SRNL-STI-2010-00589
Revision 0

Keywords: *DWPF, Tank 48, FBSR, WAC coal limit, off-gas flammability*

Retention: *Permanent*

DWPF Coal-Carbon Waste Acceptance Criteria Limit Evaluation Based on Experimental Work (Tank 48 Impact Study)

D. P. Lambert
A. S. Choi

October 2010

Savannah River National Laboratory
Savannah River Nuclear Solutions, LLC
Aiken, SC 29808

Prepared for the U.S. Department of Energy under contract number DE-AC09-08SR22470.

SRNL SAVANNAH RIVER NATIONAL LABORATORY

DISCLAIMER

Printed in the United States of America

Prepared for
U.S. Department of Energy

REVIEWS AND APPROVALS

AUTHORS:

D. P. Lambert, Process Technology Programs Date

A. S. Choi, Engineering Process Development Date

TECHNICAL REVIEW:

M. E. Stone, Process Technology Programs Date

B. R. Pickenheim, Process Technology Programs Date

F. G. Smith, Process Modeling and Computational Chemistry Date

APPROVAL:

C. C. Herman, Manager Date
Process Technology Programs

A. B. Barnes, Manager Date
Engineering Process Development

S. L. Marra, Manager Date
Environmental & Chemical Process Technology Research Programs

R. T. McNew, Manager Date
Tank 48 Projects

J. E. Occhipinti, Manager Date
Waste Solidification Engineering

EXECUTIVE SUMMARY

This report summarizes the results of both experimental and modeling studies performed using Sludge Batch 10 (SB10) simulants and FBSR product from Tank 48 simulant testing in order to develop higher levels of coal-carbon that can be managed by DWPF. Once the Fluidized Bed Steam Reforming (FBSR) process starts up for treatment of Tank 48 legacy waste, the FBSR product stream will contribute higher levels of coal-carbon in the sludge batch for processing at DWPF. Coal-carbon is added into the FBSR process as a reductant and some of it will be present in the FBSR product as unreacted coal.

The FBSR product will be slurried in water, transferred to Tank Farm and will be combined with sludge and washed to produce the sludge batch that DWPF will process. The FBSR product is high in both water soluble sodium carbonate and unreacted coal-carbon. Most of the sodium carbonate is removed during washing but all of the coal-carbon will remain and become part of the DWPF sludge batch.

A paper study was performed earlier to assess the impact of FBSR coal-carbon on the DWPF Chemical Processing Cell (CPC) operation and melter off-gas flammability by combining it with SB10-SB13. The results of the paper study are documented in Ref. 7 and the key findings included that SB10 would be the most difficult batch to process with the FBSR coal present and up to 5,000 mg/kg of coal-carbon could be fed to the melter without exceeding the off-gas flammability safety basis limits.

In the present study, a bench-scale demonstration of the DWPF CPC processing was performed using SB10 simulants spiked with varying amounts of coal, and the resulting seven CPC products were fed to the DWPF melter cold cap and off-gas dynamics models to determine the maximum coal that can be processed through the melter without exceeding the off-gas flammability safety basis limits. Based on the results of these experimental and modeling studies, the presence of coal-carbon in the sludge feed to DWPF is found to have both positive (+) and negative (-) impact as summarized below:

- Coal-carbon is a melter reductant. If excess coal-carbon is present, the resulting melter feed may be too reducing, potentially shortening the melter life. During this study, the Reduction/Oxidation Potential (REDOX) of the melter could be controlled by varying the ratio of nitric and formic acid.
- The addition of coal-carbon increases the amount of nitric acid added and decreases the amount of formic acid added to control melter REDOX. This means that the CPC with the FBSR product is much more oxidizing than current CPC processing. In this study, adequate formic acid was present in all experiments to reduce mercury and manganese, two of the main goals of CPC processing.
- Coal-carbon will be oxidized to carbon dioxide or carbon monoxide in the melter. The addition of coal-carbon to the FBSR product will lead to approximately 55% higher offgas production from formate, nitrate and carbon due to the decomposition of the carbon at the maximum levels in this testing. Higher offgas production could lead to higher cold cap coverage or melter foaming which could decrease melt rate. No testing was performed to evaluate the impact of the higher melter offgas flow.
+ The hydrogen production is greatly reduced in testing with coal as less formic acid is added in CPC processing. In the high acid run without coal, the peak hydrogen generation was 15 times higher than in the high acid run with added coal-carbon.

+ Coal-carbon is a less problematic reducing agent than formic acid, since the content of both carbon and hydrogen are important in evaluating the flammability of the melter offgas. Processing with coal-carbon decreases the amount of formic acid added in the CPC, leading to a lower flammability risk in processing with coal-carbon compared to the current DWPF flowsheet.
+ The seven SB10 formulations which were tested during the bench-scale CPC demonstration were all determined to be within the off-gas flammability safety basis limits during the 9X/5X off-gas surge for normal bubbled melter operation. The concentration of coal-carbon in these baseline melter feeds varied widely from 0 to 17,863 ppm, depending on the acid addition strategy used and the extent to which the required reductant (formic acid) was replaced with coal-carbon. All baseline feeds were redox-adjusted and three of them contained TOC higher than the current theoretical TSR limit of 18,900 ppm.
- Additional coal-carbon was then added to each baseline feed until the calculated off-gas flammability equaled the safety basis limit of 60% of the LFL at the peak of off-gas surge ("max-coal"). In doing so, however, no counterbalancing nitrate was added, thus simulating the scenario where slugs of coal enter the melter as a result of uneven distribution of coal in the slurry. The results of these "max-coal" feed simulations showed that the maximum coal-carbon concentration that can be processed through the DWPF melter without exceeding the safety basis limits varies from 3,400 ppm (SB10-8) to 19,032 ppm (SB10-1). The resulting TOC exceeded the current TSR limit in all max-coal feeds except SB10-8, whose TOC was just below the TSR limit.
- The results of flammability assessment also showed that the theoretical maximum coal-carbon limit for DWPF melter should occur when the formic acid addition is kept to a minimum, as required by the reduction of Hg and Mn and the destruction of nitrite, while maintaining as high a nitrate level as possible at a given target redox.

It should be noted that the maximum coal-carbon concentrations stated above represent the theoretical limits and the actual field limits of coal-carbon will be lower since appropriate analytical and instrument uncertainties must be subtracted from the theoretical limits.

Recommendations:

1. The results of this feasibility analysis indicate that the processing of SB10 sludge together with the FBSR product using a coal-carbon concentration of 9.5 wt % total solids basis and SWPF products is possible in the CPC. However, since every sludge batch has a different composition, this limit should be reevaluated with each new sludge batch as part of the sludge batch qualification program.
2. Minimize the coal-carbon content in the FBSR product. Minimizing the coal-carbon concentration will also limit the nonradioactive impurities added in waste processing (coal ash, carbon, sulfur, etc.).
3. Develop a method to measure the carbon concentration in washed sludge and CPC slurries. Analytical Development (AD) has been unable to accurately measure the carbon concentration with existing instruments and methods. Understanding the concentration of the carbon will be critical in DWPF processing.
4. Experimentally assess the impact of FBSR product on melt rate. Melt rate was not measured as part of this study, nor was the optimum frit used during this study.
5. Use a melter for in-situ sampling or post-mortem (destructive) analysis to assess the potential for localized reduction, the formation of metallic precipitates, and/or possible interactions of reduced species (such as nickel sulfides) on materials of construction.
6. Testing of the sludge wash material that was collected during sludge preparation should be used in testing to determine whether this large quantity of sodium carbonate produced

during sludge washing will impact the HLW evaporators or Waste Tanks. The decanted supernate from washing SB10-B simulant has been collected and retained.

7. This preliminary study should be reassessed if a new CPC flowsheet is defined and when the FBSR product stream is finalized.

TABLE OF CONTENTS

LIST OF TABLES

LIST OF FIGURES

LIST OF ABBREVIATIONS

ACTL	Aiken County Technical Laboratory
AD	Analytical Development
CPC	Chemical Processing Cell
CSTR	Continuous Stirred Tank Reactor
DOE-SR	Department of Energy – Savannah River
DWPF	Defense Waste Processing Facility
DCS	Distributed Control System
FBSR	Fluidized Bed Steam Reformer
FAVC	Formic Acid Vent Condenser
ICP-AES	Inductively Couple Plasma – Atomic Emission Spectroscopy
LFL	Lower Flammability Limit
MCU	Modular Caustic Side Solvent Extraction Unit
MOG	Melter Off-Gas
MWWT	Mercury Water Wash Tank
OGCT	Offgas Condensate Tank
PSAL	Process Support Analytical Laboratory
PTDT	Product Dissolution Tank
REDOX	Reduction/Oxidation Potential (Ratio of $Fe^{+2}/\Sigma Fe$)
SB	Sludge Batch
SME	Slurry Mix Evaporator
SMECT	Slurry Mix Evaporator Condensate Tank
SRAT	Sludge Receipt and Adjustment Tank
SRNL	Savannah River National Laboratory
SRNS	Savannah River Nuclear Solutions
SRR	Savannah River Remediation, LLC
SRS	Savannah River Site
SWPF	Salt Waste Processing Facility
TPE	Tank 48 Project Engineering
TSR	Technical Safety Requirement
TIC	Total Inorganic Carbon
TOC	Total Organic Carbon
TPB	Tetraphenylborate
TT&QAP	Task Technical and Quality Assurance Plan
TTR	Technical Task Request

UDS	Undissolved Solids
WAC	Waste Acceptance Criteria

1.0 Introduction

Currently Tank 48 has approximately 250,000 gallons of legacy waste containing organic potassium and cesium (K and Cs) tetraphenyl borate (TPB) solids from the In-Tank Precipitation (ITP) project. The waste is incompatible with other Tank Farm treatment operations. The tank has been isolated from the Tank Farm service since 1998. In order to make space in the Savannah River Site (SRS) Tank Farm, the Tank 48 waste must be processed to eliminate its organic content for downstream processing, including Tank Farm and Defense Waste Processing Facility (DWPF) processes. On June 10, 2009, the Department of Energy-Savannah River (DOE-SR) concurred with Savannah River Remediation (SRR) Business Decision Recommendation to select the THOR® sodium carbonate based Fluidized Bed Steam Reforming (FBSR) technology to treat the Tank 48 waste.[1] The FBSR processing of the Tank 48 content is expected to be completed over a two-year period from 2014 to 2016.

The FBSR process will treat the Tank 48 organic laden waste and generate organic free sodium carbonate based solid. The solids product will be slurried with water and sent to the Tank Farm for further processing. In the Tank Farm, the FBSR product slurry will be combined with sludge, washed as part of the sludge preparation process, and fed to DWPF. The FBSR product slurry will be blended with other sludge tanks to produce Sludge Batches 10-13 (SB10-SB13). Current projections of SB10-SB13[2] combined with expected composition of the FBSR product [3] will be used to predict the resulting sludge composition for SB10-SB13.

DWPF will process the washed sludge concurrently with two products from salt waste, the cesium rich strip effluent stream and the actinide rich actinide removal product from the Salt Waste Processing Facility (SWPF). Both of these streams contain organic species that must be accounted for in the requested analysis. Until the SWPF begins processing, the products from the Actinide Removal Process (ARP) and the Modular Caustic-Side Solvent Extraction Unit (MCU) will be used. These streams will be defined as salt processing streams in the rest of the report.

DWPF targets the production of a melter feed that has a balanced REDOX (defined as 0.2 $Fe^{+2}/\Sigma Fe$). An acceptable REDOX range is 0.09-0.30. It accomplishes this by using a blend of formic acid and nitric acid using a REDOX algorithm [4] shown in Eq. (1) below. If the melter feed is too reducing (REDOX >0.3), metals such as copper, nickel and the noble metals can become reduced, accumulate in the bottom of the melter, and short out the electrodes, shortening the life of the melter. If the melter feed is too oxidizing (REDOX <0.09), the glass will release oxygen, causing melter foaming, pressure upsets, and slowing melt rate.

$$REDOX=0.2358+0.1999*((2*C_{formate}+4*C_{oxalate}+4*C_{Carbon}-5*(C_{Nitrate}+C_{Nitrite})-5*C_{Mn}))*(45/TS) \quad (1)$$

Where C = species concentration, g-mole/kg melter feed, TS = total solids in melter feed in wt %, and REDOX is a molar ratio of Fe+2/ΣFe

Tank 48 contains a high organic concentration, due mainly to the potassium tetraphenylborate present. Approximately 40,000 lb of tetraphenylborate carbon is currently present in Tank 48. Processing of the waste in the FBSR will produce approximately 80,000 lb of carbon in the form of carbonate and another 120,000 lbs of carbon in the form of residual coal-carbon[13]. Neither the carbon from coal or carbonate will wind up in the final glass waste form but may impact

processing in DWPF and could lead to pluggage during CPC sampling and transferring due to the large particle size (10% greater than 177 μm[1]) of the FBSR product.

The FBSR process uses coal-carbon as a reaction additive for promoting a reducing environment in the reformer as well as for maintaining the process in an auto-thermal mode. Some levels of coal-carbon (@100% carbon) will be present in the FBSR product slurry to the Tank Farm / DWPF processing. The purpose of this study is to estimate a coal-carbon limit in the FBSR product for DWPF sludge receipt to ensure the sludge can be safely processed without impacting the DWPF safety basis. The primary products of this study are the results of the off-gas flammability assessment for the DWPF melter and the Chemical Processing Cell (CPC) demonstrations with simulant, which will provide an estimate of the total organic carbon (TOC) limit along with the associated coal-carbon limit. It should be noted that the TOC varies from sludge batch to sludge batch due to composition changes in oxalate, coal-carbon, and other carbon sources but the main contributor to the TOC in the melter feed is the formate salts originating from the addition of formic acid.

Tank 48 Projects Engineering (TPE) of Savannah River Remediation (SRR) has requested this demonstration via Technical Task Request (TTR) X-TTR-H-2009-00006.[5] The scope of the study is being controlled with the Task Technical and Quality Assurance Plan (TT&QAP).[6]

This work is Technical Baseline Research and Development (R&D) for an onsite customer (Tank 48 and DWPF).

2.0 Initial Paper Study

A paper study[7] was completed to estimate the impact of the FBSR coal-carbon on DWPF CPC processing. The paper study included a prediction of SME product composition and REDOX, a melter offgas flammability model, a cold cap model, and an off-gas dynamics model. However, a number of estimates were made for anion destruction that needed to be validated by experiments. The results of the paper study are not reproduced in this revision for brevity and because the experimental results are closer to expected processing parameters.

Four waste streams will be added to the DWPF CPC once the FBSR begins processing the Tank 48 contents. The four streams and their expected volumes are summarized in Table 2-1. As part of this study, it was assumed that DWPF will be producing 325 canisters per year (1.25 million lb/yr of glass) using the current DWPF chemical processing flowsheet and that the FBSR and salt streams will be processing at design capacity. In addition, it is assumed that no other processing facilities are providing waste to DWPF.

[1] Maximum frit particle size is 80 mesh or 177 μm

Table 2-1. DWPF Processing Streams during FBSR Processing

Waste Stream	Annual Production Rate, gal/yr	Primary carbon source
Sludge	Depends on sludge batch	Carbonate, oxalate
FBSR Product Dissolution Tank (PDT)	160,000	Unreacted Coal, carbonate
Strip Effluent	564,000	Solvent (Isopar, modifier, extractant, and suppressor)
Actinide Removal Stream	121,000	Oxalate, carbonate

Note that the assumption of 325 canisters per year in DWPF is lower than the ultimate SRR plan of 400 canisters per year. At 325 canisters per year, 19% less sludge will be processed compared to 400 canisters per year. Since the FBSR processing rate is assumed constant, production at the higher throughput will effectively dilute the coal-carbon, leading to lower coal-carbon concentrations being fed into DWPF. However, if the 325 canister per year production rate can not be achieved, the coal-carbon concentration will be higher than estimated in this study. Also it should be noted that the sludge production rate (noted in the table above as "depends on sludge batch") was calculated by difference, setting the SWPF and FBSR streams at their flowsheet targets, and calculating the volume of sludge that can be processed to achieve the 325 canister per year production rate.

The Hazen testing FBSR product[3] was between 9.3 and 17.1 wt % coal-carbon-carbon so 15% coal-carbon was used as a basis in this study. Coal is added in the FBSR product and some of this coal is unreacted and exits with the FBSR product. The coal-carbon in the 2008 Hazen product[3] was much higher than was measured in earlier processing. As a result, this study was initiated to develop waste acceptance criteria (WAC) to prevent a flammable mixture from forming in the DWPF melter offgas system.

Not all of the carbon fed to DWPF is fed to the melter. For example, formic acid, another carbon source, and nitric acid are added to the CPC to neutralize the waste. Neutralization of the waste destroys all of the carbonate and a portion of the oxalate. The addition of formic acid adds a large quantity of organic that will be fed to the melter. Also, volatile organics such as Isopar are steam stripped during processing so they do not reach the melter. However, the coal-carbon is inert during CPC processing and will be fed to the melter. The melter will oxidize all the remaining carbon to CO and CO_2 which may lead to a flammable offgas mixture if the carbon concentration in the melter feed is too high. The coal also adds other impurities that impact DWPF processing including hydrogen (impacts melter offgas flammability), sulfur, and coal ash. The coal composition of two coal sources used in FBSR testing is summarized in Table 2-2.[3] The ash content of the coal, similar to the solids present in sludge, is summarized in Table 2-3.

Table 2-2. Coal Composition, wt %

Component	Erwin	Bestac
Moisture	7.35	8.37
Ash	7.77	9.12
Al	0.81	1.26
Ca	0.17	0.14
Fe	0.15	0.44
K	0.01	0.03
Mg	0.06	0.01
Na	0.10	0.03
P	0.01	0.05
Si	2.14	2.59
Ti	0.04	0.04
Other	0.31	0.01
Carbon	80.45	78.59
Hydrogen	1.58	2.09
Oxygen	1.69	0.39
Nitrogen	0.84	0.72
Sulfur	0.30	0.72
Total	103.8	104.6

Table 2-3. Coal Ash Composition, wt %

	Normalized SRNL Ash Analysis	
Component	2006 Erwin Ash@525° C	2008 Bestac Ash@525° C
Al_2O_3	19.63%	26.10%
CaO	2.99%	2.21%
Fe_2O_3	2.70%	6.91%
K_2O	0.13%	0.34%
MgO	1.24%	0.18%
Na_2O	1.69%	0.49%
P_2O_5	0.39%	1.15%
SO_4	7.50%	1.02%
SiO_2	58.91%	60.77%
TiO_2	0.76%	0.73%
Other	4.05%	0.10%
Total	100.00%	100.00%

3.0 Results and Discussion

Seven SRAT/SME runs (SB10-1,2,3,5,7,8 and 9) were completed during this study using acid stoichiometries of 100% and 150% with a blend of SB10-A (no added FBSR) and SB10-B (added FBSR) simulant. The SB10-B simulant was prepared by producing an unwashed SB10 simulant, adding Hazen FBSR PDT slurry (high coal-carbon and sodium carbonate content), and washing to ~1 M sodium with inhibited water. These runs were completed and samples analyzed using the practices and procedures typical for CPC simulations at the Aiken County Technology Laboratory (ACTL), as described below.

3.1 Simulant Preparation

Two simulant batches were prepared, one simulating the best estimate of the SB10 composition without added FBSR PDT (SB10-A coal-free sludge simulant) and the other simulating the expected sludge composition with FBSR PDT added to the sludge preparation tank (SB10-B coal added sludge simulant). The SB10-A sludge simulant used targets were specified by the Tank 48 Project Team.[8]

3.1.1 *Analysis of 2009 Hazen PDT Sample*

A sample was pulled from one of the Hazen PDT sample drums for combining with the sludge simulant to produce a sludge simulant for this testing. Two critical analyses were performed of the PDT sample, namely a carbon estimate and a particle size measurement. The composition of the FBSR PDT product is shown in Table 3-1. A particle size distribution graph is shown in Figure 3-1.

Table 3-1 2009 Hazen PDT Sample Results

Component	FBSR PDT
Total Solids, wt %	18.73
Dissolved Solids, wt %	12.75
Undissolved Solids, wt %	5.98
Carbon Undissolved Solids, wt TS%	21.95
Non-carbon Undissolved Solids, wt % TS	10.03
Dissolved Solids, wt % TS	68.02
Carbon Undissolved Solids >80 mesh, wt % TS	0.91
Carbon Undissolved Solids 80-100 mesh, wt % TS	0.97
Carbon Undissolved Solids 100-120 mesh, wt % TS	7.40
Carbon Undissolved Solids <120 mesh, wt % TS	12.68
Non-carbon Undissolved Solids >80 mesh, wt % TS	0.02
Non-carbon Undissolved Solids 80-100 mesh, wt % TS	0.12
Non-carbon Undissolved Solids 100-120 mesh, wt % TS	1.44
Non-carbon Undissolved Solids <120 mesh, wt % TS	8.44

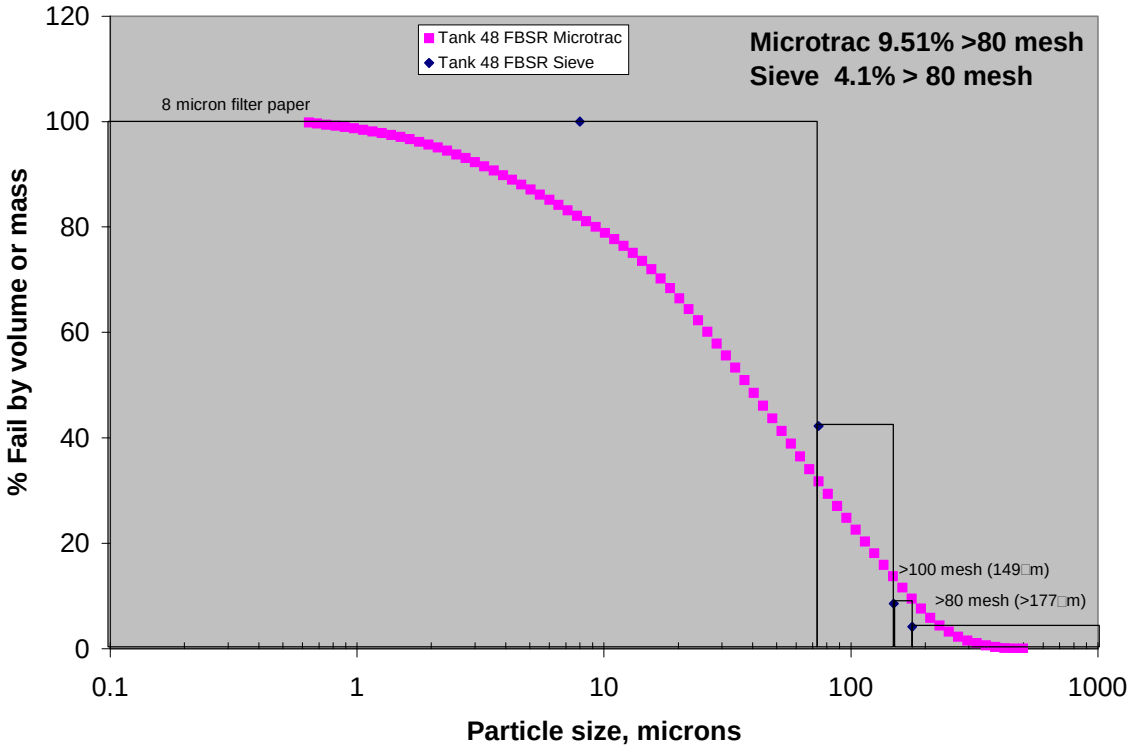

Figure 3-1. 2009 PDT Sample Particle Size Distribution Results

The concentration of the residual coal-carbon in the FBSR PDT is of critical importance to this study. The analysis of the coal-carbon in Tank 48 PDT products have led to variable results by different laboratories and different methods. The method used for estimating the coal-carbon in the FBSR PDT was developed by SRNL for coal-carbon analysis of FBSR PDT product[9]. The SRNL analysis avoids the complications of having hydrous carbonates present during the analysis and accounts for the non-carbon undissolved solids (UDS). This procedure has several steps which include (1) drying the product at 110° C to achieve a constant weight, (2) dissolution of solids at a ratio of 1 gram to 100 mL of water (considered infinite dilution), (3) filtration of the dissolved product to purge the sample of the soluble carbonates (anhydrous and hydrous), (4) redrying to a constant weight at 110° C, and (5) roasting the UDS at 525° C for two days to determine the wt% volatile carbon UDS from the wt% noncarbon UDS. The concentration of coal-carbon in the SB10-B slurry and all blends of the SB10-A and SB10-B slurries were calculated by mass balance knowing the mass of sludge and FBSR PDT solids in the SB10-B slurry.

3.1.2 *Simulant Preparation*

The preparation of a simulant for Sludge Batch 10-A involved six steps: precipitation of manganese (IV) oxide, caustic precipitation of a metal nitrate solution, addition of sodium carbonate, washing of the precipitated solids, addition of minor insoluble species, and addition of soluble species. The precipitation of metal nitrates to form insoluble oxides and hydroxides was conducted in a Continuous Stirred Tank Reactor (CSTR) and involved generation of a metal nitrate solution followed by precipitation of the metal nitrates through the addition of sodium hydroxide. Following the addition of sodium carbonate, the material was washed then

soluble/insoluble species were added. Procedure L29 ITS-00124[10], "SRS HLW Sludge Simulant Preparation" was utilized to perform the tests.

The preparation of a simulant for Sludge Batch 10-B involved eight steps. This is different than typical sludge preparation to mimic the washing of the combined unwashed sludge and FBSR PDT material that will be completed in the sludge preparation tank. The first four steps of the preparation for both sludges were identical, so the sludges were prepared as a single batch and split once step 4 met the nitrate target for SB10-B prewashing. Once SB10-B slurry was separated from the SB10-A batch, the soluble salts were added to the SB10-B slurry to produce a 5M supernate. The Tank 48 Hazen produced FBSR PDT solution was added to the sludge mixture which was washed with inhibited water down to approximately 1M Na, decanted, and the soluble/insoluble species were added.

The simulants were prepared using facilities at both ACTL and in 735-11A. The MnO_2 precipitation, the precipitation in the CSTR and the precipitation of the insoluble carbonate species were each completed in one day. The washing and concentration of the precipitate took approximately three weeks, while the final insoluble and soluble species were added in one day. The final slurry was sampled and analyzed at ACTL, the Process Science Analytical Laboratory (PSAL), and by Analytical Development (AD). The results of these analyses are summarized in Table 3-2. The SB10 simulants were very thin rheologically. The mercury and noble metals were not added to the simulant. Noble metals, mercury, and rinse water were added to the sludge simulant prior to performing the SRAT cycle. The noble metal concentrations were based on 100% of the SB6 estimated noble metals. Since the SB10 mercury content is not known, the mercury concentration was chosen so that the mercury could be steam stripped down to 0.6 wt % assuming a mercury strip factor of 750 pounds steam per pound mercury in 12 hours. The concentrations of each trim chemical added are shown in Table 3-3. Note that SB10-B has lower noble metal and mercury concentration since the FBSR product contains negligible noble metals and mercury.

In preparation for the experiments, the SB10-A and SB10-B sludge simulants were blended to provide four levels of carbon (from 0 to 9.545 wt % C) as calculated from the PDT analysis. The projected composition of the four sludge blends is summarized in Table 3-4.

Table 3-2 Simulant Composition for Flowsheet Testing

Analyses	SB10-A	SB10-B	Analyses	SB10-A	SB10-B
Elemental	**Wt% calcined solids**		**Solids Data**	**Wt %**	
Al	6.66	4.42	Total Solids	17.84	15.45
Ba	0.222	0.252	Insoluble Solids	14.37	11.65
Ca	2.50	2.92	Calcined Solids	11.16	11.58
Ce	0.742	0.802	Soluble Solids	3.47	3.80
Cr	0.138	0.150	**Anions**	**mg/kg slurry**	
Cu	0.056	0.059	Nitrite	9,430	6,680
Fe	27.9	30.9	Nitrate	5,690	4,890
K	0.202	0.253	Formate	0	0
La	0.250	0.278	Sulfate	312	323
Mg	0.330	0.367	Chloride	0	352
Mn	5.35	5.83	Phosphate	0	0
Na	14.7	13.6	Oxalate	0	140
Ni	0.736	0.830	Total Carbonate	6,960	11,500
P	<0.100	<0.100	**Other Results**		
Pb	0.186	0.190	Base Equivalents (molar)	0.909	0.664
S	0.066	0.071	Slurry Density (g/ml)	1.153	1.125
Si	2.24	3.51	Supernate Density (g/ml)	1.058	1.036
Ti	<0.010	0.141	Slurry TIC, mg/kg	1,347	2,219
Zn	0.067	0.049	Soluble TIC, mg/kg	1,151	1,719
Zr	0.450	0.483	pH	13.4	13.3
			Calculated Coal-carbon, wt % TS	0	9.545

Table 3-3 Trim Chemical Additions, wt % on Total Solids Basis

TRIM CHEMICAL	SB10-A	SB10-B
Trimmed Sludge Target Ag metal content	0.0142	0.0108
Trimmed Sludge Target wt% Hg dry basis	1.6188	1.2272
Trimmed Sludge Target Pd metal content	0.0066	0.0050
Trimmed Sludge Target Rh metal content	0.0233	0.0177
Trimmed Sludge Target Ru metal content	0.1121	0.0850

Table 3-4 Calculated Blended Sludge Composition

Analyses	SB10-1,2	SB10-3,9	SB10-5	SB10-7,8
Composition	0% A, 100% B	32.0% A, 68.0% B	66.3% A, 33.7% B	100% A,0% B
Solids Data	**Wt %**			
Total Solids	15.45%	16.21%	17.04%	17.84%
Insoluble Solids	11.58%	11.44%	11.30%	11.16%
Calcined Solids	3.87%	4.77%	5.74%	6.69%
Soluble Solids	11.65%	12.52%	13.45%	14.37%
Anions	**mg/kg slurry**			
Chloride	351.5	238.9	118.4	<100
Nitrite	6680	7562	8507	9435
Nitrate	4895	5150	5422	5690
Formate	0	0	0	0
Sulfate	323	319	316	312
Oxalate	137	95	47	<100
Phosphate	<100	0	0	<100
Total Carbonate	2219	1940	1641	1347
Other Results				
Base Equivalents (molar)	0.590	0.741	0.825	0.789
Slurry Density (g/ml)	1.125	1.134	1.144	1.153
pH	13.3	13.1	12.8	13.4
Soluble Total Inorganic C, mg/kg slurry	1719	1539	1345	1151
Calculated Coal-Carbon, Wt %	9.59	6.21	2.93	0.00

3.2 Experimental Apparatus

The testing was performed at the ACTL using the four-liter kettle setup. The SRAT rigs were assembled following the guidelines of SRNL-PSE-2006-00074[11]. The intent of the equipment is to functionally replicate the DWPF processing vessels. The 4-liter glass kettle is used to replicate both the SRAT and SME, and it is connected to the SRAT Condenser, the Mercury Water Wash Tank (MWWT), and the Formic Acid Vent Condenser (FAVC). The Slurry Mix Evaporator Condensate Tank (SMECT) is represented by a sampling bottle that is used to remove condensate through the MWWT. For the purposes of this paper, the condensers and wash tank are referred to as the offgas components. A sketch of the experimental setup is given as Figure 3-2.

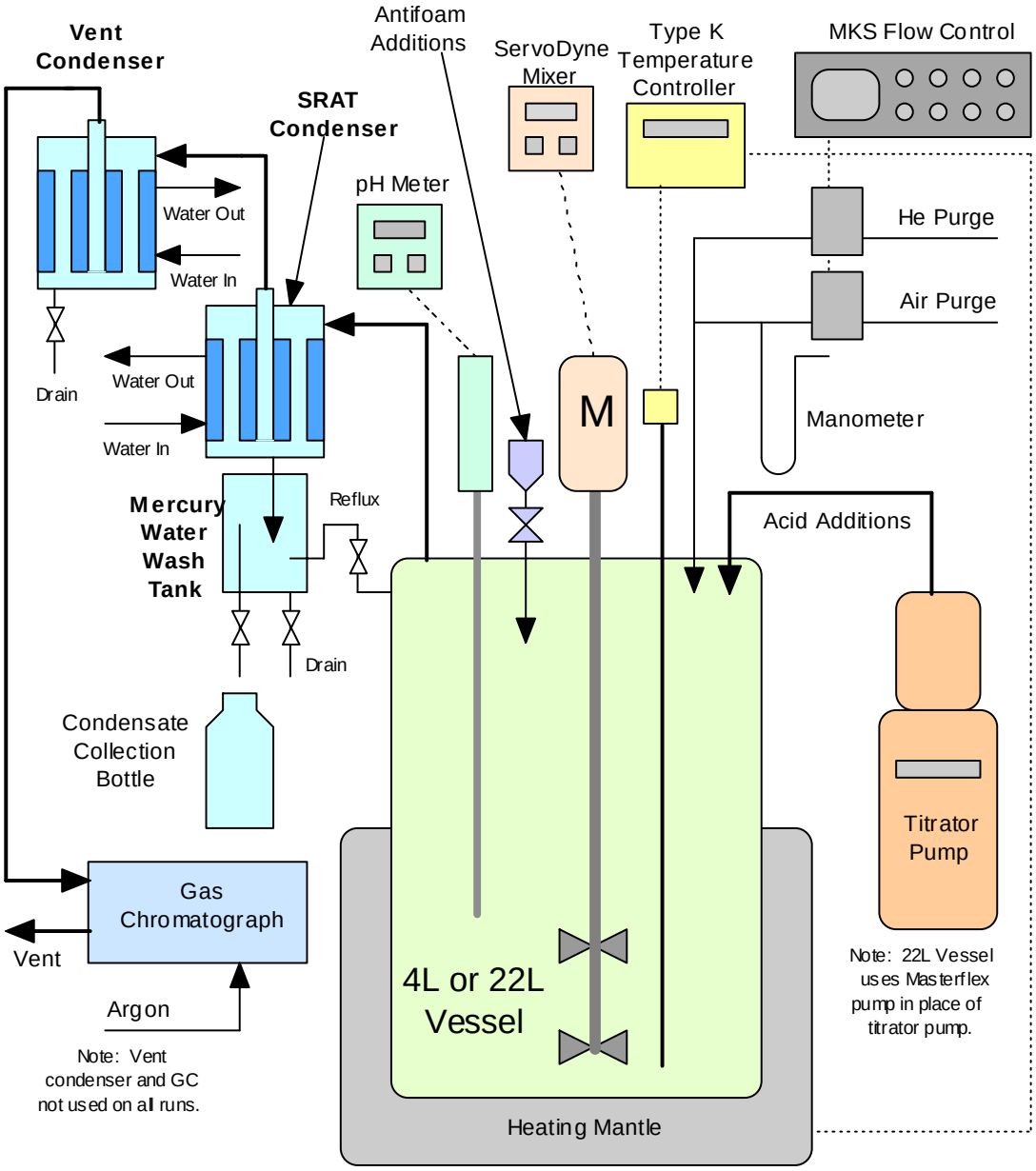

Figure 3-2. Schematic of SRAT Equipment Set-Up

The flowsheet runs were performed using the guidance of Procedure ITS-0094[12] ("Laboratory Scale Chemical Process Cell Simulations") of Manual L29. Offgas hydrogen, oxygen, nitrogen, nitrous oxide, and carbon dioxide concentrations were measured during the experiments using in-line instrumentation. Helium was introduced at a concentration of 0.5% of the total air purge as an inert tracer gas so that total amounts of generated gas and peak generation rates could be calculated. During the runs, the kettle was monitored to observe reactions that were occurring to include foaming, air entrainment, rheology changes, loss of heat transfer capabilities, and offgas carryover. Observations were recorded on data sheets and pasted into a laboratory notebook.[13]

Concentrated nitric acid (50-wt%) and formic acid (90-wt%) were used to acidify the sludge and perform neutralization and reduction reactions during processing. The amounts of acid to add for each run were determined using the proposed Koopman DWPF acid addition equation.[14] The split of the acid was determined using the REDOX equation currently being used in DWPF processing.[15] The REDOX target ($Fe^{2+}/\Sigma Fe$) was 0.2. To account for the reactions and anion destructions that occur during processing, assumptions about nitrite destruction, nitrite to nitrate conversion, and formate destruction were made for each run.

To prevent foaming during SRAT processing, 200 ppm IIT 747 antifoam was added before acid addition, 100 ppm was added after nitric acid addition was complete and 500 ppm was added at the completion of formic acid addition. SRAT processing included 12-hours at boiling (dewater time plus reflux time). The SME processing did not include the addition of canister dewaters. The frit addition was split into two equal portions. The frit was added with water and formic acid at DWPF prototypical conditions. Concentration was performed after each frit addition and then heat was removed to allow for the next frit addition. A final concentration was performed at the end of the run to meet the 50 weight percent total solids target. The SRAT condenser was maintained at 25° C during the run, while the vent condenser was maintained at 4° C.

3.3 SRAT Cycle Results

Seven SRAT/SME runs (SB10-1, 2, 3, 5, 7, 8, and 9) were completed during this study using acid stoichiometries of 100% and 150%. A unique run number was assigned to each run. SB10-1 and SB10-2 were SRAT/SME Cycles with sludge SB10-B only. SB10-7 and SB10-8 were SRAT/SME Cycles with sludge SB10-A only. SB10-3, SB10-5 and SB10-9 were SRAT/SME Cycles with blends of sludge SB10-A and SB10-B as shown in Table 3-4. All runs targeted a predicted glass REDOX ($Fe^{2+}/\Sigma Fe$) of 0.2 by adjusting the ratio of formic to nitric acid during the SRAT cycle and using the current REDOX equation.[4] The runs targeted a waste loading of 38% instead of the 40% specified in the Task Plan.

Table 3-5 SRAT/SME Test Targets

Run Number	Acid Stoichiometry	REDOX Target	Sludge Predicted Coal-carbon, mg/kg	Waste Loading
SB10-1	97%	0.2	19,800	38%
SB10-2	150%	0.2	18,500	38%
SB10-3	103%	0.2	12,900	38%
SB10-5	100%	0.2	5,870	38%
SB10-7	100%	0.2	0	38%
SB10-8	150%	0.2	0	38%
SB10-9	150%	0.2	10,000	38%

The SRAT cycles were completed using conservative design basis inputs such as acid addition flowrates, air purges, and steam flowrates.

Two processing issues were noted in this series of tests. For SB10-A sludge (no coal) runs, the high acid stoichiometry (i.e., 150%) led to high hydrogen generation and low recovery of mercury. For SB10-A sludge (no coal), the low acid stoichiometry (i.e., 100%) SRAT product had approximately 13% of the nitrite still present after 12 hours of processing.

3.3.1 *Acid Addition Calculation*

An acid calculation was completed prior to each experiment to estimate a number of scaled parameters necessary to complete each experiment at the conditions specified with the inputs such as kettle power (designed to simulate steam flow), acid addition flowrate, offgas purge, acid volume, etc. Results from the acid calculation and other run data are summarized in Appendix A.

3.3.1.1 Calculation Inputs

The SRAT cycle acid calculation utilizes the amount of nitrite, mercury, manganese, carbonate, and base equivalents to calculate the stoichiometric amount of acid to be added. Nitric acid and formic acid amounts are calculated[16] based on the applied stoichiometric factor and the ratio needed to achieve the predicted glass REDOX target of 0.2 $Fe^{+2}/\Sigma Fe$. The equation for prediction of glass REDOX utilizes estimates of the amount of formate, oxalate, nitrate, nitrite, manganese, and total solids in the SME product. The estimation of the final concentration for the anions requires assumptions to be made concerning how these species will react during the SRAT and SME cycles. Formate and oxalate are destroyed by reactions with oxidizing species and by catalytic reactions with noble metals. Nitrite is typically consumed during the SRAT cycle, but can react to form different species including nitrate, NO, NO_2 and N_2O.

Three different acid addition predictions were used. The Hsu equation, an equation with inputs for total base, slurry carbonate, nitrite, manganese and mercury, has been used for estimating the acid requirement in DWPF since startup. Two new acid equations[14], which more accurately predict the acid requirement in DWPF, have been developed. The Koopman equation adds inputs for supernate (not slurry) carbonate, calcium and magnesium to better predict the acid requirement. The cation equation uses cations (manganese, sodium, potassium, mercury, cesium, strontium, calcium, nickel, and magnesium) to predict the acid demand with credits for anions (nitrite, nitrate, sulfate, chloride, formate and phosphate). Both of these new equations were developed for minimum acid (just enough acid to destroy nitrite with very little hydrogen generation) and nominal acid (enough acid to destroy nitrite, reduce mercury, and without making too much hydrogen). The minimum Koopman equation's prediction of acid requirement was used throughout the testing and the other results are summarized in Table 3-6. The acid calculation inputs and assumptions are shown in Table 3-7 for the SRAT cycle and Table 3-8 for the SME cycle. It should be noted that the anion conversion predictions were changed between the two sets of experiments (SB10-1, SB10-2, SB10-7 and SB10-8) and the second set of experiments (SB10-3, SB10-5, and SB10-9). Sample results from the first set of experiments were used to predict the anion conversions for the second set of experiments.

Table 3-6 Acid Calculation Results

Equation	SB10-1	SB10-2	SB10-3	SB10-5	SB10-7	SB10-8	SB10-9
Hsu Equation, M	3.87	3.87	3.87	3.87	3.87	3.87	3.65
Nominal Koopman, M	4.51	4.51	4.51	4.51	4.51	4.51	4.38
Minimum Koopman, M	3.80	3.80	3.80	3.80	3.80	3.80	3.73
Nominal Cation, M	3.74	3.74	3.74	3.74	3.74	3.74	4.06
Minimum Cation, M	3.16	3.16	3.16	3.16	3.16	3.16	3.53

Table 3-7 SRAT Cycle Processing Parameters and Assumptions

Description	Units	SB10-1	SB10-2	SB10-3	SB10-5	SB10-7	SB10-8	SB10-9
Sludge SB10-A		**0%**	**0%**	**32.0%**	**66.3%**	**100%**	**100%**	**32.0%**
Sludge SB10-B		**100%**	**100%**	**68.0%**	**33.7%**	**0%**	**0%**	**68.0%**
Conversion of Nitrite to Nitrate in SRAT Cycle	gmol NO_3/100 gmol NO_2	22.0	25.0	-6.0	-5.9	22.0	28.0	-27.3
Destruction of Nitrite in SRAT and SME cycle	% of starting nitrite	100	100	91.1	100	100	100	100
Destruction of Formic acid charged in SRAT	%	100	60	20.7	20.7	20.0	35.0	27.2
Destruction of oxalate charged	%	50	50	50	50	50	50	50
Percent Koopman Acid in Excess Stoichiometric Ratio	%	97	150	103	100	100	150	150
SRAT Product Target Solids	%	25	25	25	25	25	25	25
Nitric Acid Molarity	Molar	10.53	10.60	10.40	10.40	10.60	10.53	10.40
Formic Acid Molarity	Molar	23.80	23.80	23.84	23.84	23.80	23.80	23.84
Scaled Nitric Acid addition Rate	gallons per minute	2	2	2	2	2	2	2
Scaled Formic Acid addition Rate	gallons per minute	2	2	2	2	2	2	2
REDOX Target	Fe^{+2} / ΣFe	0.2	0.2	0.2	0.2	0.2	0.2	0.2
Trimmed Sludge Target Ag metal content	total wt% dry basis	0.0108	0.0108	0.0123	0.0119	0.0142	0.0142	0.0119
Trimmed Sludge Target wt% Hg dry basis	total wt% dry basis	1.23	1.23	1.40	1.35	1.62	1.62	1.35
Trimmed Sludge Target Pd metal content	total wt% dry basis	0.0050	0.0050	0.0057	0.0055	0.0066	0.0066	0.0055
Trimmed Sludge Target Rh metal content	total wt% dry basis	0.0177	0.0177	0.0202	0.0195	0.0233	0.0233	0.0195
Trimmed Sludge Target Ru metal content	total wt% dry basis	0.0850	0.0850	0.0962	0.0937	0.1121	0.1121	0.0937
Wt% Active Agent In Antifoam Solution	%	10	10	10	10	10	10	10
Basis Antifoam Addition for SRAT (generally 100 mg antifoam/kg slurry)	mg/kg slurry	100	100	100	100	100	100	100
Number of basis antifoam additions added during SRAT cycle		8	8	8	8	8	8	1212

Table 3-8 SME Processing Parameters and Assumptions

Description	Units	SB10-1,2,3,5,7,8,9
Frit type	N/A	418
Destruction of Formic acid in SME	%	5.0
Destruction of Nitrate in SME	%	5.0
Assumed SME density	kg / L	1.450
Basis Antifoam Addition for SME cycle	mg/kg slurry	100
Number of basis antifoam additions added during SME cycle	N/A	6
Sludge Oxide Contribution in SME (Waste Loading)	%	38
Frit Slurry Formic Acid Ratio	g 90 wt% FA/100 g Frit	1.50
Target SME Solids total Wt%	wt%	50.0
Number of frit additions in SME Cycle	N/A	2

3.3.1.2 Acid Calculation Results

Three different acid addition predictions were used. The Hsu equation, an equation with inputs for total base, slurry carbonate, nitrite, manganese and mercury, has been used for estimating the acid requirement in DWPF since startup. Two new acid equations[9], which more accurately predict the acid requirement in DWPF, have been developed. The Koopman equation adds inputs for supernate (not slurry) carbonate, calcium and magnesium to better predict the acid requirement. The acid calculation determines the values for a large number of processing parameters as well as the amount of formic and nitric acid to be used. Selected values are shown in Table 3-6. The stoichiometric acid addition for the sludge simulant was calculated to be 1.61 moles per liter for SB6-A and 1.83 moles per liter for SB6-B. The cation equation uses cations (manganese, sodium, potassium, mercury, cesium, strontium, calcium, nickel, and magnesium) to predict the acid demand with credits for anions (nitrite, nitrate, sulfate, chloride, formate and phosphate). Both of these new equations were developed for minimum acid (just enough acid to destroy nitrite with very little hydrogen generation) and nominal acid (enough acid to destroy nitrite, reduce mercury, and without making too much hydrogen). The minimum Koopman equation's prediction of acid requirement was used throughout the testing and the other results are summarized in Table 3-6.

The acid calculation determines the values for a large number of processing parameters as well as the amount of formic and nitric acid to be used. Selected values are shown in Table 3-9. The stoichiometric acid addition for the sludge simulant was calculated to be 1.61 moles per liter for SB10-A and 1.83 moles per liter for SB10-B. The minimum stoichiometric acid requirement is based on a new acid addition equation developed by David Koopman.[14] As acid stoichiometry increased, the ratio of formic acid to the total amount of acid decreased. This decrease is due to the presence of nitrate and nitrite in the initial sludge simulant lowering the amount of nitrate or oxidizers needed to balance the formic acid at lower acid stoichiometries. The frit addition increased slightly due to the process samples being more dilute in terms of the original feed as acid stoichiometry increased.

Table 3-9 Selected Process Values for Testing

Run Number	Sludge Blend	Acid Stoichiometry	Total Acid Required (mol/L)	Formic Acid Ratio (% of Total Acid)	Frit Addition Amount (grams)
SB10-1	0% A	97	1.31	14.09%	535.92
SB10-2	0% A	150	2.03	25.60%	543.55
SB10-3	32.03% A	103	1.46	23.40%	587.31
SB10-5	66.30% A	100	1.57	44.70%	637.62
SB10-7	100% A	100	1.69	73.53%	691.16
SB10-8	100% A	150	2.53	74.41%	695.81
SB10-9	32.02%A	150	2.50	38.79%	593.56

3.3.2 *SRAT Cycle Processing Observations*

Overall processing during the testing went smoothly with no interruptions or upsets occurring during process runs. The sludge became less viscous during acid additions and no problems were noted with mixing during the runs. Agitator speeds of 250 RPM[2] were sufficient to mix the sludge simulants.

3.3.2.1 SRAT Cycle Foaming

The FBSR PDT slurry is high in carbonate. Approximately 80% of the soluble carbonate is washed out of the slurry during sludge preparation. However the carbonate concentration in the SB10-B slurry was approximately 1.5X higher than the SB10-A slurry. Since carbonate is neutralized during acid addition and CO_2 is evolved, the excess carbonate means that CO_2 continues evolving for a long time during acid addition so there is a potential for more foaming in testing with the SB10-B slurry. However, no foaming was noted in any of the experiments. No additional antifoam was required during any of the seven experiments. Note that the SB10-9 experiment had additional antifoam added because of the longer processing time and higher antifoam addition during caustic boiling (ARP addition).

3.3.2.2 SRAT Cycle pH Profiles

The pH profiles of the seven runs in general matched profiles noted during previous CPC simulations.[17] As shown in Figure 3-3 the pH of the runs was lower for runs with coal and little change in pH occurred during boiling in runs with coal. Formic acid decomposition during high acid, no coal runs resulted in a higher final pH.

[2] The mixing geometry of the lab-scale apparatus is not prototypic of the DWPF SRAT/SME vessels and mixing was adjusted as required during testing to ensure that the process chemistry was captured. Agitator speed is reported only to give an indication of changes in rheological properties during the testing.

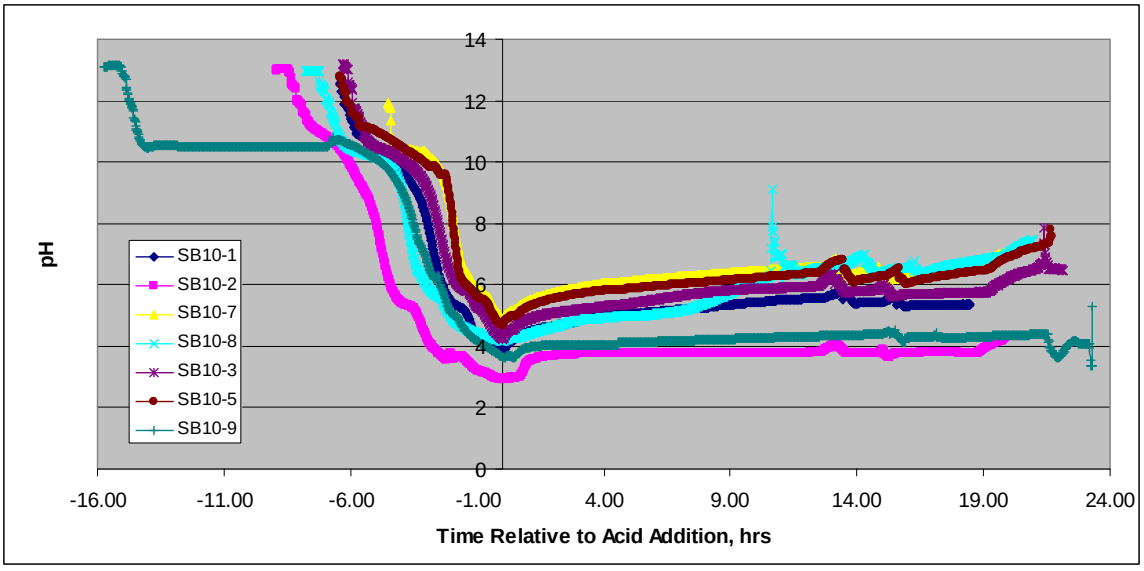

Figure 3-3. CPC Flowsheet Testing pH Profiles

3.3.3 *SRAT Cycle Sample Results*

Samples were pulled throughout and at the conclusion of the SRAT cycle. The total solids, mercury, anions, and soluble elemental species were analyzed for all samples. Samples were taken of the SRAT dewater and the MWWT contents at the completion of the SRAT cycle. All sample results are tabulated in Appendix B.

3.3.3.1 Nitrite, Nitrate, Formate

Nitrite destruction met the process requirement of <1000 mg/kg slurry at the end of the SRAT cycle for all runs except the low acid stoichiometry run with SB10-A simulant (no coal). For all runs with coal, there was no detectable nitrite at the end of the SRAT cycle. Note that the total time at boiling was 12 hours for each of these experiments. Anion results are summarized in Table 3-10.

Table 3-10 SRAT Product Anion Concentration from Tests, mg/kg slurry

Run ID & Acid Stoichiometry	F	Cl	NO_2	NO_3	SO_4	PO_4	HCO_2
100% SB10-1	<100	<100	<100	68,100	<100	<100	11,800
150% SB10-2	<100	<100	<100	65,450	<100	<100	24,800
100% SB10-3	<100	361	<100	64,100	<100	NM	18,350
100% SB10-5	<100	291	<100	41,450	<100	NM	37,100
100% SB10-7	<100	<100	1315	18,150	<100	<100	53,250
150% SB10-8	<100	<100	<100	17,150	<100	<100	59,300
150% SB10-9	<100	295	<100	56,800	<100	NM	36,200

NM = Not Measured

In a "typical run", approximately one-third of the nitrite is converted to nitrate and the other two-thirds are converted to NO_x and N_2O. In all of these runs (Table 3-11), some additional nitrate was present in the SRAT product due to the destruction of nitrite. However, in four of these runs,

(SB10-1, 2, 7, and 8) all lost significant nitrate (negative nitrite to nitrate conversion) suggesting that ammonia was likely produced during testing both with and without coal.

Formate is destroyed by reduction of Mn, Hg and catalytic destruction of nitrite ion to primarily produce NO, N_2O, NO_2, and CO_2. Formic acid is destroyed catalytically to produce primarily CO_2, and hydrogen. An overall trend of higher formate loss with higher acid stoichiometry is indicated, which matches previous results and the amount of formate loss is consistent with previous testing.

Table 3-11 SRAT Anion Conversions

Run ID & Acid Stoichiometry	SRAT Cycle		
	Formate Destruction	Nitrite to Nitrate Conversion	Nitrite Destruction
SB10-1 97%	36.6%	-7.9%	100%
SB10-2 150%	36.0%	-32.4%	100%
SB10-3 103%	42.5%	1.2%	100%
SB10-5 100%	24.9%	7.6%	100%
SB10-7 100%	13.4%	-5.3%	87.0%
SB10-8 150%	28.9%	-37.2%	100%
SB10-9 150%	26.3%	22.8%	100%

3.3.3.2 Mercury

The SRAT product samples were analyzed for mercury content to evaluate the stripping of mercury during the SRAT cycle. The current DWPF SRAT product target is 0.6 wt% (solids basis) mercury to meet process specifications. The mercury concentration in the six hour sample and in the SRAT product sample (12-hour of boiling) is summarized in Table 3-12 and Figure 3-4.

Table 3-12 SRAT Product Mercury Results

Run ID & Acid Stoichiometry	Calculated Initial Mercury (Wt % Total Solid Basis)	SRAT 6-hour Mercury (Wt % Total Solids Basis)	SRAT Product Mercury (Wt % Total Solids Basis)	SME Product Mercury (Wt % Total Solids Basis)
SB10-1 97%	1.05%	0.62%	0.45%	0.22%
SB10-2 150%	0.92%	0.60%	0.39%	0.01%
SB10-3 103%	1.09%	0.80%	0.65%	0.19%
SB10-5 150%	1.26%	0.86%	0.59%	0.18%
SB10-7 100%	1.38%	1.02%	0.89%	0.52%
SB10-8 150%	1.28%	0.01%	0.01%	0.00%
SB10-9 150%	1.03%	0.68%	0.27%	0.06%

3.3.3.3 SRAT Product Solids, Density, and pH

The solids, density and pH results are summarized in Table 3-13. The total solids target for the runs was 25 wt % so the measured solids is higher than targeted for all runs. The insoluble solids and pH results are lowest for run SB10-2 (highest coal-carbon, 150% acid stoichiometry) and the supernate density was highest. This demonstrates that more of the insoluble solids were dissolved in the high acid runs with coal-carbon. Nitric acid is a stronger acid (pKa -1.5) compared to formic acid (pKa 3.75). In addition, less nitric acid is consumed due to catalytic reactions so the resulting SRAT product pH is much lower for the runs with coal-carbon than without coal-carbon.

Table 3-13 SRAT Product Solids, Density, and pH Results

Run ID	Total Solids wt %	Insoluble Solids wt %	Soluble Solids wt %	Calcined Solids wt %	Slurry Density g/mL	Supernate Density g/mL	pH
SB10-1	27.87	15.69	12.19	17.29	1.165	1.1001	6.52
SB10-2	25.29	11.99	13.30	17.43	1.213	1.1159	3.85
SB10-3	26.98	15.25	11.74	18.70	1.214	Not Measured	6.87
SB10-5	27.18	15.57	11.61	17.48	1.207	Not Measured	7.47
SB10-7	27.63	16.79	10.85	16.94	1.232	1.0856	7.37
SB10-8	26.49	15.46	11.03	17.48	1.210	1.0865	7.91
SB10-9	26.82	13.31	13.51	16.63	1.221	Not Measured	4.61

3.3.3.4 SRAT Slurry and Filtrate Sample ICP-AES Results

The slurry elemental results from Inductively Coupled Plasma – Atomic Emission Spectroscopy (ICP-AES) analyses are summarized in Table 3-14, and the filtrate elemental results from ICP-AES analyses are summarized in Table 3-15. The solubility of each element was then calculated based on these results and summarized in Table 3-16. In runs SB10-2 and SB10-9, both high acid runs with coal-carbon, iron and nickel are moderately soluble compared to being insoluble in the rest of the experiments.

Table 3-14 SRAT ICP-AES Slurry Results, wt % Calcined Solids Basis

Element	SB10-1	SB10-2	SB10-3	SB10-5	SB10-7	SB10-8	SB10-9
Ag	<0.0100	<0.0100	NM	NM	<0.0100	<0.0100	NM
Al	4.94	4.82	5.51	6.28	6.98	6.96	5.81
Ba	0.24	0.23	0.23	0.22	0.21	0.22	0.20
Ca	2.79	2.84	2.15	2.08	2.64	2.64	2.03
Cd	<0.0100	<0.0100	<0.0100	<0.0100	<0.0100	<0.0100	<0.0100
Cr	0.16	0.17	0.14	0.14	0.16	0.17	0.12
Cu	0.06	0.05	NM	NM	0.06	<0.0100	NM
Fe	30.00	29.80	29.96	29.27	28.65	28.35	25.24
K	0.25	0.23	0.27	0.21	0.16	0.16	0.20
Mg	0.37	0.39	0.32	0.31	0.35	0.40	0.37
Mn	5.55	5.46	3.72	3.79	5.45	5.37	3.16
Na	12.75	12.60	13.78	14.46	13.25	13.30	16.52
Ni	0.80	0.83	0.72	0.71	0.76	0.84	0.61
P	<0.100	<0.100	<0.100	<0.100	<0.100	<0.100	<0.100
Pb	NM	NM	0.14	0.18	NM	NM	0.18
Pd	<0.100	<0.100	<0.100	<0.100	<0.100	<0.100	<0.100
Rh	0.02	0.02	0.09	0.09	0.02	0.02	0.07
Ru	<0.100	<0.100	<0.100	<0.100	<0.100	<0.100	<0.100
S	0.08	0.08	<0.100	<0.100	0.07	0.08	<0.100
Si	3.05	3.02	2.56	2.31	2.02	2.04	2.22
Sn	0.04	0.04	0.08	0.04	0.03	0.04	0.18
Ti	0.15	0.15	0.085	0.037	<0.0100	<0.0100	2.33
Zn	0.08	0.08	0.07	0.07	0.07	0.08	0.07
Zr	0.44	0.44	0.44	0.46	0.47	0.51	0.40

Note that the sum of the oxides was between 87.6 and 92.5 for all analyses. Typically this is between 95 and 105 so the samples may not have been completely digested. Note that the sum of the oxides for the SME products were all between 95 and 105.

Table 3-15 SRAT Product ICP-AES Filtrate Results, mg/L

Element	SB10-1	SB10-2	SB10-3	SB10-5	SB10-7	SB10-8	SB10-9
Ag	<0.010	<0.010	<0.100	<0.100	<0.010	<0.010	<0.100
Al	0.98	92.37	1.86	1.90	0.88	0.92	26.83
B	7.13	37.55	54.53	18.97	3.71	3.50	0.71
Ca	5,455	5,180	5,550	5,132	4,380	4,505	3,796
Cd	NM	NM	<0.010	<0.010	NM	NM	<0.010
Ce	2.38	403.55	NM	NM	0.28	1.73	NM
Cr	<0.010	0.55	0.26	<0.010	<0.010	<0.010	0.84
Cu	0.08	6.84	0.95	0.93	0.07	0.15	5.51
Fe	<0.010	5,160	<0.010	<0.010	<0.010	<0.010	674
K	975	826	1,142	973	848	811	852
La	0.17	205.20	NM	NM	<0.010	<0.010	NM
Li	3.54	3.87	NM	NM	2.36	2.48	NM
Mg	562	625	471	436	503	571	635
Mn	4,215	11,000	3,796	1,008	670	2,615	9,579
Mo	0.59	0.35	NM	NM	0.70	0.41	NM
Na	32,600	25,300	NM	NM	38,450	35,900	NM
Ni	0.42	675	0.26	<0.010	<0.010	<0.010	167
Pr	NM	NM	<1.00	<1.00	NM	NM	<1.00
Pb	NM	NM	<0.010	<0.010	NM	NM	<0.010
Pd	NM	NM	0.15	0.14	NM	NM	0.09
Pr	2.02	5.79	2.74	2.30	1.54	1.56	1.57
Rh	NM	NM	0.52	0.48	NM	NM	0.51
Ru	NM	NM	<0.010	<0.010	NM	NM	<0.010
S	19.67	23.62	24.83	35.37	41.04	30.94	263.1
Si	25.48	77.01	22.16	13.10	9.04	23.84	94.67
Sr	17.50	18.40	NM	NM	3.69	4.16	NM
Ti	<0.010	<0.010	<0.010	<0.010	<0.010	<0.010	<0.010
Zn	<0.010	15.34	<0.010	<0.010	<0.010	<0.010	7.40
Zr	<0.010	0.16	0.02	0.02	<0.010	<0.010	0.06

NM= Not Measured

Table 3-16 SRAT Product Percent of ICP-ES Elements Soluble

Element	SB10-1	SB10-2	SB10-3	SB10-5	SB10-7	SB10-8	SB10-9
Al	0.0%	1.0%	0.0%	0.0%	0.0%	0.0%	0.2%
B	1.3%	8.3%	10.6%	3.5%	0.7%	0.7%	0.2%
Ca	86.8%	94.6%	113.7%	101.2%	65.1%	71.2%	88.8%
Cr	LDL	0.2%	0.1%	LDL	LDL	LDL	0.3%
Cu	0.1%	7.0%	NM	NM	0.0%	LDL	NM
Fe	LDL	9.0%	LDL	LDL	LDL	LDL	1.3%
K	171.1%	190.1%	187.6%	189.9%	202.0%	211.2%	200.1%
La	NM	NM	0.0%	0.0%	LDL	LDL	0.0%
Li	NM	NM	0.0%	0.0%	NM	NM	0.0%
Mg	67.7%	83.9%	65.2%	57.6%	55.6%	59.4%	80.8%
Mn	33.7%	104.6%	45.0%	10.9%	4.8%	20.3%	143.7%
Mo	NM	NM	0.0%	0.0%	NM	NM	0.0%
Na	113.3%	104.2%	NM	NM	113.7%	112.3%	NM
Ni	0.0%	42.2%	0.0%	0.0%	LDL	LDL	12.9%
Pb	0.0%	0.0%	LDL	LDL	0.0%	0.0%	LDL
Rh	0.0%	0.0%	0.8%	0.8%	0.0%	0.0%	1.1%
S	11.2%	15.3%	16.8%	24.7%	23.0%	16.7%	68.8%
Si	0.4%	1.3%	0.4%	0.2%	0.2%	0.5%	2.0%
Sn	0.0%	0.0%	0.0%	0.0%	0.0%	0.0%	0.0%
Sr	NM	NM	0.0%	0.0%	NM	NM	0.0%
Zn	LDL	10.3%	LDL	LDL	LDL	LDL	5.1%
Zr	LDL	0.0%	0.0%	0.0%	LDL	LDL	0.0%

LDL = Below Lower Detection Limit
NM = Not Measured

3.3.4 *SRAT Cycle Offgas Composition Results*

A typical offgas concentration profile is shown in Figure 3-5, while charts from all runs are shown in Appendix C. Helium and nitrogen show reduced concentrations during periods with large quantities of offgas generation due to dilution, while oxygen showed reduced concentrations during these periods due to dilution and from consumption. In general, hydrogen generation began after nitrous oxide emissions had ceased and carbon dioxide emission was noted in conjunction with the hydrogen. The patterns of offgas emissions noted during the runs were typical of offgas generation during the SRAT cycle.

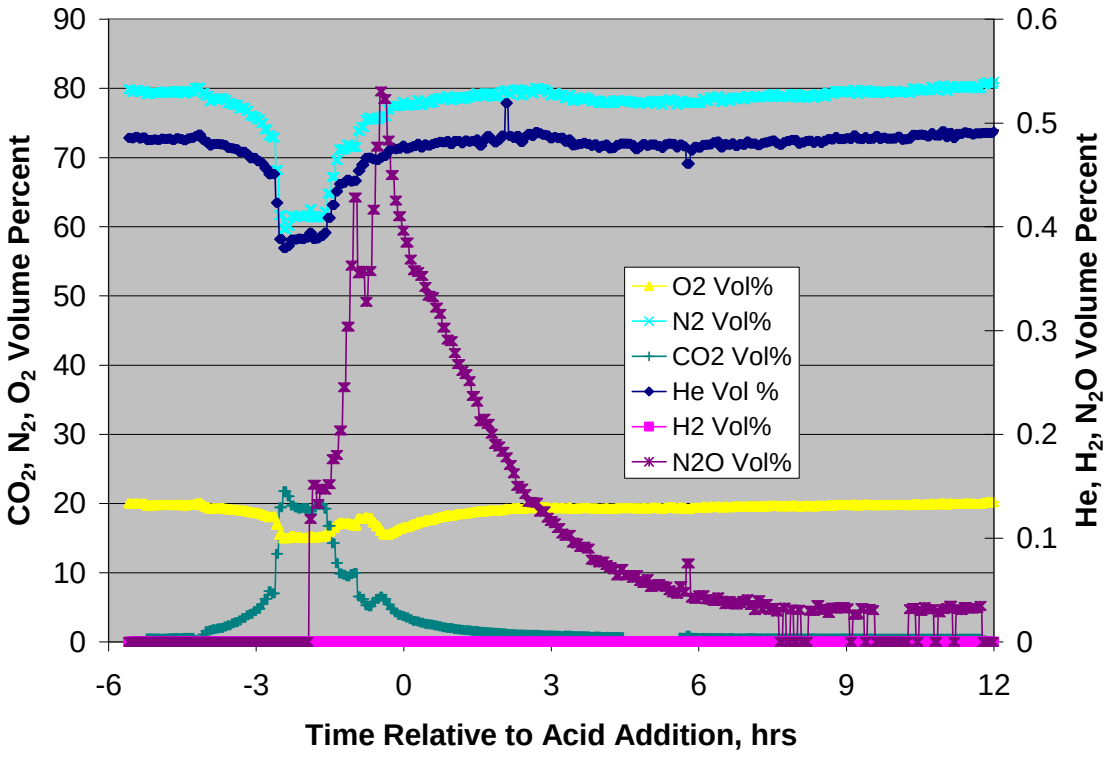

Figure 3-4. Typical SRAT Offgas Profile 100% Acid Stoichiometry, no coal

3.3.4.1 SRAT Cycle Hydrogen Evolution

The peak hydrogen concentration for each run is shown in Figure 3-6. In general, the peak hydrogen generation rate increased with increased acid addition. Also, in runs with SB10-B sludge, very little hydrogen was formed. In the SB10-8 run with SB10-A simulant (no FBSR coal) at 150% acid stoichiometry, the hydrogen generation exceeded the DWPF SRAT processing limits of 0.65 lb/hr, which shows the peak hydrogen generation after scaling to the DWPF process. It should be noted that the noble metal concentrations for these runs was conservative (SB6 levels of noble metals were used). Processing with the SB10-B simulant significantly decreased the hydrogen generation due to the low formic acid addition amounts resulting from REDOX adjustment with nitric acid due to the presence of coal. Results are shown in Table 3-17.

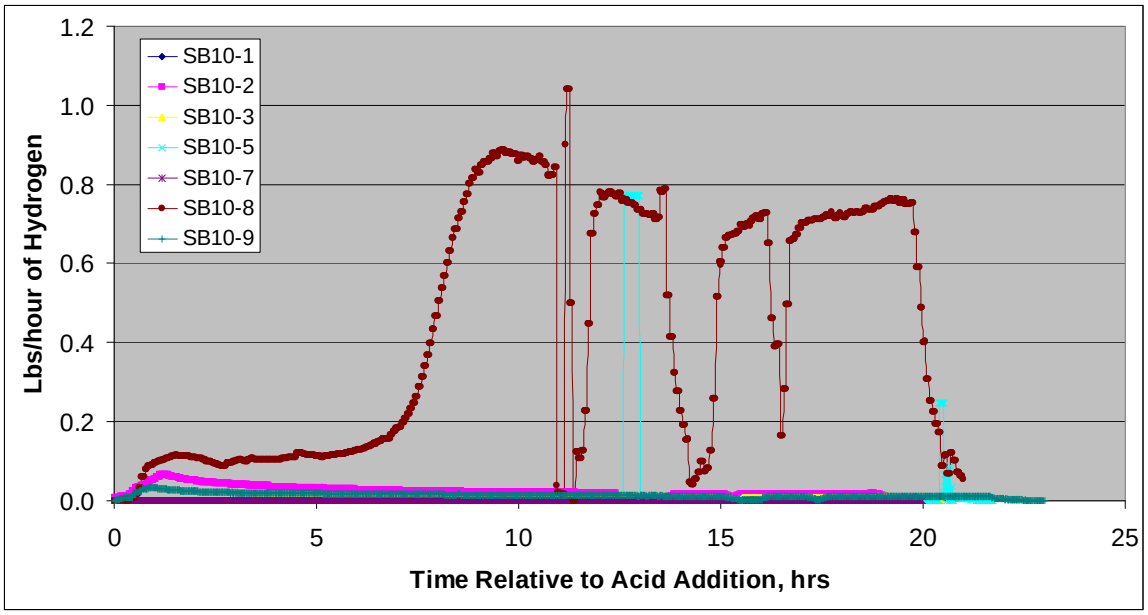

Figure 3-5. SRAT Cycle Hydrogen Peaks

Table 3-17 SRAT Cycle Hydrogen Peak Generation Rate

Run ID	Sludge Composition	Slurry Predicted Coal, mg/kg	Acid Stoichiometry	Hydrogen (lb/hr)
SB10-1	0.00% A, 100% B	19,800	97%	0.01
SB10-2	0.00% A, 100% B	18,500	150%	0.07
SB10-3	32.0% A, 68.0% B	12,900	103%	0.01
SB10-5	66.3% A, 33.7% B	5,870	100%	0.00
SB10-7	100% A, 0.00% B	0	100%	0.00
SB10-8	100% A, 0.00% B	0	150%	1.04
SB10-9	32.0% A, 68.0% B	10,000	150%	0.03

3.3.4.2 SRAT Cycle Other Offgas Species

The nitrous oxide peak concentrations slightly increased as acid addition was increased. The carbon dioxide peak was very similar for all runs. The peak generation of these species is less dependent on acid concentration than hydrogen since more acid is added than needed to destroy carbonate and nitrite, the compounds that are responsible for the highest emissions. The peak generation rates are shown in Table 3-18 after scaling to the DWPF process scale.

Table 3-18 SRAT Cycle Nitrous Oxide and Carbon Dioxide Peak Generation Rates

Run ID	Sludge Composition	Slurry Predicted Coal-carbon, mg/kg	Acid Stoichiometry	CO_2 Peak (lb/hr)	N_2O Peak (lb/hr)
SB10-1	0.00% A, 100% B	19,800	97%	323	6.95
SB10-2	0.00% A, 100% B	18,500	150%	500	13.14
SB10-3	32.0% A, 68.0% B	12,900	103%	422	10.50
SB10-5	66.3% A, 33.7% B	5,870	100%	438	7.19
SB10-7	100% A, 0.00% B	0	100%	533	10.56
SB10-8	100% A, 0.00% B	0	150%	459	47.79
SB10-9	32.0% A, 68.0% B	10,000	150%	233	19.23

The volumes of both carbon dioxide and nitrous oxide generated were smaller in runs with coal (SB10-1, SB10-2) compared to runs without coal (SB10-7, SB10-8), Figure 3-7. Since the sodium carbonate concentration in runs with coal was 1.5X the runs without coal, this was unexpected. It was expected that more CO_2 would be produced during runs with the coal but that did not happen. More CO_2 production would increase the potential for foam during acid addition.

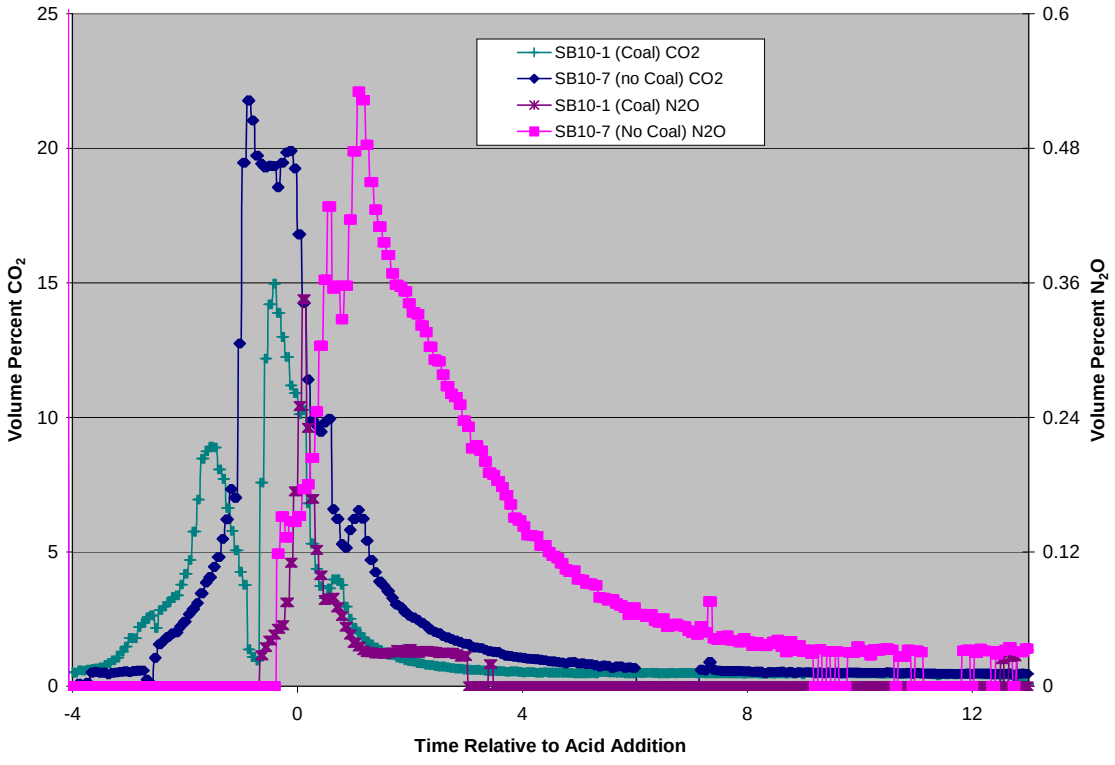

Figure 3-6. Carbon Dioxide and Nitrous Oxide Concentration in Runs SB10-2 and SB10-8 SRAT Cycle

3.3.5 *SRAT Product Rheological Properties*

The rheological properties of SRAT products were measured for the four runs produced with the simulant (SB10-A). The rheological properties were outside the design basis limits for yield stress or consistency for SRAT products (yield stress 1.5 to 5 Pa and Consistency 5 to 12 cP) except for the low acid, high coal run (SB10-1) and the high acid, no coal run (SB10-8) which was within the limits for yield stress and consistency. The yield stress and consistency of the SRAT products are shown in Table 3-19. Note that the high acid runs with coal had very low yield stress values so could have been further concentrated.

Table 3-19 SRAT Product Rheological Properties

Run ID	Acid %	Yield Stress, Pa	Consistency, cP	Total Solids, wt %	Insoluble Solids, wt %
SB10-1	97	2.60	10.22	27.87	15.69
SB10-2	150	0.34	5.21	25.29	11.99
SB10-3	103	8.65	3.47	26.98	15.25
SB10-5	100	7.89	33.42	27.18	15.57
SB10-7	100	10.52	25.16	27.63	16.79
SB10-8	150	1.59	8.48	26.49	15.46
SB10-9	150	0.56	5.85	26.82	13.31

3.4 SME Cycle Results

The seven SME cycles were performed immediately following the SRAT cycle and utilized the estimated amount of frit based on the initial sludge additions and the expected amount of SRAT samples. The SME cycles did not include the addition of water simulating decon water additions but all included two frit slurry additions. As stated earlier, the SME cycle targeted a final solids concentration of 50 wt % total solids.[18]

3.4.1 *SME Cycle Processing Observations*

Only hydrogen generation was noted as a potential processing issue during the SME cycle. The hydrogen generation in the highest acid run with the SB10-A simulant (no coal) exceeded the DWPF hydrogen limit during the final dewater at the completion of the SME cycle. Mixing was not an issue during processing. Mixer speed was maintained at 250 RPM throughout each run.

As shown in Figure 3-8, the pH profile of each SME cycle followed a similar profile with a dip in pH as the frit is added due to the formic acid content of the frit slurry followed by a gradual rise in pH as the slurry mix is concentrated.

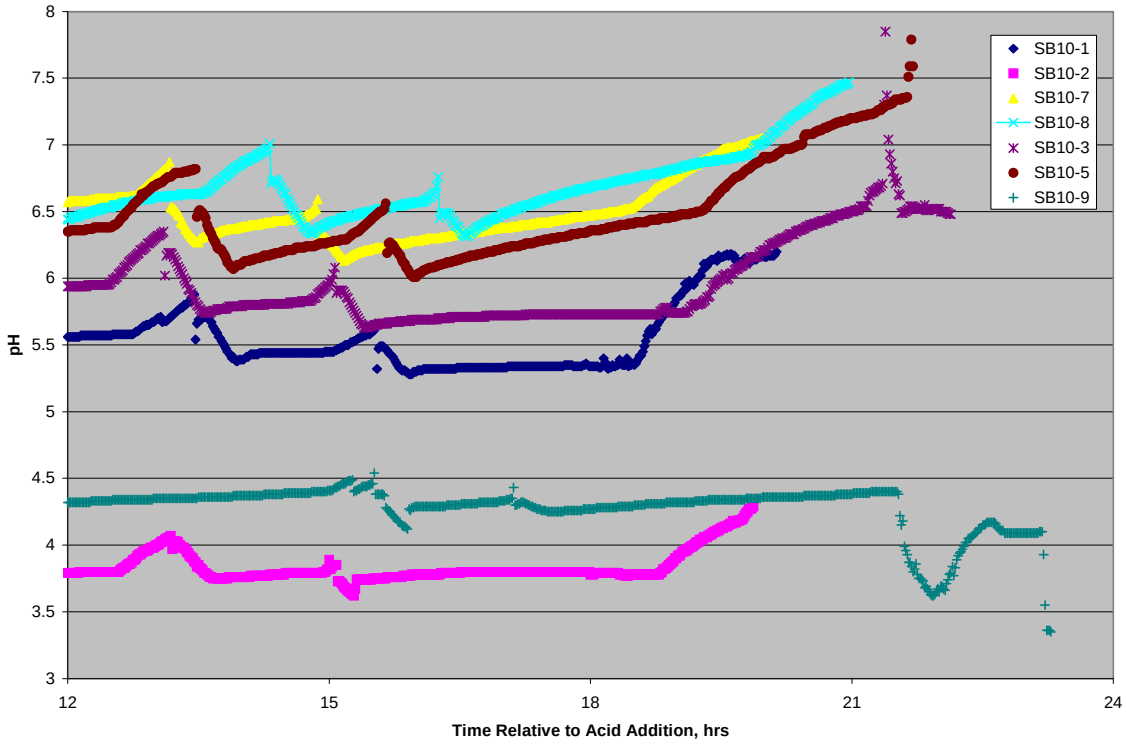

Figure 3-7. SME pH Profile

3.4.2 *SME Cycle Sample Results*

Samples were pulled at the conclusion of the SME cycle and analyzed for total solids, anions, soluble elemental species, and mercury. Samples were also taken of the composite SME dewater and the FAVC contents at the completion of the SME cycle.

3.4.2.1 SME Cycle Waste Loading

The lithium oxide content of the SME products is shown in Table 3-20 along with the calculated waste loading. The solids contents generally were higher than targeted, and the waste loading targets were slightly higher than the 38% target. Waste loadings were calculated from the PSAL analyzed lithium content of the SME product (the frit 418 was 7.42% Li). The waste loadings were within 2% of the planned targets.

Table 3-20 SME Product Lithium Oxide Concentration and Waste Loading Results

Run	Lithium Oxide Content (wt % Calcined solids)	Waste Loading, Wt %
SB10-1	4.55	38.7
SB10-2	4.52	37.5
SB10-3	4.60	38.0
SB10-5	4.51	39.2
SB10-7	4.46	39.8
SB10-8	4.53	38.9
SB10-9	4.54	38.8

3.4.2.2 SME Cycle Anion Concentrations and Anion Conversion Results

The SME products anion results are shown in Table 3-21. Loss of formate varied during the SME cycles, as shown in Table 3-22. The range of values noted during the testing is similar to results from previous runs.

Table 3-21 SME Product Anion Results, mg/kg slurry

Run ID & Acid Stoichiometry	F	Cl	NO_2	NO_3	SO_4	PO_4	HCO_2	$C_2O_4^{2-}$
SB10-1 97%	<100	348	<100	78,650	<100	<100	13,100	<100
SB10-2 150%	<100	307	<100	76,300	<100	<100	24,850	<100
SB10-3 103%	<100	389	<100	67,900	<100	<100	22,800	<100
SB10-5 100%	<100	298	<100	41,650	<100	<100	40,100	<100
SB10-7 100%	<100	276	<100	20,600	<100	<100	55,350	<100
SB10-8 100%	<100	286	<100	17,850	<100	<100	52,400	<100
SB10-9 150%	<100	320	<100	61,950	<100	<100	36,200	<100

Table 3-22 SME Product Anion Conversions (%)

Run ID	Formate Destruction		Nitrate Destruction	
	Planned	Actual	Planned	Actual
SB10-1	5	21.0	5	-3.8
SB10-2	5	24.9	5	5.6
SB10-3	5	2.2	5	0.9
SB10-5	5	8.5	5	6.6
SB10-7	5	19.7	5	7.2
SB10-8	5	30.9	5	14.3
SB10-9	5	24.5	5	11.3

3.4.2.3 SME Cycle Carbon Sample Results

The measurement of the carbon content of the SME product is the key to predicting the glass REDOX. REDOX is important since a melter feed with an oxidizing REDOX melts slower and a melter feed with a reducing REDOX may shorten melter life as the reduction of Ni, Cu and noble metals to their elemental state have the potential to short the melter. Of key importance in this analysis is the determination of the nitrite, nitrate, formate, oxalate, and coal-carbon concentration of the SME product. The SME product anions were summarized in Table 3-21.

No reliable carbon data was available for the starting sludge with coal (SB10-B), SRAT products or SME products. As a result of this, coal-carbon estimates were used in all calculations throughout this report based on the coal-carbon measurement of the PDT sample. No estimates can be made of any possible decomposition of the coal during SRAT and SME processing. It is recommended that a coal-carbon method be developed for sludge, SRAT products and SME products.

Estimates of the carbon concentration were performed using two different methods. The first method used an AD carbon analyzer to measure the CO_2 produced when heating the sample to 900°C (total carbon or TC) and to add acid to the sample to measure the CO_2 evolved from the carbonate present (TIC). The TOC is calculated by subtracting TIC from TC. The TOC value includes all organic forms of carbon including oxalate and formate. To determine the coal-carbon concentration, the carbon in the oxalate and formate must be subtracted from the TOC. The second method was a thermal method to determine the coal-carbon concentration. This method dries the sample at 110 °C ° for > 2 hours. Approximately 5 g of dried solids are added to 500 ml of water. The slurry is filtered to remove soluble carbonate, formate and oxalate from the dried solids. Lastly, the solids are put in a 525 °C ° furnace for two days to oxidize the coal-carbon to CO_2. The coal-carbon concentration is estimated by measuring the mass loss at 525 °C.

The AD method is specific for carbon since it measures CO_2. The Ion Chromatography (IC) anion analysis is another technique specific for the other forms of organic carbon (formate, oxalate) that are present in the SME products. Thus the coal-carbon estimate is expected to be an accurate measurement. However, the thermal method is not specific for coal-carbon. A number of other reactions can occur including anion decomposition and loss of waters of hydration so this method may overestimate the coal-carbon concentration. For example, the two sludges were each analyzed by this method. The mass loss of the SB10-B sludge simulant was 15.21 % and the mass loss of the SB10-A sludge simulant (no coal) had a mass loss of 10.61 %.

Due to analytical difficulties, no reliable carbon data was available at the time this report was issued. As a result of this, coal-carbon estimates were used in all calculations throughout this report based on the coal-carbon measurement of the PDT sample.

3.4.2.4 SME Sample Solids, Density and pH Results

The SME Product solids, density and pH results are summarized in Table 3-23. The experiments with the highest pH were the two experiments without coal. The general trend in these experiments is that the more nitric acid added (less formic acid), the lower the final pH.

Table 3-23 SME Product Slurry Solids, Density and pH

Run ID	Total Solids wt %	Insoluble Solids wt %	Calcined Solids wt %	Supernate Solids wt %	Soluble Solids wt %	Density g/mL	pH
SB10-1	52.56	40.50	42.28	20.27	12.06%	1.480	6.38
SB10-2	50.53	37.44	40.09	20.93	13.10%	1.435	4.44
SB10-3	54.39	42.06	44.76	21.28	12.33%	1.510	6.68
SB10-5	53.85	41.66	45.74	20.89	12.19%	1.504	7.33
SB10-7	53.33	42.73	45.56	18.50	10.59%	1.495	7.68
SB10-8	54.34	45.03	46.62	16.93	9.30%	1.508	8.19
SB10-9	53.50	40.75	42.83	21.53	12.76%	1.466	5.42

3.4.2.5 SME Slurry and Filtrate Sample ICP-AES Results and Calculated Percent Soluble

The slurry elemental results from ICP-AES analyses are summarized in Table 3-24, the filtrate elemental results from ICP-AES analyses are summarized in Table 3-25, and the fraction of each element that is soluble is summarized in Table 3-26. In runs SB10-2 and SB10-9, both high acid runs with coal, iron and nickel are moderately soluble compared to being insoluble in the rest of the experiments. Note that the fraction of elements that are soluble decreased during the SME cycle. For example, the iron solubility dropped from 9.0 % in the SB10-2 post SRAT sample to 1.33 % in the SB10-2 post SME sample.

Table 3-24 SME ICP-AES Slurry Results, wt % Calcined Solids Basis

Element	SB10-1	SB10-2	SB10-3	SB10-5	SB10-7	SB10-8	SB10-9
Al	2.15	2.11	2.44	2.72	3.04	3.03	2.62
B	1.35	1.37	1.35	1.32	1.32	1.32	1.32
Ba	0.105	0.103	0.100	0.100	0.101	0.098	0.091
Ca	1.20	1.17	1.14	1.11	1.07	1.09	1.01
Cr	0.0682	0.0713	0.0694	0.0707	0.0750	0.0733	0.0644
Fe	12.7	12.5	12.1	12.1	12.4	12.1	10.7
K	0.168	0.165	0.170	0.121	0.105	0.122	0.128
Li	2.12	2.13	2.14	2.10	2.08	2.11	2.11
Mg	0.169	0.165	0.160	0.163	0.164	0.158	0.194
Mn	1.96	1.99	1.88	1.92	1.97	1.88	1.74
Na	8.87	8.78	8.91	9.09	9.22	8.91	9.72
Ni	0.324	0.326	0.348	0.342	0.353	0.363	0.294
Pb	0.164	0.162	0.157	0.162	0.168	0.158	0.140
S	0.0309	0.0280	0.0266	0.0263	0.0226	0.0318	0.0643
Si	24.18	24.09	24.00	23.87	23.48	23.62	23.76
Ti	0.102	0.100	0.076	0.058	0.036	0.041	1.183
Zn	0.0347	0.0317	0.0298	0.0290	0.0299	0.0301	0.0320
Zr	0.299	0.294	0.285	0.295	0.285	0.285	0.268

Table 3-25 SME Product ICP-AES Filtrate Results, mg/L

Element	SB10-1	SB10-2	SB10-3	SB10-4	SB10-5	SB10-6	SB10-7
Ag	<0.100	<0.100	<0.100	<0.100	<0.100	<0.100	<0.100
Al	<1.00	3.87	<1.00	<1.00	<1.00	<1.00	7.82
B	10.7	76.7	9.5	5.5	13.6	5.4	66.4
Ba	65.9	112.1	44.8	15.3	8.5	8.9	0.9
Ca	8220	7935	8265	6850	6675	3770	5250
Cd	<0.100	<0.100	<0.100	<0.100	<0.100	<0.100	<0.100
Cr	<1.00	<1.00	<1.00	<1.00	<1.00	<1.00	<1.00
Fe	<1.00	1170	<1.00	<1.00	<1.00	<1.00	2.72
K	1155	984	1275	1015	936	995	974
Li	251	256	296	300	344	259	290
Mg	781	866	827	676	720	393	985
Mn	6810	11350	6105	2500	1675	202	7520
Na	47700	40700	51150	53850	57100	57850	57450
Ni	<1.00	536.35	<1.00	<1.00	<1.00	<1.00	179.82
P	<10.0	<10.0	<10.0	<10.0	<10.0	<10.0	<10.0
Pb	<1.00	3.37	<1.00	<1.00	<1.00	<1.00	<1.00
Pd	<1.00	<1.00	<1.00	<1.00	<1.00	<1.00	<1.00
Pr	<0.100	<0.100	<0.100	<0.100	<0.100	<0.100	<0.100
Rh	<1.00	<1.00	<1.00	<1.00	<1.00	3.31	<1.00
Ru	<1.00	<1.00	<1.00	<1.00	<1.00	11.44	<1.00
S	33.16	33.01	40.73	53.18	66.07	54.15	547.95
Si	83.85	87.29	43.21	34.61	21.06	54.41	120.58
Ti	<0.100	<0.100	<0.100	<0.100	<0.100	<0.100	<0.100
Zn	<0.100	7.18	<0.100	<0.100	<0.100	<0.100	3.66
Zr	<0.100	<0.100	<0.100	<0.100	<0.100	<0.100	<0.100

Table 3-26 SME Product Percent of ICP-AES Elements Soluble

Element	SB10-1	SB10-2	SB10-3	SB10-5	SB10-7	SB10-8	SB10-9
Al	LDL	0.03%	LDL	LDL	LDL	LDL	0.03%
B	0.10%	0.79%	0.08%	0.05%	0.11%	0.04%	0.63%
Ba	8.05%	15.5%	5.03%	1.73%	0.97%	0.95%	0.11%
Ca	87.5%	96.3%	81.0%	67.9%	66.8%	36.5%	61.8%
Fe	LDL	1.33%	LDL	LDL	LDL	LDL	0.00%
K	88.3%	84.7%	89.6%	71.4%	62.9%	88.3%	117%
Li	1.51%	1.71%	1.65%	1.64%	1.84%	1.33%	1.76%
Mg	59.2%	74.5%	57.7%	47.5%	51.3%	25.9%	75.5%
Mn	44.5%	81.0%	36.7%	14.6%	10.2%	1.13%	48.1%
Na	68.8%	65.8%	67.8%	71.1%	73.2%	68.2%	78.4%
Ni	LDL	23.37%	LDL	LDL	LDL	LDL	6.47%
P	LDL	LDL	LDL	LDL	LDL	LDL	LDL
Pb	LDL	0.30%	LDL	LDL	LDL	LDL	LDL
S	13.8%	16.8%	15.6%	22.1%	28.4%	22.1%	311%^
Si	0.04%	0.05%	0.02%	0.02%	0.01%	0.02%	0.06%
Ti	LDL	LDL	LDL	LDL	LDL	LDL	LDL
Zn	LDL	3.24%	LDL	LDL	LDL	LDL	1.54%

LDL = Below Lower Detection Limit
^Supernate S was approximately 3x higher than slurry S or Slurry S from SO_4.

3.4.2.6 SME Slurry Rheological Results

The rheological properties of each SME product were measured. Higher acid stoichiometry lowered the yield stress and consistency of the SME products. Most of the runs were outside the design basis limits for yield stress (2.5 to 15 Pa) and consistency (10 to 40 cP)[19] as shown in Table 3-27. Note that all samples were higher than the 50 wt % total solids target which contributed to the high yield stress values. The high acid runs with coal (SB10-2 and SB10-9) had the lowest (and acceptable) yield stress values. The products with added coal had higher yield stress values, but also had slightly higher total solids measurements.

Table 3-27 SME Product Rheological Properties

Run ID	Acid %	Yield Stress, Pa	Consistency, cP	Total Solids, wt %	Insoluble Solids, wt %
SB10-1	97	23.1	34.4	52.56	40.50
SB10-2	150	4.43	30.9	50.53	37.44
SB10-3	103	44.0	28.1	54.39	42.06
SB10-5	100	34.0	87.0	53.85	41.66
SB10-7	100	29.5	51.6	53.33	42.73
SB10-8	150	25.8	40.7	54.34	45.03
SB10-9	150	7.44	40.5	53.50	40.75

3.4.3 *SME Cycle Offgas Composition Results*

The offgas stream was analyzed for nitrogen, oxygen, hydrogen, helium, nitrous oxide, carbon dioxide using a gas chromatograph. The amount of offgas generated during the runs generally increased as acid stoichiometry increased, as indicated by the helium concentration in the offgas since helium is added at a constant 0.5 wt% of the incoming air purge. A typical offgas concentration profile is shown in Figure 3-9. The patterns of offgas emissions noted during the runs were typical of offgas generation during the SME cycle with hydrogen and carbon dioxide emissions occurring during dewatering after each frit slurry (with formic) addition.

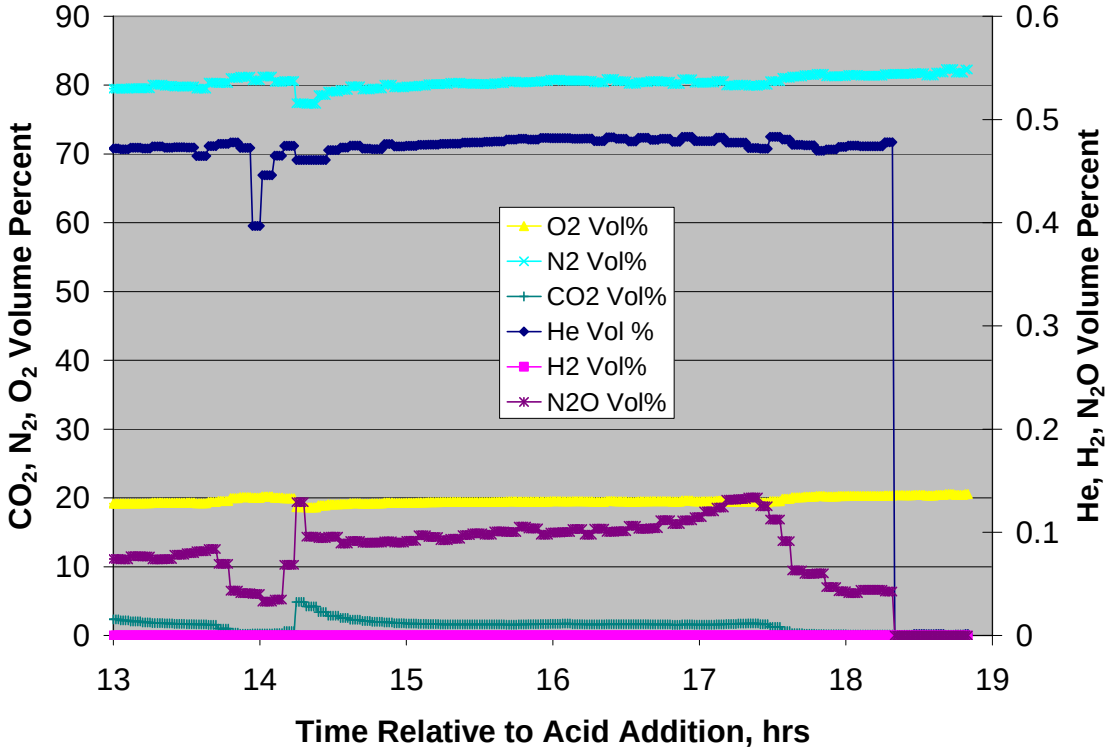

Figure 3-8. Typical SME Offgas Profile 100% Acid Stoichiometry

3.4.3.1 Hydrogen Evolution

The peak hydrogen generation rates were generally noted as sharp spikes in the data immediately following the start of dewater, as shown in Figure 3-9. Peak generation rates scaled to the DWPF process are shown in Table 3-28 and were all below the SME process limit of 0.223 lb/hr, except for the SB10-A (no coal) sludge at 150% stoichiometry run (run SB10-8). This run exceeded the SME limit by 3.5X.

Table 3-28 SME Cycle Hydrogen Peak Generation Rate

Run ID	Sludge Predicted Coal-carbon, mg/kg	% Acid Stoichiometry	Hydrogen (lb/hr)
SB10-1	19,800	97	0.0197
SB10-2	18,500	150	0.0215
SB10-3	12,900	103	0.0110
SB10-5	5,870	100	0.0010
SB10-7	0	100	0.0010
SB10-8	0	150	0.7915
SB10-9	10,000	150	0.0115

3.4.3.2 Other Species

Carbon dioxide, as shown in Table 3-29, was generally the only other gas of any significance emitted during the SME cycle (the lower acid runs contained a small amount of nitrous oxide emissions).

Table 3-29 SME Cycle Nitrous Oxide and Carbon Dioxide Peak Generation Rates, lb/hr

Run ID	Sludge Predicted Coal-carbon, mg/kg	% Acid Stoichiometry	CO_2 Peak (lb/hr)	N_2O Peak (lb/hr)
SB10-1	19,800	97	29.6	1.37
SB10-2	18,500	150	30.3	2.17
SB10-3	12,900	103	37.2	2.71
SB10-5	5,870	100	118.5	0.23
SB10-7	0	100	28.6	0.80
SB10-8	0	150	128.5	0.36
SB10-9	10,000	150	0.0	0.68

3.5 Glass Results

Glass was produced from the SME products to allow the measurement of REDOX. In addition, the glass was sectioned and visually observed to look for crystals and reduced metals. Note that Frit 418 was used and no attempt was made to optimize the glass formulation. The glass shop noted that the glass was very hard compared to other glasses they have been sectioning.

3.5.1 *Glass REDOX Results*

The SME products were dried and melted using the REDOX Measurement Procedure.[20] This method can produce overly oxidizing results (REDOX of 0) if the sample is overdried or the crucible seal is inadequate during melting. For example the two replicates might have a REDOX of 0.25 and 0.28, while the third result is 0.00. The procedure utilizes a nepheline gel seal which can be lost if excessive offgas is produced during melting (a problem with high acid stoichiometry runs, SB10-2, SB10-8, and SB10-9). In runs where the seal was obviously

inadequate, no measure of the REDOX was performed. The measured and predicted REDOX results are summarized in Table 3-30. Note that the maximum REDOX result is reported as this might be the best REDOX measurement as problems with the seal during melting might lead to overly oxidized results.

Most of the REDOX results ($Fe^{2+}/\Sigma Fe$) were within 0.1 of the predicted values. However, some of the values were higher than predicted and some were lower than predicted. A concern in using coal-carbon as a reductant is that the coal-carbon is such a good reductant that it can be difficult to control. It is similar to a pH titration curve where a small amount of acid near pH 7 can make a big change in pH. Based on the results of this study, the REDOX can likely be controlled in processing sludge with added coal-carbon.

Table 3-30 SME Product REDOX Results, $Fe^{2+}/\Sigma Fe$

Run ID	Average Measured $Fe^{2+}/\Sigma Fe$	Standard Deviation	% Relative Standard Deviation	Maximum $Fe^{2+}/\Sigma Fe$	Predicted $Fe^{2+}/\Sigma Fe$
SB10-1	0.300	0.082	27.4	0.373	0.310
SB10-2	0.208	0.049	23.5	0.268	0.318
SB10-3	0.225*	0.117	52.0	0.328	0.124
SB10-5	0.235	0.147	62.4	0.352	0.178
SB10-7	0.237	0.039	16.4	0.288	0.225
SB10-8	0.218#	0.002	0.9	0.219	0.251
SB10-9	0.332#	0.002	0.5	0.333	0.113

* Average of two glasses, not three as one was overly oxidized.
# Only one glass was analyzed as the seal was lost during melting for the other two glasses.

3.5.2 *SME Product MAR Assessment of Sectioned Glass Samples*

A Measurement Acceptability Region (MAR) assessment approach for glass systems was developed by Peeler and Edwards to facilitate formulation of waste glasses for DWPF[21]. The MAR approach allows for efficient evaluation of glass compositions against the Product Composition Control System (PCCS) constraints developed for DWPF[22] for various glass quality and processing properties. A MAR assessment was conducted for the compositions of the seven experiments in this study. The MAR assessment concluded that all of the MAR criteria were met for all seven experiments.

3.6 DWPF Melter Processing Review

A review was completed by SRNL concerning the processing of a melter feed containing the Tank 48 FBSR product in the DWPF melter. From a glass formulation and melter processing perspective, the introduction of the FSBR product into the DWPF flowsheet does require a review of the possible impacts to current operations. Jantzen[23] indicates that the current flowsheet for Tank 48 FBSR processing produces a sodium carbonate based granular product that is 85-90 wt% soluble in water. The remaining 10-15 wt% are insolubles composed of (1) insoluble carbonates and sulfates such as $PbCO_3$ and $BaSO_4$, (2) alumina/bauxite bed material, (3) coal used to generate heat for autothermal processing, and (4) aluminosilicate containing coal ash and sodium aluminosilicates. From a glass formulation and melter processing perspective, the introduction of

the FSBR product into the DWPF flowsheet does require a review of the possible impacts to current operations. Potential impacts or technical areas to assess include (but are not limited to):

(a) redox control primarily associated with the introduction of coal-carbon into the melter which, if not accounted for, could led to precipitation of metallic species within the melter or (if over compensated for) foaming within the melter,
(b) flammability concerns within the melter plenum again primarily due to the presence of coal-carbon in the incoming melter feed,
(c) the possibility of localized reduction within the glass pool from coal and the impact of precipitated phases (such as nickel sulfides on melter operation or materials of corrosion),
(d) the ability of frit development efforts to compensate for the FBSR secondary stream with respect to melter processing (e.g., viscosity, ability to attain waste loading requirements, melt rate, cold cap behavior, etc) and product performance (durability) constraints.

The potential impacts on the FBSR product on REDOX control (via modifications or changes to the acid addition strategy to ensure REDOX of the melter feed is maintained within acceptable limits) and melter flammability (through off-gas flammability calculations) are addressed in Section 3.7 of this report.

With respect to the ability of frit development efforts to accommodate the FBSR product, the current flowsheet has the FBSR product being added to Tank 51 followed by a washing strategy that ultimately establishes the same Na concentration (endpoint) as a flowsheet without the FBSR product. If this is the case, then the impact of Na_2O from the FBSR product on glass formulation is not anticipated to be an issue.

The remaining issues that have been identified thus far are the potential impacts of the FSBR product on melt rate (for example, will the aluminate based products dissolve easily into the melt) and the potential for localized REDOX reductions assuming coal-carbon accumulation in the cold cap or within the glass pool. Given DWPF contractual agreements for canister production rates, the impact of the FBSR product on melt rate should be experimentally assessed. Historically, melt rate impacts have utilized a simulant SRAT product coupled with a candidate frit composition (targeting the anticipated waste loading). It is recommended that a slurry-fed, joule heated melter be utilized to assess the impact of the FBSR product on melt rate given the form of the FBSR product and potential processing impacts. A baseline flowsheet (specific sludge batch – frit system without the FBSR product) could be compared to the FBSR-based flowsheet (including acid additions strategy modifications to control REDOX) with respect to melt rate and other melter processing issues. Based on potential issues of localized reduction due to the presence of coal, one should consider the possible use of a melter platform that could allow for in-situ sampling or post-mortem (destructive) analysis to assess the potential for localized reduction, the formation of metallic precipitates, and/or possible interactions of reduced species (such as nickel sulfides) on materials of construction. To minimize programmatic risks, preliminary testing using small scale testing (crucibles and/or smaller melters) should be considered when technically feasible to address this latter issue.

3.7 DWPF Melter Off-Gas Flammability Assessment

Melter off-gas flammability is determined largely by: (1) total organic carbon (TOC) in the feed, (2) feed rate, (3) air purges for combustion and cooling, (4) melter vapor space temperature, and (5) off-gas surge. In essence, all these variables are controlled either by the choice of flowsheet or by the mode of operation, and their impact on off-gas flammability is highly interdependent. For example, when TOC is increased at fixed air flows, the melter vapor space temperature would have to be increased in order to burn excess carbon. The melter vapor space temperature can be increased by reducing the feed rate, thereby exposing a greater area of melt surface for increased radiation shine into the vapor space. Reduced feed rate in turn not only reduces the rate of TOC fed to the melter but decreases the likelihood of off-gas surging as well. It is also to be noted that the degree of variability in TOC without counterbalancing changes in nitrate is limited since a proper balance between the reductant (carbon) and oxidant (nitrate) is required to ensure that the redox ($Fe^{+2}/\Sigma Fe$) of the resulting glass remains within the acceptable range of 0.09-0.33.

Two computer models have been used to describe these complex interdependencies quantitatively and further set the operating limits of these variables in the form of feed interlocks and technical safety requirements (TSR).[24,25] The first model, called the 4-stage cold cap model, describes the chemistry of cold cap reactions thermodynamically and predicts the compositions of both glass and calcine gases from a given feed chemistry. The composition of calcine gases thus calculated is used as the input to the second model, called the off-gas dynamics model, which predicts the transient behavior of the DWPF melter off-gas system, including the off-gas flammability, under various upset scenarios. The baseline upset scenario used in the off-gas flammability assessment for bubbled melter operation is the 9X/5X off-gas surge, which is defined later in this section.

The following theoretical limits have been established for SB6 in order to ensure full compliance with the off-gas flammability safety bases for both normal and seismic melter operations:[26]

- TOC ≤18,900 ppm (SME product).
- Melter Feed rate ≤1.5 GPM
- Total melter air purge (FIC3221A) ≥ 900 lb/hr (nominally at 1,070 lb/hr)
- Backup film cooler air purge (FIC3221B) ≥233 lb/hr (nominally at 340 lb/hr)
- Melter vapor space temperature (TI4085D) ≥ 460 °C.

It is noted that the actual TSR and feed interlock limits used in the field are set by applying appropriate analytical or instrument uncertainties to these theoretical limits.

Of those variables affecting off-gas flammability listed above, the focus of this assessment is on TOC, particularly the maximum amount of coal-carbon that can be fed to the DWPF melter without exceeding the off-gas flammability safety basis limits. Specifically, the potential for off-gas flammability for all seven SB10 feed formulations that were tested during the bench-scale CPC demonstration was assessed in this study. In addition, if the calculated off-gas flammability for any of the feeds was below the safety basis limit of 60 % of the lower flammability limit (LFL) for normal operation, additional coal was added to each “baseline” feed until the safety basis limit was reached. It is to be noted that coal-carbon was added without any redox considerations, i.e., without the addition of counterbalancing nitrate for redox control. These hypothetical feeds containing extra coal-carbon are termed the “max-coal” feeds in this study.

3.7.1 *Flammability Assessment of Baseline Feeds*

3.7.1.1 Cold Cap Model Input

The input to the cold cap model was constructed by blending the SRAT products with Frit 418 at specified waste loadings to simulate the melter feed compositions. This required reconciling the SRAT product analytical data given in Table 3-10 to Table 3-16 until electroneutrality was achieved in the resulting slurries. Since the anion data particularly the formate has a direct impact on TOC and off-gas flammability, any charge imbalances were reconciled by adjusting the sodium data.

The results of charge balance are shown in Table 3-31. The sum of formate and nitrate accounted for practically 100 % of the total anion charges in all SRAT products. The calculated charge imbalances were all quite large, except for SB10-1 and SB10-5, requiring significant adjustments in sodium concentration; for example, the reported sodium data for SB10-2 had to be reduced by 44.1 % to achieve charge balance. It is noted that the SB10-2 SRAT product had the lowest pH at 3.85 and had the highest concentration of dissolved metals.

Table 3-31. Results of Charge Balance of SB10 SRAT Products.

Run #	COOH (ppm)	NO3 (ppm)	Total Anion (equiv M)	Na (M)	Dissolved Metals (equiv M)	Total Cation (equiv M)	Cation-Anion (equiv M)	Charge Imbalance (% Na)
SB10-1	11,800	68,100	1.59	1.26	0.48	1.74	0.15	12.1
SB10-2	24,800	65,450	1.95	1.41	1.16	2.57	0.62	44.1
SB10-3	18,350	64,100	1.76	1.75	0.54	2.30	0.53	30.4
SB10-5	37,100	41,450	1.81	1.61	0.36	1.96	0.15	9.4
SB10-7	53,250	18,150	1.86	1.27	0.29	1.56	-0.30	-23.2
SB10-8	59,300	17,150	1.93	1.31	0.37	1.68	-0.25	-19.2
SB10-9	36,200	56,800	2.13	1.80	0.63	2.43	0.30	16.9

Table 3-32 shows that 7.67% of the iron in SB10 was soluble at the pH of 3.85 and, as expected, its solubility fell to 1.25% at the pH of 4.61 in SB10-9, while iron remained essentially insoluble at higher pH's. Since iron was by far the most abundant element in the SB10 feeds making up 25-30 wt% of the calcine solids (Table 3-14), its impact on the overall charge balance of SB10-2 was significant. The solubility of manganese also increased in general with decreasing pH, while both calcium and magnesium remained quite soluble in the measured pH range. It is noted that the calculated solubilities in the charge-balanced slurries are somewhat lower than those given in Table 3-16 which are based on analytical data.

Table 3-32. Varying Solubility of Major Metal Species with pH.

Run #	Acid Stoichiometry	pH	Soluble Fe (% total Fe)	Soluble Ca (% total Ca)	Soluble Mn (% total Mn)	Soluble Mg (% total Mg)
SB10-1	100%	6.52	0.00	84.44	32.80	65.60
SB10-2	150%	3.85	7.67	80.81	89.26	71.00
SB10-3	100%	6.87	0.00	103.82	41.04	65.60
SB10-5	100%	7.47	0.00	105.72	11.40	65.60
SB10-7	100%	7.37	0.00	73.18	5.42	65.60
SB10-8	150%	7.91	0.00	74.24	21.19	62.11
SB10-9	150%	4.61	1.25	87.61	142.01	80.40

The resulting charge-reconciled SB10 melter feed compositions are shown in Tables D-1 to D-7 in Appendix D. It is to be noted that the given feed component flows are set to give the current DWPF maximum feed rate of 1.5 GPM. Both SB10-7 and SB10-8 feeds did not contain any coal, while SB10-9 was the only feed that contained the ARP/MCU streams. The amount of coal-carbon in each feed was calculated based on the actual recipe given in Table 3-33, since available analytical results of coal-carbon were not conclusive.

Table 3-33. Recipe for Coal-carbon Addition to SB10 SRAT Product.

	SB10-1	SB10-2	SB10-3	SB10-5	SB10-7	SB10-8	SB10-9
Coal added (gmol)	3.467	3.517	2.403	1.203	0	0	1.940
SRAT Product (g)	2,124.55	2,535.51	2,244.60	2,311.69	2,696.96	2,799.22	2,570.92
Density (g/ml)	1.165	1.213	1.214	1.207	1.232	1.210	1.221

The feed compositions given in Tables D-1 to D-7 were further decomposed into the final input form for the 4-stage cold cap model, as shown in Table 3-34 to Table 3-40. As described elsewhere[27] the model approximates the complex melting process as a continuous, 4-stage countercurrent equilibrium reactor, and the temperature of each stage is set progressively higher from the top (Stage 1) to bottom stage (Stage 4) at 1,150° C. The non ideality that exists among various melt phases that form is partially accounted for in lower stages with the use of the Gibbs free energy database for the complex liquids, which was developed at the National Institute of Standards and Technology (NIST).[27] In forming these model input vectors, all salts except sulfates were pre-decomposed into oxides and corresponding gases as follows:

$$2\,Fe(OH)_3 = Fe_2O_3 + 3\,H_2O \quad (2)$$

$$2\,NaCOOH = Na_2C_2O_4 + H_2 \quad (3)$$

$$Na_2C_2O_4 = Na_2O + CO + CO_2 \quad (4)$$

$$2\,NaNO_3 = 2\,NaNO_2 + O_2 \quad (5)$$

$$2\ NaNO_2 = Na_2O + NO + NO_2 \quad (6)$$

In particular, the decomposition of sodium nitrate is known to begin with the release of oxygen, thereby converting to nitrite at low temperatures, e.g., ~350 °C, and the subsequent decomposition of nitrite, which can take several different routes depending on the presence or absence of air and other gases, can persist beyond 850 °C. Based on this ample experimental evidence, the model assumes that the decomposition of nitrite shown in Rxn. (6) occurs at 40:60 split between Stages 1 and 2, respectively. Coal-carbon was assumed to react over a wider temperature range, and the cold cap model input vectors reflect a 60:30:10 split of coal-carbon among Stages 1 to 3, respectively. It is also to be noted that the H_2O shown in the model input vectors represent water produced from the decomposition reactions, e.g., Rxn. (2), not the free H_2O that constituted ~50 wt% of the slurry feed. Although SB10-9 contained $NaTi_2O_5H$ as part of the MCU/ARP streams (Table B-7), one of its decomposition products, TiO_2, was omitted from the cold cap model input vector (Table 3-40), since it is not known to affect glass redox or off-gas flammability.

Table 3-34. 4-Stage Cold Cap Model Input for SB10-1 at 1.5 GPM.

Species	Stage 1 (gmole/hr)	Stage 2 (gmole/hr)	Stage 3 (gmole/hr)
Al2O3	0	82.086	0
B2O3	144.613	0	0
CaO	0	61.955	0
CuO	0.847	0	0
Fe2O3	240.815	0	0
K2O	2.866	0	0
Li2O	0	336.945	0
MgO	0	0	13.647
MnO2	0	60.870	0
MnO	29.708	0	0
Na2O	218.386	162.438	0
NiO	12.218	0	0
SiO2	1689.056	0	0
CaSO4	0	0	0.460
Na2SO4	0	0	0.210
Coal-Carbon	450.330	225.165	75.055
H2O	519.322	0	0
CO	0	60.248	0
CO2	0	60.248	0
H2	60.248	0	0
O2	100.946	151.420	0
NO	100.946	151.420	0
NO2	100.946	151.420	0

Table 3-35. 4-Stage Cold Cap Model Input for SB10-2 at 1.5 GPM.

Species	Stage 1 (gmole/hr)	Stage 2 (gmole/hr)	Stage 3 (gmole/hr)
Al2O3	0	77.915	0
B2O3	137.676	0	0
CaO	0	61.326	0
CuO	0.645	0	0
Fe2O3	232.706	0	0
K2O	2.565	0	0
Li2O	0	320.783	0
MgO	0	0	13.993
MnO2	0	9.314	0
MnO	77.372	0	0
Na2O	133.393	154.714	0
NiO	12.331	0	0
SiO2	1609.128	0	0
CaSO4	0	0	0.481
Na2SO4	0	0	0.235
Coal-Carbon	343.559	171.779	57.260
H2O	480.058	0	0
CO	0	113.649	0
CO2	0	113.605	0
H2	113.649	0	0
O2	97.778	146.667	0
NO	87.067	130.601	0
NO2	87.067	130.601	0

Table 3-36. 4-Stage Cold Cap Model Input for SB10-3 at 1.5 GPM.

Species	Stage 1 (gmole/hr)	Stage 2 (gmole/hr)	Stage 3 (gmole/hr)
Al2O3	0	109.860	0
B2O3	156.444	0	0
CaO	0	57.712	0
CuO	0.000	0	0
Fe2O3	288.567	0	0
K2O	3.715	0	0
Li2O	0	364.513	0
MgO	0	0	14.162
MnO2	0	42.949	0
MnO	29.898	0	0
Na2O	221.941	175.699	0
NiO	13.194	0	0
SiO2	1724.607	0	0
CaSO4	0	0	0
Na2SO4	0	0	0.260
Coal-Carbon	286.884	143.442	47.814
H2O	643.299	0	0
CO	0	90.980	0
CO2	0	90.951	0
H2	90.980	0	0
O2	92.268	138.402	0
NO	92.268	138.402	0
NO2	92.268	138.402	0

Table 3-37. 4-Stage Cold Cap Model Input for SB10-5 at 1.5 GPM.

Species	Stage 1 (gmole/hr)	Stage 2 (gmole/hr)	Stage 3 (gmole/hr)
Al2O3	0	120.241	0
B2O3	152.082	0	0
CaO	0	53.617	0
CuO	0.000	0	0
Fe2O3	270.729	0	0
K2O	2.774	0	0
Li2O	0	354.349	0
MgO	0	0	13.175
MnO2	0	63.150	0
MnO	8.122	0	0
Na2O	291.946	170.519	0
NiO	12.494	0	0
SiO2	1676.119	0	0
CaSO4	0	0	0
Na2SO4	0	0	0.403
Coal-Carbon	152.559	76.279	25.426
H2O	654.873	0	0
CO	0	201.224	0
CO2	0	200.915	0
H2	201.224	0	0
O2	65.270	97.905	0
NO	65.270	97.905	0
NO2	65.270	97.905	0

Table 3-38. 4-Stage Cold Cap Model Input for SB10-7 at 1.5 GPM.

Species	Stage 1 (gmole/hr)	Stage 2 (gmole/hr)	Stage 3 (gmole/hr)
Al2O3	0	119.431	0
B2O3	151.519	0	0
CaO	0	60.703	0
CuO	0.872	0	0
Fe2O3	236.813	0	0
K2O	1.889	0	0
Li2O	0	353.037	0
MgO	0	0	13.293
MnO2	0	86.622	0
MnO	4.966	0	0
Na2O	327.377	170.196	0
NiO	11.952	0	0
SiO2	1734.112	0	0
CaSO4	0	0	0.112
Na2SO4	0	0	0.492
Coal-Carbon	0	0	0
H2O	634.246	0	0
CO	0	304.482	0
CO2	0	304.482	0
H2	304.482	0	0
O2	30.131	45.196	0
NO	33.073	49.609	0
NO2	33.073	49.609	0

Table 3-39. 4-Stage Cold Cap Model Input for SB10-8 at 1.5 GPM.

Species	Stage 1 (gmole/hr)	Stage 2 (gmole/hr)	Stage 3 (gmole/hr)
Al2O3	0	121.208	0
B2O3	158.555	0	0
CaO	0	61.427	0
CuO	0.000	0	0
Fe2O3	238.503	0	0
K2O	1.923	0	0
Li2O	0	369.431	0
MgO	0	0	15.462
MnO2	0	72.390	0
MnO	19.460	0	0
Na2O	323.700	178.100	0
NiO	13.445	0	0
SiO2	1813.407	0	0
CaSO4	0	0	0.470496
Na2SO4	0	0	0.369
Coal-Carbon	0	0	0
H2O	642.661	0	0
CO	0	331.134	0
CO2	0	331.134	0
H2	331.134	0	0
O2	27.803	41.705	0
NO	27.803	41.705	0
NO2	27.803	41.705	0

Table 3-40. 4-Stage Cold Cap Model Input for SB10-9 at 1.5 GPM.

Species	Stage 1 (gmole/hr)	Stage 2 (gmole/hr)	Stage 3 (gmole/hr)
Al2O3	0	106.149	0
B2O3	145.157	0	0
CaO	0	43.743	0
CuO	0.000	0	0
Fe2O3	222.765	0	0
K2O	2.521	0	0
Li2O	0	338.214	0
MgO	0	0	15.005
MnO2	0	0.000	0
MnO	56.703	0	0
Na2O	289.103	174.735	0
NiO	10.243	0	0
SiO2	1604.011	0	0
CaSO4	0	0	6.191
Na2SO4	0	0	3.080
Coal-Carbon	218.234	109.117	36.372
H2O	569.411	0	0
CO	0	193.703	0
CO2	0	193.798	0
H2	193.703	0	0
O2	89.908	134.863	0
NO	88.236	132.354	0
NO2	88.236	132.354	0

3.7.1.2 Cold Cap Model Output

The compositions of both calcine gases and glasses predicted by the cold cap model are shown in Table 3-41 and Table 3-42, respectively, for the seven SB10 cases considered. It is noted that the calculated TOC's were much higher than that of the SB6; the TOC's for SB10-1 and SB10-2 were even higher than the current DWPF TSR limit of 18,900 ppm. The molar ratios of CO/CO_2 and $H_2/(CO+CO_2)$ represent the relative flammability of calcine gas flows, and they are expected to increase as TOC increases. However, no clear trend can be seen between those ratios and TOC in SB10 feeds, since the makeup of TOC and the counterbalancing nitrate level were all different from one feed to the next. It is interesting to note that both SB10-3 and SB10-9 calcine gases had no flammable components despite high TOC levels. These seemingly-counterintuitive results illustrate the fact that not only the TOC but the nitrate (oxidant) levels determine the flammability potential of each feed. Therefore, the TOC data must be taken in along with the corresponding nitrate data in order to provide an accurate measure of the flammability potential of each feed.

Table 3-41. Calculated Calcine Gas Compositions of Baseline Feeds at 1.5 GPM.

	SB10-1 (gmole/hr)	**SB10-2** (gmole/hr)	**SB10-3** (gmole/hr)	**SB10-5** (gmole/hr)	**SB10-7** (gmole/hr)	**SB10-8** (gmole/hr)	**SB10-9** (gmole/hr)
H_2O	453.749	492.030	734.330	835.214	870.868	882.308	763.104
CO_2	743.117	708.993	659.952	646.399	580.776	622.017	751.069
H_2	125.799	101.674	0	20.806	67.894	91.473	0
N_2	252.405	217.649	230.712	163.164	82.683	69.505	220.557
CO	127.964	90.998	0	10.001	28.123	40.054	0
O_2	0	0.000	40.987	0	0	0	7.312
SO_2	0.014	0.016	0.011	0.009	0	0	0.014
NO	0	0	0.006	0	0	0	0.003
NO_2	0	0	0	0	0	0	0
$NaBO_2$	0	0	0.001	0	0	0	0.001
Total	1,703.049	1611.360	1665.999	1675.594	1630.344	1705.357	1742.059
CO/CO_2	0.172	0.128	0	0.015	0.048	0.064	0
$H_2/(CO+CO_2)$	0.144	0.127	0	0.032	0.112	0.138	0
TOC (ppm)	20,727	19,628	15,393	15,370	14,332	15,452	18,037

This point is further illustrated in Table 3-41; the molar ratios of CO/CO_2 and $H_2/(CO+CO_2)$ are generally low for their TOC, since all SB10 baseline feeds were redox-adjusted. By contrast, the existing method of determining the maximum TOC limit is by increasing the concentrations of all formate salts in the baseline feed by the same ratio without any redox considerations until the peak flammable gas concentration during the design basis off-gas surge equals the safety basis limits. As a result, the calculated REDOX of such a maximum-TOC feed would become much higher than that of the baseline feed, and the resulting calcine gases more flammable. This approach of increasing the formate level without the accompanying increase in nitrate level was originally used to simulate the situation where slugs of insoluble, high-boiling aromatic carbon species from the precipitate hydrolysis process enter the melter. Since the formate salts are highly

Table 3-42. Calculated Glass Compositions of Baseline Feeds at 1.5 GPM.

	SB10-1 (gmole/hr)	**SB10-2** (gmole/hr)	**SB10-3** (gmole/hr)	**SB10-5** (gmole/hr)	**SB10-7** (gmole/hr)	**SB10-8** (gmole/hr)	**SB10-9** (gmole/hr)
Melt Phase							
SiO_2 l	1,265.016	1,279.120	1,286.718	1,178.336	1,197.349	1,249.091	1,105.081
Na_2SiO_3	381.051	288.283	397.946	462.828	498.093	502.163	466.910
$LiBO_2$ l	288.824	275.084	312.440	303.650	302.663	316.643	289.950
$LiAlO_2$ l	164.167	155.813	219.758	240.578	238.900	242.381	212.356
Fe_3O_4 l	116.925	90.086	76.324	41.870	92.334	121.127	58.769
$MgSiO_3$ l	10.848	11.023	11.607	10.880	10.695	12.175	13.152
FeO l	25.174	19.396	16.433	9.015	19.880	58.364	12.653
$CaFe_2O_4$	14.562	13.590	14.138	13.609	15.132	7.603	11.502
B_2O_3 l	8.8E-05	8.4E-05	1.2E-04	1.3E-04	1.3E-04	1.3E-04	1.1E-04
Ca_2SiO_4	19.550	19.427	17.943	16.468	18.770	21.796	11.925
Ca_3MgSi_2*	2.718	2.890	2.481	2.222	2.524	3.287	1.777
Fe_2SiO_4	4.551	3.082	1.888	0.563	2.512	19.975	1.124
KBO_2	0.404	0.360	0.528	0.492	82.273	89.955	0.442
Li_2O l	110.375	105.316	98.465	82.334	1.685	1.716	87.139
K_2SiO_3	2.664	2.385	3.449	2.528	0.408	0.416	2.300
Spinel Phase							
$NiFe_2O_4$	12.218	12.332	13.185	12.502	11.951	0	10.243
Mn_3O_4	30.193	28.894	24.283	23.756	30.530	0	18.900
$CuFe_2O_4$	0.846	0.645	0	0	0.873	0	0
$MgFe_2O_4$	0.081	0.079	0.074	0.073	0.085	0	0.076
ICP							
Fe_2O_3	20.560	58.070	136.563	176.617	57.776	0	105.310
$CaSO_4$	0.657	0.702	0.244	0.396	0.604	0.417	9.255
Ni	0	0	0	0	0	0	0
NiO	0	0	0	0	0	13.444	0
Ni_3S_2	0	0	0	0	0	0	0
Cu	0	0	0	0	0	0	0
MnO	0	0	0	0	0	91.847	0
Redox (Fe^{+2}/Fe^{total})							
Calculated	0.314	0.249	0.167	0.096	0.248	0.460	0.165
Predicted	0.326	0.285	0.109	0.182	0.232	0.291	0.148
Measured	0.300	0.208	0.225	0.235	0.237	0.218	0.332
TOC (ppm)	20,727	19,628	15,393	15,370	14,332	15,452	18,037

* The melt species Ca_3MgSi_2 is a truncated name for $Ca_3MgSi_2O_8$ or $3CaO.MgO.2SiO_2$.

soluble in aqueous solutions, applying the same approach to the formate carbon would make the resulting TOC limit conservative. However, the selective increase in reductant level without the accompanying increase in oxidant level seems more justified for coal-carbon, since it is insoluble and its wide particle size distribution makes its segregation in the slurry more likely. Therefore, the scenario of slugs of coal-carbon entering the melter is plausible.

The predicted SB10 glass oxides are split into groups or phases in Table 3-42. The letter **l** after each species in the melt phase denotes "liquid." These liquid or melt species were taken from the NIST database;[30] they do not necessarily represent independent molecular or ionic species but serve to represent the local associative order. Due to structural similarities, the spinels readily form solid solutions with one another and thus are assumed to form a separate phase of their own. On the other hand, each species included in the Invariant Condensed Phase (ICP) is assumed to form a separate phase by itself. Therefore, as more species are included in the ICP, the total number of phases to be considered in the equilibrium calculations increases, and this makes it more difficult to achieve convergence. It is noted that at the calculated redox of 0.46 for SB10-8 the glass was reducing enough to form no hematite and all manganese was in a +2 oxidation state as in MnO, rather than in a hybrid of +2 (33%) and +3 (67%) oxidation states as in Hausmannite (Mn_3O_4). Furthermore, at the redox ratio of 0.46, nickel is predicted to precipitate as NiO instead of forming a multiple oxide with iron as $NiO.Fe_2O_3$ as part of the spinel phase.

The calculated redox ratios using the cold cap model are next plotted in Figure 3-9 against the net reducing potential, which is defined as F-3N+2C where F, N and C are molar concentrations of formate, nitrate and coal-carbon, respectively. Also plotted are the redox ratios predicted from Eq. (1) along with measured data. As expected, both the calculated and predicted redox ratios increase with increasing net reducing potential, and the exponential functions that best fit each data set are quite similar until they begin to diverge at (F-3N+2C) > ~0.35. On the other hand, the measured redox ratios remained more or less flat, showing no dependence on the net reducing potential.

3.7.1.3 Off-Gas Dynamics Model Input

The calculated calcine gas compositions given in Table 3-41 were next used as the input to the off-gas dynamics model in order to check if the off-gas flammability safety basis limit of 60% of the LFL for normal operation is exceeded during a design basis off-gas surge. Briefly, the model predicts the time-dependent responses of both the primary and backup DWPF melter off-gas systems under a variety of upset conditions.[25] It calculates 5-component mass and energy balances for the condensable and non-condensable gases from first principles. It simulates all major DWPF melter off-gas system hardware, including 22 Proportional-Integral (PI) controllers and 26 valves, and the Distributed Control System (DCS) software logic to provide protection against extreme pressure transients and other operational anomalies such as equipment malfunction. It employs a 2-step global reaction scheme using the empirical first-order oxidation kinetics of CO and H_2 to model combustion of calcine gases in the melter vapor space.

The design basis 9X/5X off-gas surge for bubbled melter operation is assumed to proceed as follows: [26]

- At time zero, the baseline flow rates of steam and non-condensable gases increase 9- and 5-fold, respectively, instantly and then immediately start to decrease linearly to 3.5 times (3.5X) and 2 times (2X) the normal condensable and non-condensable flows during the first 1 minute.
- The flow rates of both steam and non-condensable gases further decrease linearly to the normal values (1X) during the next 7 minutes.

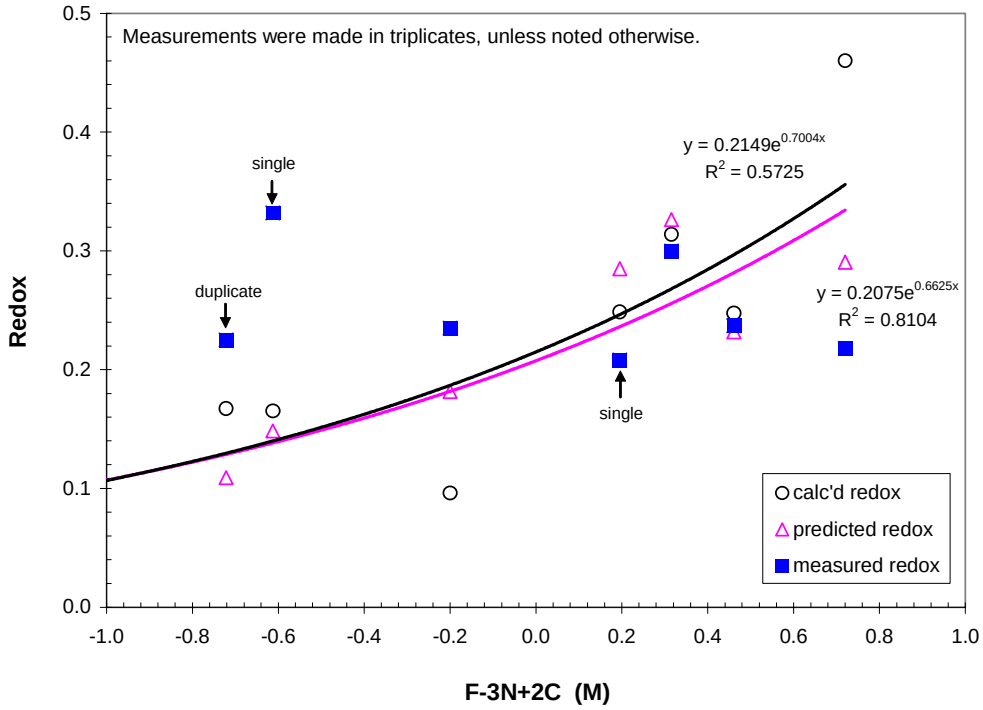

Figure 3-9. Calculated, Predicted, and Measured Redox vs. Net Reducing Potential of Baseline SB10 Feeds.

3.7.1.4 Results of Off-Gas Dynamics Model Runs

Typical results of the 9X/5X off-gas surge simulation for normal bubbled melter operation are shown in Figure 3-10 for the baseline SB10-1 feed as an example. It shows the transient profiles of the calcine gas flow into the melter vapor space, melter pressure, melter vapor space gas temperature and the concentration of flammable gases in the Off-Gas Condensate Tank (OGCT) in terms of percent of the LFL during the first 2 and 1/2 minutes into the surge. The magnitude of 9X/5X surge is clearly seen from the melter pressure peaking at over +15" H_2O, compared to +2" H_2O for the 3X non-bubbled off-gas surge. After steam has condensed out in the quencher, the concentration of flammable gases in the remaining off-gas is shown to peak at ~45% of the LFL from the initial value of 13% of the LFL about 20 seconds after the gas temperature reached its minimum during normal bubbled operation. It is noted that this peak off-gas flammability is well under the safety basis limit of < 60% of the LFL for normal operation.

The peak concentrations of flammable gases read off from these figures are summarized in Table 3-43 along with key input variables. It is shown that the calculated peak off-gas flammability for all seven SB10 baseline feeds is well under the safety basis limit. Although not presented here, the calculated peak flammability for seismic operation is also significantly below the safety basis limit of <95% of the LFL. Therefore, it can be concluded that there is no flammability concern for all SB10 baseline feeds for both normal and seismic operations. Furthermore, there appears to

Figure 3-10. Results of 9X/5X Off-Gas Surge Simulation with Baseline SB10-1 Feed.

(Normal Operation, 100% Acid Stoichiometry, 20,727 ppm TOC, 17,863 ppm Coal-carbon, 1.5 GPM Feed Rate; TI4085D = 460° C; FIC3221A = 900 PPH; FIC3221B = 233 PPH).

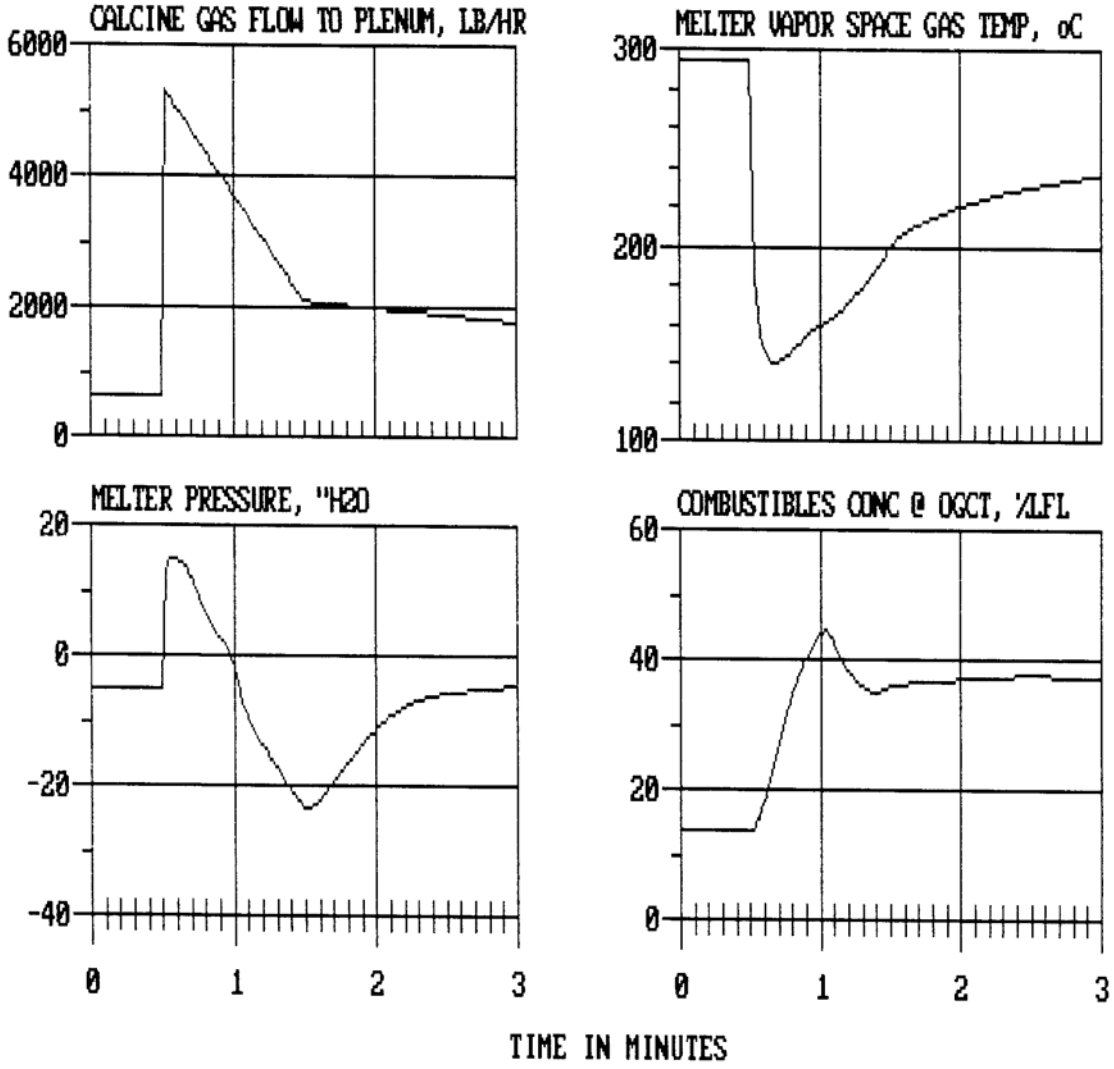

Table 3-43. Calculated Peak Flammability of Baseline SB10 Off-Gas @ OGCT during 9X/5X Surge at 1.5 GPM.

Feed	NO3 (ppm)	Formate Carbon (ppm)	Coal-carbon (ppm)	TOC (ppm)	F-3N+2C (M)	Calculated Redox	Peak Flammability (%LFL)
SB10-1	62,064	2,865	17,863	20,727	0.315	.314	45
SB10-2	55,209	5,573	14,055	19,628	0.195	0.249	34
SB10-3	55,601	4,240	11,153	15,393	-0.721	0.167	~0
SB10-5	39,489	9,415	5,955	15,370	-0.200	0.096	7
SB10-7	18,339	14,332	0	14,332	0.461	0.248	21
SB10-8	16,776	15,452	0	15,452	0.720	0.460	28
SB10-9	54,767	9,298	8,739	18,037	-0.613	0.165	~0

be no definite correlation between TOC and off-gas flammability. For example, despite high TOC, the peak flammability of SB10-9 off-gas is zero, while other feeds with lower TOC like SB10-7 are predicted to have much higher flammability potential. However, this is not unexpected since the TOC only reflects the reductant, whereas the reducing effect of TOC can be overwhelmed by a high concentration of nitrate as in SB10-9, resulting in a very oxidizing feed.

By contrast, the calculated peak off-gas flammability appears to be better correlated with the net reducing potential, as expected. It is also of interest to note that the model predicts more sharply increasing off-gas flammability with increasing net reducing potential for feeds with coal than those without coal. Table 3-43 also shows that the coal carbon has a greater reducing potential than the formate carbon, thus making glass more reducing and off-gas more flammable. For example, when SB10-2 and SB10-9 are compared, the former has only about 8% higher TOC than the latter at a comparable nitrate level but the peak off-gas flammability of the former is 34% of the LFL compared to 0% for the latter. The difference is in the TOC makeup; the TOC of SB10-9 is split roughly 50:50 between the formate carbon and coal-carbon, while the split for SB10-2 is 28:72 in favor of coal-carbon. However, the impact of TOC makeup on redox does not appear to be as pronounced as on the off-gas flammability; the glass redox was increased from 0.165 (SB10-9) to 0.249 (SB10-2).

3.7.2 *Flammability Assessment of Max-Coal Feeds*

Since the potential for off-gas flammability of all baseline feeds was well below the safety basis limits, additional coal-carbon was added to each baseline feed iteratively until the calculated peak off-gas flammability equaled the safety basis limit for normal operation, 60% of the LFL. It is noted that in all the cases considered for DWPF the safety basis limit for normal operation has been more controlling than the seismic limit (95% of the LFL); therefore, the former limit was used here.

3.7.2.1 Cold Cap Model Input

Since coal-carbon was the only species added to the baseline feeds, the input vectors for the max-coal feeds were identical to those shown in Table 3-34 to Table 3-40 except that the feed rate of coal-carbon to Stages 1 to 3 for each baseline feed were increased by the same factor. Therefore, the equivalent cold cap model input tables for the max-coal SB10 feeds are not repeated here. Likewise, the charge-reconciled max-coal SB10 melter feed compositions are identical to Tables D-1 to D-7 except for higher coal-carbon flows so they are not repeated in Appendix D either.

3.7.2.2 Cold Cap Model Output

The compositions of both calcine gases and glasses predicted by the cold cap model are shown in Table 3-44 and Table 3-45, respectively, for the SB10 max-coal feed cases; these compositions or flow rates were found after several iterations to give the peak off-gas flammability equaling 60% of the LFL during the 9X/5X off-gas surge. It is noted that the max-coal feeds have 6-33% higher TOC than the baseline feeds and all exceed or at least equal the TSR limit. As a result, the calcine gases for the max-coal feeds are more reduced, as indicated by higher molar ratios of CO/CO_2 and $H_2/(CO+CO_2)$ than those of the baseline feeds, particularly for SB10-3 and SB10-9. The higher flammability potential of the max-coal feeds is due in part to the fact that additional coal-carbon was added without adding counterbalancing nitrate, whereas all baseline feeds were redox-balanced. As stated earlier, the intent of adding extra coal-carbon without the accompanying increase in nitrate is to simulate the scenario of slugs of coal-carbon entering the melter.

Table 3-44. Calculated Calcine Gas Compositions for Max-Coal Feeds at 1.5 GPM.

	SB10-1 (gmole/hr)	**SB10-2** (gmole/hr)	**SB10-3** (gmole/hr)	**SB10-5** (gmole/hr)	**SB10-7** (gmole/hr)	**SB10-8** (gmole/hr)	**SB10-9** (gmole/hr)
H_2O	410.791	413.663	558.697	666.841	734.296	774.739	588.502
CO_2	732.082	734.302	722.367	720.065	689.810	696.967	821.754
H_2	164.188	177.294	169.661	184.629	197.497	199.408	185.414
N_2	250.415	216.641	228.837	162.297	82.060	69.523	223.684
CO	181.740	195.474	136.248	123.827	115.236	111.422	160.807
O_2	0	0	0	0	0	0	0
SO_2	0.015	0.003	0.022	0.007	4.32E-04	4.43E-04	0.008
NO	0	0	0	0	0	0	0
NO_2	0	0	0	0	0	0	0
$NaBO_2$	3.20E-04	3.09E-04	3.68E-04	3.89E-04	3.86E-04	3.99E-04	3.99E-04
Total	1,739.231	1737.378	1815.832	1857.666	1818.900	1852.059	1980.171
CO/CO_2	0.248	0.266	0.189	0.172	0.167	0.160	0.196
$H_2/(CO+CO_2)$	0.180	0.191	0.198	0.219	0.245	0.247	0.189
TOC (ppm)	21,894	22,849	20,009	19,815	19,003	18,798	23,147

The calculated redox ratios of the max-coal glasses are shown in Table 3-45 to be much higher than those of the baseline glasses. At redox ratio > ~0.45, all nickel and manganese spinels are converted to their oxides. At even higher redox ratios of SB10-7 and SB10-8, some or all of the nickel oxide is further reduced mostly to elemental Ni and some to Ni_3S_2. At redox ratio > ~0.35 no hematite is predicted to form. The abundance ranking of the melt-phase species remains fairly constant except for those containing iron, e.g., ferrous oxide (*FeO l*), ferrous silicate (*Fe_2SiO_4 l*), magnetite (*Fe_3O_4 l*); this is not surprising since redox is the manifestation of how iron partitions itself among various oxidation states. It is also noted that the redox of all SB10 max-coal glasses except for SB10-3 exceeded the DWPF upper limit of 0.3. Furthermore, since both SB10-7 and SB10-8 baseline feeds did not contain any coal, the max-coal to baseline feed coal ratios for these feeds are infinite; for the remaining feeds the ratio ranged from 1.06 (SB10-1) to 1.75 (SB10-5).

Table 3-45. Calculated Glass Compositions of Max-Coal Feeds at 1.5 GPM.

	SB10-1 (gmole/hr)	**SB10-2** (gmole/hr)	**SB10-3** (gmole/hr)	**SB10-5** (gmole/hr)	**SB10-7** (gmole/hr)	**SB10-8** (gmole/hr)	**SB10-9** (gmole/hr)
Melt Phase							
SiO_2 l	1,254.511	1,244.441	1,274.699	1,152.072	1,067.715	1,147.092	1,103.854
Na_2SiO_3	378.047	286.949	394.604	460.367	494.340	502.186	473.626
$LiBO_2$ l	286.546	273.802	309.895	302.018	300.358	316.711	294.048
$LiAlO_2$ l	162.873	155.092	217.970	239.299	237.099	242.444	215.365
Fe_3O_4 l	123.409	111.352	106.928	140.439	30.473	29.637	118.849
$MgSiO_3$ l	10.772	10.538	11.551	10.614	9.660	11.570	13.076
FeO l	26.570	60.679	23.022	54.522	144.545	148.258	49.688
$CaFe_2O_4$	14.501	5.954	14.234	8.521	0.840	0.808	6.776
B_2O_3 l	8.72E-05	8.31E-05	1.14E-04	1.29E-04	1.28E-04	1.30E-04	1.14E-04
Ca_2SiO_4	19.384	22.348	17.752	18.490	24.459	24.497	14.029
Ca_3MgSi_2*	2.687	3.390	2.423	2.476	3.532	3.896	2.140
Fe_2SiO_4	5.070	28.229	3.617	18.138	116.175	119.121	15.583
KBO_2	0.402	0.366	0.528	0.508	0.429	0.432	0.459
Li_2O l	109.505	104.925	97.667	81.905	81.665	89.986	88.380
K_2SiO_3	2.643	2.370	3.419	2.506	1.660	1.708	2.327
Spinel Phase							
$NiFe_2O_4$	12.122	0	13.078	4.645	0	0	0.411
Mn_3O_4	29.955	0	24.086	9.234	0	0	0.912
$CuFe_2O_4$	0.839	0	0	0	0	0	0
$MgFe_2O_4$	0.080	0	0.074	0.015	0	0	0.002
ICP							
Fe_2O_3	7.883	0	83.299	0	0	0	0
$CaSO_4$	0.652	0.712	0.235	0.396	0	0	9.394
Ni	0	0	0	0	4.779	12.822	0
NiO	0.652	12.275	0	7.791	6.183	0	9.976
Ni_3S_2	0	0	0	0	0.300	0.209	0
Cu	0	0.642	0	0	0.866	0	0
MnO	7.883	86.282	0	43.187	90.899	91.871	54.769
Redox (Fe^{+2}/Fe^{total})							
Calculated	0.335	0.493	0.240	0.429	0.867	0.872	0.442
Predicted	0.394	0.479	0.372	0.433	0.497	0.477	0.440
Measured	n/a	n/a	n/a	n/a	n/a	n/a	n/a
TOC (ppm)	21,894	22,849	20,009	19,815	19,003	18,798	23,147

* The melt species Ca_3MgSi_2 is a truncated name for $Ca_3MgSi_2O_8$ or $3CaO.MgO.2SiO_2$.

The calculated redox ratios of both the max-coal and baseline glasses using the cold cap model are next plotted in Figure 3-11 against the net reducing potential. Both data sets were regressed using an exponential function and the resulting curves are shown to maintain a good continuity at the net reducing potential between 0.6 and 0.7. However, the curve for the max-coal feed is seen to have a steeper slope than the baseline curve. Since no redox data are available at these high net reducing potentials, it is not certain that a sharper upturn in redox at high net reduction potential is a real trend or the model is simply over predicting redox. However, comparison of the calculated redox ratios for SB10-7 and SB10-8 against those predicted from Eq. (1) suggests that it is likely the latter.

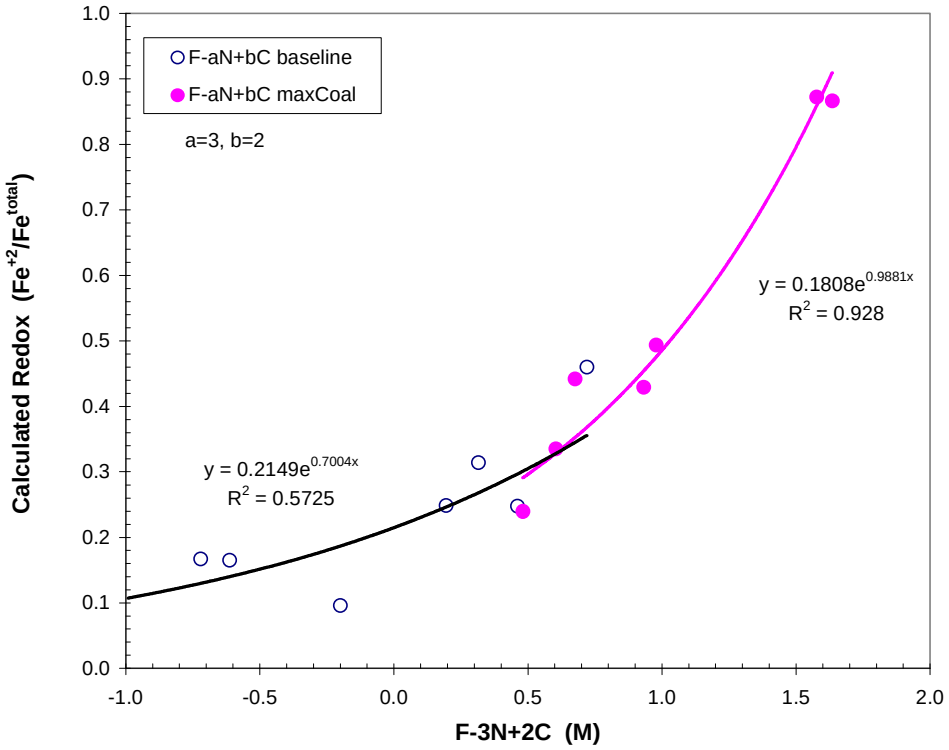

Figure 3-11. Calculated Redox vs. Net Reducing Potential of Max-Coal SB10 Feeds.

3.7.2.3 Off-Gas Dynamics Model Input

The calcine gas compositions given in Table 3-44 for the max-coal feeds were used as the input to the off-gas dynamics model. As stated above, these calcine gas flows were found to give the peak off-gas flammability equaling the safety basis limit for normal operation for each max-coal feed. It is to be noted that all other input parameters of the model such as process and controller constants remained the same as in the baseline feed cases.

3.7.2.4 Results of Off-Gas Dynamics Model Runs

Typical results of the 9X/5X off-gas surge simulation for normal bubbled melter operation are shown in Figure 3-12 for the SB10-1 max-coal feed as an example. Since the amount of extra coal added to the baseline feeds was not large, ranging from 1,200 to 5,200 ppm, the transient profiles of the calcine gas flow into the melter vapor space, melter pressure, and melter vapor space gas temperature are virtually identical to those shown in Figure 3-10. The only difference

is in the concentration profile for the flammable gases in the OGCT. As discussed earlier, the flammable gas concentration profile was set to peak at the safety basis limit of 60% of the LFL for each max-coal feed. It is interesting to note that while the melter pressure is shown to recover within ~2 minutes after the onset of surge, the flammable gas concentration remains relatively high for a longer period of time after the initial quick descent from its peak value in both the baseline and max-coal feed cases. It is not clear why this is the case but it could be the result of high surge magnitudes of bubbled melter operation coupled with the slow recovery of the melter vapor space temperature.

The maximum coal content that each SB10 feed can accommodate without exceeding the off-gas flammability safety basis for normal operation are summarized in Table 3-47 along with other input variables. The maximum coal content is further broken down into that included in each baseline feed and the extra added later. It is shown that the maximum coal limit can vary widely from 3,400 ppm to over 19,000 ppm, depending on how each feed was blended from two SB10 simulants and, more importantly, how the acid addition was done, as outlined in Table 3-10.

For example, the lower bound for the maximum coal limit is set by SB10-8 and this was expected since it contains the most formate carbon and least nitrate. As a result, SB10-8 has the smallest TOC and one of the largest net reducing potential. On the other hand, the upper bound for the maximum coal-carbon limit is set by SB10-1, since it contains the least formate carbon and most nitrate, resulting in the smallest net reducing potential. Because of this counterbalancing between the formate carbon and coal-carbon at a given nitrate level, the resulting TOC at the safety basis limit does not vary as widely as the maximum coal-carbon limit, ranging from 19,000 ppm to 23,100 ppm.

Table 3-46. Maximum Coal-carbon Limits for SB10 Feeds at 60% of LFL.

Feed	NO_3 (ppm)	Formate Carbon (ppm)	Baseline Coal (ppm)	Additional Coal-carbon (ppm)	Maximum Coal-carbon (ppm)	TOC (ppm)	F-3N+2C (M)
SB10-1	61,990	2,861	17,841	1,191	19,032	21,894	0.605
SB10-2	55,028	5,555	14,009	3,285	17,294	22,849	0.979
SB10-3	55,115	4,203	11,056	4,750	15,806	20,009	0.481
SB10-5	39,310	9,372	5,928	4,515	10,443	19,815	0.932
SB10-7	18,252	14,264	0	4,739	4,739	19,003	1.635
SB10-8	16,719	15,399	0	3,399	3,399	18,798	1.577
SB10-9	54,482	9,249	8,694	5,204	13,898	23,147	0.675

Figure 3-12. Results of 9X/5X Off-Gas Surge Simulation with SB10-1 Max-Coal Feed.

(Normal Operation, 100% Acid Stoichiometry, 21,894 ppm TOC, 19,032 ppm Coal, 1.5 GPM Feed Rate; TI4085D = 460° C; FIC3221A = 900 PPH; FIC3221B = 233 PPH).

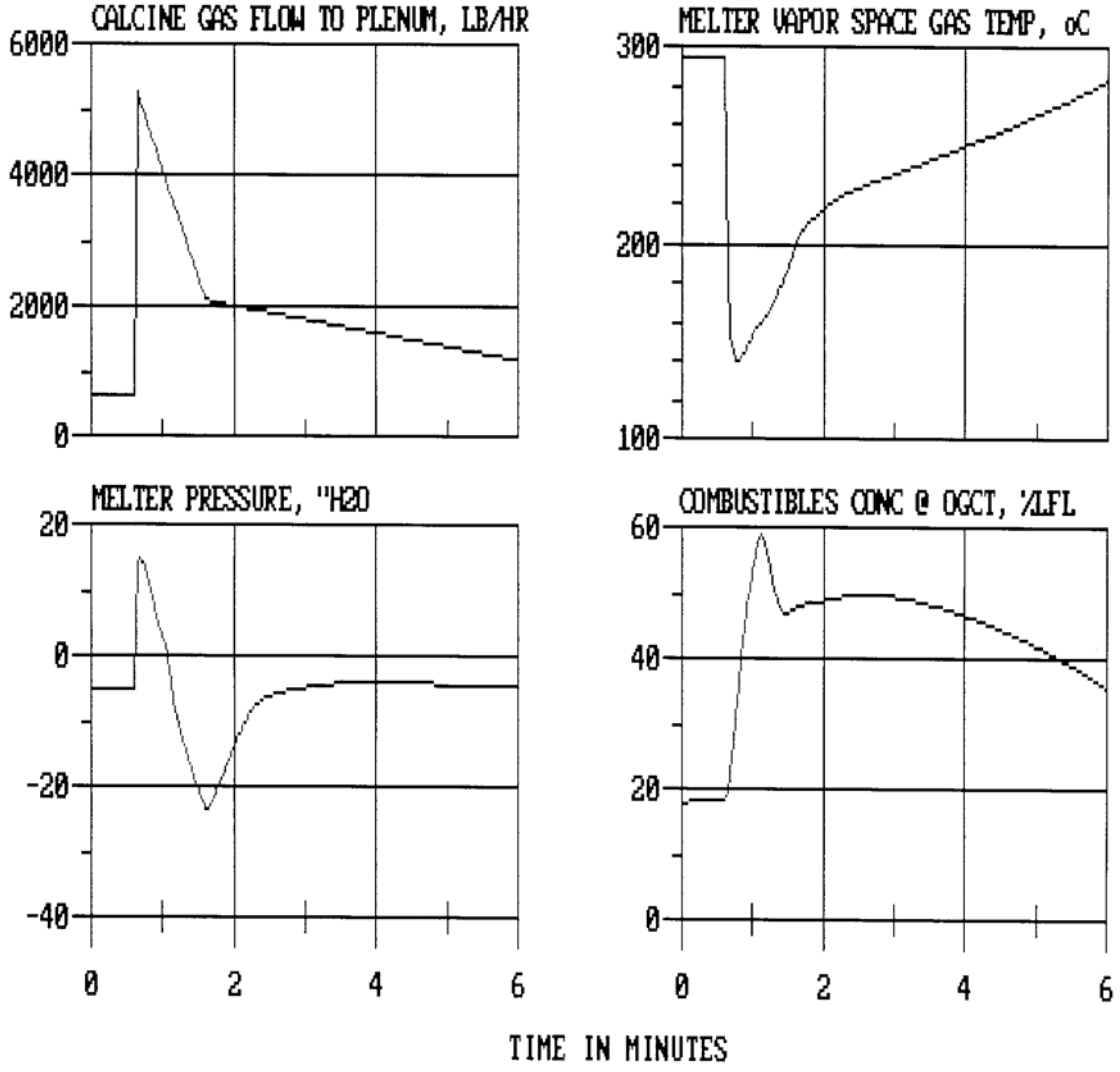

However, the counterbalancing between the formate carbon and coal-carbon is not clearly seen in Table 3-47 for the remaining "non-extreme" cases. When SB10-2 and SB10-3 are compared, both have comparable nitrate levels but it is the former that can accommodate more coal-carbon despite having more formate carbon than the latter. As a result, SB10-2 has a higher TOC but still end up with the same peak off-gas flammability as SB10-3. Nevertheless, the larger net reducing potential of SB10-2 had the expected impact on glass redox, i.e., 0.49 vs. 0.24 for SB10-3 (see Table 3-46) and the resulting speciation in the spinel phase and ICP of SB10-2 glass was quite the opposite of SB10-3. This could mean that the larger net reducing potential of SB10-2 was affecting the glass phase more heavily, thus leaving more oxygen available for the oxidation of calcine gases.

On the other hand, the impact of nitrate (oxidant) on the coal-carbon and TOC limits can be clearly seen when SB10-5 and SB10-9 are compared. Both have comparable formate carbon; however, since SB10-9 has 39% higher nitrate, it could accommodate 33% more coal-carbon, resulting in a 17% higher TOC. It is be noted that although the nitrate and format remained the same in the baseline and max-coal feeds, their concentrations given in Table 3-44 and Table 3-47 are not quite identical. The slight differences are due to the fact that just by adding additional coal-carbon the density of the max-coal feeds became a little higher than their baseline counterparts, thereby lowering their concentrations in the max-coal feed slightly.

3.8 Impact of FBSR Stream on Tank Farm and Other Processing Facilities

The FBSR PDT material will be transferred into Tank 42 and Tank 51 for washing prior to transferring to Tank 40 prior to feeding to DWPF. All three tanks will contain some coal-carbon once the FBSR facility begins transferring product. Large insoluble solids are harder to suspend and will settle faster if mixing is inadequate or not being performed. It should be noted that after redissolution of the PDT material and settling, the insoluble solids were difficult to resuspend. However, during SRNL washing and preparation of the sludge simulants, after combining the PDT material and the sludge, the settled solids were easily resuspended. They also settled quickly making the washing of this material much easier than many sludges. In addition, no solids were seen floating or sticking to the plastic vessels during washing nor did solids accumulate in the SRAT/SME glassware. Note that no carbon steel equipment was used in the testing.

One impact that may be significant is the quantity of sodium carbonate that will be transferred to the Tank Farm during the washing operations. Depending on the size of the decant, at least 90% of the sodium carbonate in the PDT material will be removed from the sludge and will need to be processed in the Tank Farm. It is recommended that future testing be completed with the wash solution to determine whether this large quantity of sodium carbonate will impact the HLW evaporators or evaporator drop tank. The decanted supernate from washing SB10-B simulant has been collected and retained. These could be used for future downstream testing. No analysis was completed on these decanted supernates.

4.0 Conclusions

In order to determine the carbon limit for the Defense Waste Processing Facility (DWPF), seven different SB10 feed simulants were formulated at varying coal-carbon concentrations and tested during a bench-scale CPC demonstration to assess the impact of coal-carbon on the CPC processing goals such as nitrite destruction and redox. The resulting melter feed compositions were then assessed in terms of the potential for melter off-gas flammability using the DWPF cold cap and off-gas dynamics models. This report summarizes the results of these experimental and modeling studies and draws several conclusions including the maximum allowable coal-carbon limit for DWPF without exceeding the off-gas flammability safety basis limits.

Carbon (coal) will be added to the sludge processed by DWPF once the Fluidized Bed Steam Reformer (FBSR) process starts up in order to destroy the tetraphenylborate (TPB) present in Tank 48. Carbon is present in the FBSR product due to unreacted coal-carbon, an FBSR additive.

The FBSR product will be combined with sludge and washed together to produce the sludge batch that DWPF will process. The FBSR product is high in both sodium carbonate and coal-carbon. Most of the sodium carbonate is removed during washing but all of the coal-carbon will become part of the DWPF sludge batch.

An earlier report was issued based on paper studies with no insight from experimental data. This report adds the results and analysis of the experiments. The presence of coal-carbon in the sludge feed to DWPF has both positive and negative impact as summarized below:

- Coal-carbon is a melter reductant. If excess coal-carbon is present, the resulting melter feed may be too reducing, potentially shortening the melter life. During this study, the Reduction/Oxidation Potential (REDOX) of the melter could be controlled by varying the ratio of nitric and formic acid. However, higher coal-carbon concentrations than were studied could lead to glass that is too reducing if not balanced.
- The addition of coal-carbon increases the amount of nitric acid added and decreases the amount of formic acid added to control melter REDOX. This means the DWPF flowsheet with the FBSR product is much more oxidizing than current CPC processing. In this study, adequate formic acid was present in all experiments to reduce mercury and manganese, two of the main goals of CPC processing, but did not lead to adequate mercury stripping in the SRAT cycle in two of the experiments. However, higher coal-carbon concentrations than were studied could lead to glass that is too reducing if not balanced.
- Coal-carbon will decompose to carbon dioxide or carbon monoxide in the melter. The addition of coal-carbon to the FBSR product will lead to approximately 55 % higher offgas production from formate, nitrate and carbon due to the decomposition of the carbon at the maximum levels in this testing. Higher offgas production could lead to higher cold cap coverage or melter foaming which could decrease melt rate. No testing was performed to evaluate the impact of the higher melter offgas flow.
- The FBSR product contains 4.1 to 9.5 % by mass coal-carbon particles with a particle size >177 μm (maximum particle size for frit). There is concern that the large sludge particles may lead to localized reducing pockets as the large carbon particles react in the melt pool. In addition, the larger particles may plug smaller diameter piping in the DWPF sampling system and will settle faster than smaller particles. No testing was performed to evaluate the impact of the larger particle size on DWPF processing.

- The hydrogen production is greatly reduced in testing with coal-carbon as less formic acid is added in CPC processing. In the high acid runs, the peak hydrogen generation was 15 times higher in the run with added coal-carbon.
- Coal-carbon is a better melter reducing agent than formic acid, since the content of both carbon and hydrogen are important in evaluating the flammability of the melter offgas. Processing with coal-carbon decreases the amount of formic acid added in the CPC, leading to a lower flammability risk in processing with coal-carbon compared to the current DWPF flowsheet.

A total of 14 cases were considered in the assessment of DWPF melter off-gas flammability using two computer models that describe the cold cap chemistry and off-gas combustion and dynamics. Seven of those cases involved the SB10 simulants which were tested during the bench-scale CPC demonstration, and the resulting baseline SB10 melter feeds were all shown to be well under the off-gas flammability safety basis limits at the peak of the 9X/5X off-gas surge for bubbled melter operation. The concentration of coal-carbon in the baseline melter feeds varied widely from 0 to 17,863 ppm, depending on the acid addition strategy used and the extent to which the required reductant (formic acid) was replaced with coal-carbon. The highest coal-carbon concentration in the baseline SB10 melter feeds occurred when the least amount of formic acid was used at the highest nitrate concentration (SB10-1). On the other hand, the coal-carbon concentration was zero at the two highest formate concentrations coupled with the two lowest nitrate concentrations (SB10-7 and SB10-8). Therefore, the theoretical maximum coal-carbon limit for the melter feed will occur when the formic acid addition is kept to a minimum, as required by the reduction of Hg and Mn and the destruction of nitrite, while maintaining as high a nitrate level as possible at a target redox. All baseline feeds were redox-adjusted, and three of the seven baseline melter feeds contained TOC higher than the current DWPF theoretical limit of 18,900 ppm.

Since the off-gas flammability potential for all seven baseline feeds was below the safety basis limits, additional coal-carbon was added to each baseline feed next until the calculated peak off-gas flammability during the 9X/5X off-gas surge equaled the safety basis limit of 60 % of the LFL for normal operation. In doing so, however, no counterbalancing nitrate was added, thus simulating the scenario where slugs of coal-carbon enter the melter as a result of uneven distribution of coal-carbon in the slurry. The results of this “max-coal” feed simulation showed that the amount of additional coal-carbon that can be added before the safety basis limit is exceeded varies from 1,190 ppm (SB10-1) to 5,200 ppm (SB10-9). Including the coal-carbon contained in the baseline feeds, the theoretical maximum coal-carbon concentration that can be processed through the DWPF melter without exceeding the safety basis limits varies from 3,400 ppm (SB10-8) to 19,032 ppm (SB10-1). The resulting TOC, including the excess coal-carbon, would exceed the current DWPF theoretical limit in all SB10 max-coal feeds except SB10-8 whose TOC is just below the theoretical maximum.

5.0 Recommendations

The following recommendations are the result of a number of lessons learned during the performance of this testing.

1. The results of this feasibility analysis indicate that the processing of SB10 sludge together with the FBSR product using a coal-carbon concentration of <9.5 wt % (<14,700 mg/kg carbon) and SWPF products is possible in the CPC. However, since every sludge batch has a different composition and requires different acid addition amounts, this limit should be reevaluated with each new sludge batch as part of the sludge batch qualification program.

2. The Tank 48 team should attempt to minimize the coal-carbon content in the FBSR product. Minimizing the coal-carbon concentration will also limit the nonradioactive impurities added in waste processing (coal ash, carbon, sulfur, etc.).
3. Develop a method to measure the carbon concentration in washed sludge and CPC slurries. AD has been unable to accurately measure the carbon concentration with existing instruments and methods.
4. Limit the FBSR product particle size to <177 μm. This may require FBSR product particle size reduction.
5. Given the contractual commitments for canister production and waste loading, the impact of FBSR product on melt rate should be experimentally assessed. Melt rate was not measured as part of this study, nor was the optimum frit used during this study.
6. Use a melter for in-situ sampling or post-mortem (destructive) analysis to assess the potential for localized reduction, the formation of metallic precipitates, and/or possible interactions of reduced species (such as nickel sulfides) on materials of construction.
7. Testing of the sludge wash material that was collected during sludge preparation should be used in testing to determine whether this large quantity of sodium carbonate produced during sludge washing will impact the HLW evaporators or Waste Tanks. The decanted supernate from washing SB10-B simulant have been collected and retained.
8. This preliminary study should be reassessed if a new CPC flowsheet is defined and when the FBSR product stream is finalized.

6.0 Acknowledgements

The sludge projections for future sludge batches were estimated by Jeff Gillam and David Larsen.

The SWPF cesium and actinide stream projections were provided by Azi Samadi and Celia Aponte.

The experiments were capably performed by SRNL technicians Phyllis Workman, Irene Reamer, Vickie Williams, Jon Duvall, David Healy and Tony Burkhalter. Their long hours, shift work, and careful control of the experiments are greatly appreciated.

The technical support offered by David Koopman, Michael Stone, and Brad Pickenheim in planning these experiments and reviewing the plans and results is very much appreciated.

The calibration, set up and post run analysis of the offgas data by Frances Williams and John Pareizs is appreciated.

The preparation of the simulants by David Healy and David Newell is also appreciated.

The analysis of the hundreds of samples by David Best, Whitney Riley, and Pat Simmons is greatly appreciated. In addition, analysis of rheology samples by Beverly Walls and the carbon analyses by Mike Williams, Sherry Vissage, Carol Jantzen and Kathy White were also appreciated.

The REDOX analysis by David Newell, Holly Hall, and Whitney Riley along with support from Gary Dobos and Curt Sexton of the SRNL glass shop was appreciated.

7.0 References

[1] WDPD-09-041, 'Letter of Direction - Tank 48 Business Decision (Re: Letter, Olson to Spears, LWO-EVP-2009-00025, 6/2/09)', June 10, 2009-07-28.
[2] Sludge Batch Plan 2009, SRR-LWP-2009-00009, Rev. 0, Oct 2009.
[3] Daniel W. E., M. R. Williams, C. M. Jantzen. 2009 THOR® (Thermal Organic Reduction) Engineering Scale Test Demonstration (ESTD) Fluidized Bed Steam Reformer (FBSR) Phase 3 Analytical Results, SRNL-TR-2009-00437, Revision 0, Savannah River Site, Aiken, SC 29808 (2010).
[4] Jantzen, C. M. and J. D. Newell, Defense Waste Processing Facility (DWPF) Sludge Batch 5 (SB5) REDOX Validation, SRNL-PSE-2008-00184, Savannah River Site, Aiken, SC 29808 (2008).
[5] Fellinger, T. L. 2009 Tank 7F Sludge Slurry Characterization and Wash Studies: Technical Task Request, HLW-DWPF-TTR-2009-0027, Rev. 0, Savannah River Site, Aiken, SC 29808 (2009).
[6] Lambert, D. P. , Task Technical and Quality Assurance Plan for DWPF Coal-Carbon WAC Limit Evaluation (Tank 48 Impact Study), SRNL-RP-2010-0126, Rev. 0, Savannah River Site, Aiken, SC 29808 (2010).
[7] Lambert, D. P., Choi, A. S., DWPF Coal-Carbon Waste Acceptance Criteria (WAC) Limit Evaluation (Tank 48 Impact Study), SRNL-RP-2010-00155, Rev. 0, Savannah River Site, Aiken, SC 29808 (2010).
[8] Samadi, A, Input Sheet for DWPF Coal WAC limit Evaluation (Tank 48 Impact Study), SRR-SPT-2010-00010, Rev 0, Savannah River Site, Aiken, SC 29808 (2010).
[9] C. M. Jantzen , Comparative Laboratory Measurement of Coal in Tank 48 Fluidized Bed Steam Reformer Samples, SRNL-TR-2010-00165, Rev 0, Savannah River Site, Aiken, SC 29808 (2010).
[10] Manual L29, Procedure ITS-00124, Rev 2, SRS HLW Sludge Simulant Preparation Savannah River Site, Aiken, SC 29808 (2008).
[11] Stone, M. E., Lab-Scale CPC Equipment Set-up, SRNL-ITS-2006-00074, Savannah River Site, Aiken, SC 29808 (2008).
[12] Manual L29, Procedure ITS-0094, Rev. 3, Laboratory Scale Chemical Process Cell Simulations, Savannah River Site, Aiken, SC 29808 (2006)
[13] Tank 48 Coal Carbon Study, WSRC-NB-2010-00017.
[14] Koopman, D.C., A.I. Fernandez, B.R. Pickenheim, Preliminary Evaluations of Two Proposed Stoichiometric Acid Equations, Revision 0, Savannah River Site, Aiken, SC 29808 (2009).
[15] Jantzen, C.M., J.R. Zamecnik, D.C. Koopman, C.C. Herman, and J.B. Pickett, Electron Equivalents Model for Controlling Reduction-Oxidation (REDOX) Equilibrium during High Level Waste (HLW) Vitrification, WSRC-TR-2003-00126, Savannah River Site, Aiken, SC 29808 (2003).
[16] Lambert, D. P., Acid Calculation Spreadsheet for DWPF Simulations, Revision 1 (Dated 8/14/06), SRNL-PSE-2006-00173, Savannah River Site, Aiken, SC 29808 (2006).
[17] Lambert, D.P., M. E. Stone, B. R. Pickenheim, D. R. Best, D. C. Koopman, Sludge Batch 5 Simulant Flowsheet Studies, SRNS-STI-2008-00024, Revision 0, Savannah River Site, Aiken, SC 29808 (2008).
[18] Stone, M. E., FY06 Feed Preparation for Melt Rate Testing, WSRC-STI-2006-0007, Savannah River Site, Aiken, SC 29808 (2006).
[19] PT Technical Data Summary for the Defense Waste Processing Facility: Sludge Plant", DPSTD-80-38-2

[20] Manual L29, Procedure ITS-0052, Rev. 2, Heat Treatment of Waste Slurries for REDOX ($Fe^{2+}/\Sigma Fe$) & Chemical Composition Measurement, Savannah River Site, Aiken, SC 29808 (2009).
[21] C.M. Jantzen, J.B. Pickett, K.G. Brown, T.B. Edwards and D.C. Beam, Process/Product Models for the Defense Waste Processing Facility (DWPF): Part I Predicting Glass Durability from Composition Using a Thermodynamic Hydration Energy Reaction Model (THERMO), WSRC-TR-93-672, Westinghouse Savannah River Company, Aiken, SC (1995).
[22] D.K. Peeler AND T.B. Edwards, Frit Development for Sludge Batch 3, WSRC-TR-2002-00491, Westinghouse Savannah River Company, Aiken, SC (2002).
[23] CM Jantzen, Comparative Laboratory Measurement of Coal in Tank 48 Fluidized Bed Steam Reforming Samples, SRNL-TR-2010-00165, Revision 0, Savannah River National Laboratory, Aiken, SC 29808 (2010).
[24] Choi, A. S., Validation of DWPF Melter Off-Gas Combustion Model, WSRC-TR-2000-00100, Savannah River Site, Aiken, SC 29808 (2000).
[25] Choi, A. S., Validation of DWPF MOG Dynamics Model - Phase I, WSRC-TR-96-0307, Savannah River Site, Aiken, SC 29808 (1997).
[26] Choi, A. S., DWPF Melter Off-Gas Flammability Assessment, X-CLC-S-00164, Rev. 4 (2010).
[27] Plante, E. R., Bonnell, D. W., and Hastie, J. W., Experimental and Theoretical Determination of Oxide Glass Vapor Pressures and Activities, Advances in the Fusion of Glass, Am. Cer. Soc., pp26.1-26.18 (1988).

Appendix A: Acid Calculation Results from Experiments

Table A-1. SRNL Acid, Trim Chemical, Dewater and Redox Calculations								
Run #	**SB10-1**	**SB10-2**	**SB10-3**	**SB10-5**	**SB10-7**	**SB10-8**	**SB10-9**	**Units**
Run Description:	Highest FBSR, 100% acid stoichiometry, redox 0.2	Highest FBSR, 150% acid stoichiometry, redox 0.2	Highest FBSR, 100% acid stoichiometry, redox 0.2	Lowest FBSR, 100% acid stoichiometry, redox 0.2	No FBSR, 100% acid stoichiometry, redox 0.2	No FBSR, 150% acid stoichiometry, redox 0.2	Med FBSR, 150% acid stoichiometry, redox 0.2 with ARP/MCU	
Sludge Feed Batch #	SB10-B	SB10-B	Blend of SB10-A and SB10-B	SB10-A and Sludge 10-B Lowest FBSR Blend	SB10-A	SB10-A	SB10-A/B Blend	
SRAT Vessel Volume, L	4	4	4	4	4	4	4	
Table A-1a -- Sludge Analyses for Acid Calculations								
Fresh Sludge Mass without trim chemicals	3,153.5	3,152.2	3,174.0	3,202.8	3,231.6	3,230.4	2,537.0	g slurry
Fresh Sludge Weight % Total Solids	15.45	15.45	16.21	17.04	17.84	17.84	16.21	wt%
Fresh Sludge Weight % Calcined Solids	11.65	11.65	12.52	13.45	14.37	14.37	12.52	wt%
Fresh Sludge Weight % Insoluble Solids	11.58	11.58	11.44	11.30	11.16	11.16	11.44	wt%
Fresh Sludge Density	1.125	1.125	1.134	1.144	1.153	1.153	1.134	kg / L slurry
Fresh Sludge Supernate density	1.036	1.036	1.043	1.051	1.058	1.058	1.043	kg / L supernate
Fresh Sludge Nitrite	6,680	6,680	7,562	8,507	9,435	9,435	7,562	mg/kg slurry
Fresh Sludge Nitrate	4,895	4,895	5,150	5,422	5,690	5,690	5,150	mg/kg slurry
Fresh Sludge Formate	0	0	0	0			0	mg/kg slurry
Fresh Sludge Sulfate (mg/kg)	323	323	319	316	312	312	319	mg/kg slurry
Fresh Sludge Chloride (mg/kg)	352	352	239	118	0	0	239	mg/kg slurry
Fresh Sludge Phosphate (mg/kg)	0	0	0	0	0	0	0	mg/kg slurry
Fresh Sludge Oxalate	140	140	95	47	0	0	95	mg/kg slurry
Fresh Sludge Slurry TIC (treated as	2,219	2,219	1,940	1,641	1,347	1,347	1,940	mg/kg slurry

Table A-1. SRNL Acid, Trim Chemical, Dewater and Redox Calculations								
Run #	**SB10-1**	**SB10-2**	**SB10-3**	**SB10-5**	**SB10-7**	**SB10-8**	**SB10-9**	**Units**
carbonate)								
Fresh Supernate TIC (treated as carbonate)	1,719	1,719	1,539	1,345	1,151	1,151	1,539	mg/L supernate
Fresh Sludge Hydroxide (Base Equivalents) pH = 7	0.664	0.664	0.741	0.825	0.909	0.909	0.741	Equiv Moles Base/L slurry
Fresh Sludge Coal-carbon/Carbon source	9.595	9.595	6.213	2.931	0.000	0.000	6.214	wt% dry basis
Fresh Sludge Manganese (% of Calcined Solids)	5.825	5.825	5.652	5.492	5.355	5.355	5.652	wt % calcined basis
Fresh Sludge Mercury (% of Total Solids in untrimmed sludge)	0.0000	0.0000	0.0000	0.0000	0.0000	0.0000	0.0000	wt% dry basis
Fresh Sludge Magnesium (% of Calcined Solids)	0.367	0.367	0.353	0.340	0.330	0.330	0.353	wt % calcined basis
Fresh Sludge Sodium (% of Calcined Solids)	13.600	13.600	14.021	14.410	14.745	14.745	14.021	wt % calcined basis
Fresh Sludge Potassium (% of Calcined Solids)	0.253	0.253	0.234	0.217	0.202	0.202	0.234	wt % calcined basis
Fresh Sludge Cesium (% of Calcined Solids)	0.000	0.000	0.000	0.000	0.000	0.000	0.000	wt % calcined basis
Fresh Sludge Calcium (% of Calcined Solids)	2.915	2.915	2.762	2.620	2.499	2.499	2.762	wt % calcined basis
Fresh Sludge Strontium (% of Calcined Solids)	0.000	0.000	0.000	0.000	0.000	0.000	0.000	wt % calcined basis
Fresh Sludge Nickel (% of Calcined Solids)	0.830	0.830	0.796	0.764	0.736	0.736	0.796	wt % calcined basis
Fresh Sludge Supernate manganese	0.000	0.000	0.000	0.000	0.000	0.000	0.000	mg/L supernate

Table A-1. SRNL Acid, Trim Chemical, Dewater and Redox Calculations								
Run #	**SB10-1**	**SB10-2**	**SB10-3**	**SB10-5**	**SB10-7**	**SB10-8**	**SB10-9**	**Units**
Table A-1b -- ARP Analyses for Acid Calculations								
ARP Mass without trim chemicals	No ARP						2691.00	g slurry
ARP Weight % Total Solids							4.43	wt%
ARP Weight % Calcined Solids							2.98	wt%
ARP Weight % Insoluble Solids							2.15	wt%
ARP Density							1.0314	kg / L slurry
ARP Supernate density							1.01	kg / L supernate
ARP Nitrite							592.5	mg/kg slurry
ARP Nitrate							6325	mg/kg slurry
ARP Oxalate							3910	mg/kg slurry
ARP Formate							0	mg/kg slurry
ARP Sulfate (mg/kg)							812	mg/kg slurry
ARP Chloride (mg/kg)							0	mg/kg slurry
ARP Phosphate (mg/kg)							0	mg/kg slurry
ARP Coal/Carbon source							0	wt% dry basis
ARP Slurry TIC (treated as carbonate)							202	mg/kg slurry
ARP Supernate TIC (treated as carbonate)							151	mg/L supernate
ARP Hydroxide (Base Equivalents) pH = 7							0.14816	Equiv Moles Base/L slurry
ARP Mercury (% of Total Solids in untrimmed sludge)							0	wt% dry basis
ARP Manganese (% of Calcined Solids)							1.67	wt % calcined basis

Table A-1. SRNL Acid, Trim Chemical, Dewater and Redox Calculations								
Run #	**SB10-1**	**SB10-2**	**SB10-3**	**SB10-5**	**SB10-7**	**SB10-8**	**SB10-9**	**Units**
ARP Magnesium (% of Calcined Solids)							0.65	wt % calcined basis
ARP Sodium (% of Calcined Solids)							27.55	wt % calcined basis
ARP Potassium (% of Calcined Solids)							0.11	wt % calcined basis
ARP Cesium (% of Calcined Solids)							0	wt % calcined basis
ARP Calcium (% of Calcined Solids)							1.03	wt % calcined basis
ARP Strontium (% of Calcined Solids)							0	wt % calcined basis
ARP Nickel (% of Calcined Solids)							0.3	wt % calcined basis
ARP Supernate manganese							0	mg/L supernate
Table A-1c -- MCU Analyses for Acid Calculations,								
MCU Mass without trim chemicals,	No MCU						2985.00	g
MCU Weight % Total Solids							0.2	wt % total solids
MCU Density							1.001	g/mL
MCU Supernate density							1.001	g/mL
MCU Nitrite							0	mg/kg slurry
MCU Nitrate							2,044	mg/kg slurry
MCU Hydroxide (Base Equivalents) pH = 7							-0.033	Equiv Moles Base/L slurry
Table 2 -- SRAT Processing Assumptions, Run #								
Conversion of Nitrite to Nitrate in SRAT Cycle	22.00	25.00	-5.95	-6.97	22.00	28.00	-27.26	gmol NO_3^- /100 gmol NO_2^-
Destruction of Nitrite	100.00	100.00	100.00	100.00	100.00	100.00	100.00	% of starting

Table A-1. SRNL Acid, Trim Chemical, Dewater and Redox Calculations								
Run #	**SB10-1**	**SB10-2**	**SB10-3**	**SB10-5**	**SB10-7**	**SB10-8**	**SB10-9**	**Units**
in SRAT and SME cycle								nitrite destroyed
Destruction of Formic acid charged in SRAT	100.00	60.00	20.72	28.67	20.00	35.00	27.24	% formate converted to CO_2 etc.
Destruction of Oxalate charged	50.00	50.00	50.00	50.00	50.00	50.00	50.00	% of total oxalate destroyed
Percent Acid in Excess Stoichiometric Ratio	96.78	150.00	100.00	100.00	100.00	150.00	150.00	%
SRAT Product Target Solids	25.00	25.00	25.00	25.00	25.00	25.00	25.00	%
Nitric Acid Molarity	10.534	10.600	10.400	10.400	10.600	10.534	10.400	Molar
Formic Acid Molarity	23.800	23.800	23.840	23.840	23.800	23.800	23.840	Molar
DWPF Nitric Acid addition Rate	2.0	2.0	2.0	2.0	2.0	2.0	2.0	gallons per minute
DWPF Formic Acid addition Rate	2.0	2.0	2.0	2.0	2.0	2.0	2.0	gallons per minute
REDOX Target	0.200	0.200	0.200	0.200	0.200	0.200	0.200	Fe^{+2} / ΣFe
Trimmed Sludge Target Ag metal content	0.0108	0.0108	0.0119	0.0130	0.0142	0.0142	0.0119	total wt% dry basis after trim
Trimmed Sludge Target wt% Hg dry basis	1.2272	1.2272	1.3526	1.4868	1.6188	1.6188	1.3526	total wt% dry basis after trim
Trimmed Sludge Target Pd metal content	0.0050	0.0050	0.0055	0.0061	0.0066	0.0066	0.0055	total wt% dry basis after trim
Trimmed Sludge Target Rh metal content	0.0177	0.0177	0.0195	0.0214	0.0233	0.0233	0.0195	total wt% dry basis after trim
Trimmed Sludge Target Ru metal	0.0850	0.0850	0.0937	0.1030	0.1121	0.1121	0.0937	total wt% dry basis after

Table A-1. SRNL Acid, Trim Chemical, Dewater and Redox Calculations								
Run #	**SB10-1**	**SB10-2**	**SB10-3**	**SB10-5**	**SB10-7**	**SB10-8**	**SB10-9**	**Units**
content								trim
Trimmed Sludge Target Wt% Coal-carbon/carbon source dry basis	9.4406	9.4406	6.1032	2.8744	0.0000	0.0000	6.1036	total wt% dry basis after trim
Trimmed Sludge Target oxalate after trim (wt % not mg/kg)	0.0892	0.0892	0.0576	0.0272	0.0000	0.0000	0.0447	total wt% dry basis after trim
Water to dilute fresh sludge and/or rinse trim chemicals	100.00	100.00	100.00	100.00	100.00	100.00	100.00	g
Mass of SRAT cycle samples	250.00	250.00	250.00	250.00	250.00	250.00	250.00	g
Wt% Active Agent In Antifoam Solution	10	10	10	10	10	10	10	%
Basis Antifoam Addition for SRAT (generally 100 mg antifoam/kg slurry)	100	100	100	100	100	100	100	mg/kg slurry
Number of basis antifoam additions added during SRAT cycle	8	8	8	8	8	8	12	
SRAT air purge	230	230	230	230	230	230	230	scfm
SRAT boil-up rate	5000	5000	5000	5000	5000	5000	5000	lbs/hr
SRAT total boil-up (reflux)	60,000	60,000	60,000	60,000	60,000	60,000	60,000	lbs
SRAT Steam Stripping Factor	750	750	750	750	750	750	750	(g steam/g mercury)
Table 3 -- SME Processing Assumptions								
Frit type	418	418	418	418	418	418	418	
Destruction of Formic acid in SME	5.00	5.00	5.00	5.00	5.00	5.00	5.00	% Formate converted to CO_2 etc.

Table A-1. SRNL Acid, Trim Chemical, Dewater and Redox Calculations								
Run #	**SB10-1**	**SB10-2**	**SB10-3**	**SB10-5**	**SB10-7**	**SB10-8**	**SB10-9**	**Units**
Destruction of Nitrate in SME	5.00	5.00	5.00	5.00	5.00	5.00	5.00	% Nitrate destroyed in SME
Assumed SME density	1.450	1.450	1.450	1.450	1.450	1.450	1.450	kg / L
Sludge Oxide Contribution in SME (Waste Loading)	38.00	38.00	38.00	38.00	38.00	38.00	38.00	%
Frit Slurry Formic Acid Ratio	1.50	1.50	1.50	1.50	1.50	1.50	1.50	g 90 wt% FA/100 g Frit
Target SME Solids total Wt%	50.0	50.0	50.0	50.0	50.0	50.0	50.0	wt%
Number of frit additions in SME Cycle	2	2	2	2	2	2	2	
# DWPF Canister decons simulated	0.0	0.0	0.0	0.0	0.0	0.0	0.0	
Volume of water per deconned can	1,000	1,000	1,000	1,000	1,000	1,000	1,000	gal at DWPF scale
Water flush volume after frit slurry addition	0.0	0.0	0.0	0.0	0.0	0.0	0.0	gal
SME air purge	74	74	74	74	74	74	74	scfm
SME boil-up rate	5000	5000	5000	5000	5000	5000	5000	lbs/hr
Acid and Glass Calculation Base Values								
Total nitrite	0.458	0.458	0.522	0.592	0.663	0.663	0.452	gmol
Total Mn minus soluble Mn	0.390	0.389	0.409	0.431	0.453	0.452	0.351	gmol
Total carbonate	0.583	0.582	0.513	0.438	0.362	0.362	0.455	gmol
Total hydroxide	1.861	1.860	2.075	2.311	2.548	2.547	1.947	gmol
Total mercury	0.030	0.030	0.035	0.040	0.047	0.047	0.028	gmol
Total oxalate	0.005	0.005	0.003	0.002	0.000	0.000	0.122	gmol
Total grams of calcined oxides	367.465	367.314	397.471	430.905	464.364	464.191	397.891	g
Trim Chemicals	7.9623	7.9590	9.2829	10.8328	12.4809	12.4762	9.5685	

Table A-1. SRNL Acid, Trim Chemical, Dewater and Redox Calculations								
Run #	**SB10-1**	**SB10-2**	**SB10-3**	**SB10-5**	**SB10-7**	**SB10-8**	**SB10-9**	**Units**
Calculations								
Fresh Sludge Calcine Factor (1100° C), g oxide/g dry solids (calculated)	0.7543	0.7543	0.7723	0.7897	0.8053	0.8053	0.7723	g/g
ARP calcine factor	0.0000	0.0000	0.0000	0.0000	0.0000	0.0000	0.6727	g/g
Total solids before trim addition	487.1300	486.9291	514.6610	545.6458	576.6522	576.4380	530.5815	g
Total solids before trim less HgO, NaOxalate, coal-carbon)	439.73	439.55	482.23	529.42	576.65	576.44	497.25	g
Predicted total solids at target levels	495.0923	494.8882	523.9439	556.4786	589.1330	588.9143	540.1500	g
Predicted total mass at target levels	3,261.4623	3,261.7956	3,285.1926	3,315.8625	3,346.6510	3,345.4454	5,339.3161	g
Target Ag metal content in trimmed sludge	0.010765	0.010765	0.011865	0.013043	0.014200	0.014200	0.011865	total wt% dry basis
$AgNO_3$ to add (CF=0.682)	0.00000	0.08390	0.09790	0.11430	0.13174	0.13170	0.08959	g
Ag2O calcined solids	0.00000	0.05723	0.06678	0.07796	0.08986	0.08983	0.06111	g
Water added with Ag	0.00000	0.00000	0.00000	0.00000	0.00000	0.00000	0.00000	g
Target wt% Hg dry basis	1.227	1.227	1.353	1.487	1.619	1.619	1.353	total wt% dry basis
Total HgO in fresh Sludge	0.000	0.000	0.000	0.000	0.000	0.000	0.000	g
Total HgO in trimmed Sludge	6.56029	6.55758	7.65205	8.93374	10.29730	10.29348	7.88867	g
HgO to add	0.00000	6.55758	7.65205	8.93374	10.29730	10.29348	7.00246	g
HgO calcined solids	0.00000	0.00000	0.00000	0.00000	0.00000	0.00000	0.00000	g
Water added with Hg	0.00000	0.00000	0.00000	0.00000	0.00000	0.00000	0.00000	g
Calculated total wt%	0.0000	1.2272	1.3526	1.4868	1.6188	1.6188	1.2006	wt% dry basis

Table A-1. SRNL Acid, Trim Chemical, Dewater and Redox Calculations								
Run #	**SB10-1**	**SB10-2**	**SB10-3**	**SB10-5**	**SB10-7**	**SB10-8**	**SB10-9**	**Units**
Hg dry basis								
Target Pd metal content in trimmed sludge	0.0050	0.0050	0.0055	0.0061	0.0066	0.0066	0.0055	total wt% dry basis
Wt % Pd in reagent solution	15.2700	15.2700	15.2700	15.2700	15.2700	15.2700	15.2700	wt% in solution
$Pd(NO_3)_2*H_2O$ solution to add (CF=1.150 g metal oxide/g metal)	0.00000	0.16216	0.18922	0.22092	0.25464	0.25454	0.17316	g of solution
Pd(NO3)2 to add	0.00000	0.05362	0.06256	0.07304	0.08419	0.08416	0.05725	g
PdO calcined solids	0.00000	0.02848	0.03324	0.03881	0.04473	0.04471	0.03042	g
Water added with Pd	0.000	0.109	0.127	0.148	0.170	0.170	0.116	g
Target Rh metal content in trimmed sludge	0.0177	0.0177	0.0195	0.0214	0.0233	0.0233	0.0195	total wt% dry basis
Wt% Rh in reagent solution	4.93	4.93	4.93	4.93	4.93	4.93	4.93	wt% in solution
$Rh(NO_3)_3*2H_2O$ (CF=1.311g metal oxide/g metal)	0.0000	1.7731	2.0691	2.4156	2.7843	2.7833	1.8934	g of solution
Rh(NO3)3 to add	0.00000	0.24543	0.28639	0.33436	0.38540	0.38525	0.26208	g
Rh2O3 calcined solids	0.00000	0.10780	0.12579	0.14686	0.16928	0.16922	0.11512	g
Water added with Rh	0.000	1.528	1.783	2.081	2.399	2.398	1.631	g
Target Ru metal content in trimmed sludge	0.0850	0.0850	0.0937	0.1030	0.1121	0.1121	0.0937	total wt% dry basis
Wt% Ru in $RuCl_3$ reagent solids	41.74	41.74	41.74	41.74	41.74	41.74	41.74	wt% in solids
$RuCl_3$ to add (CF=1.0)	0.0000	1.0076	1.1758	1.3727	1.5822	1.5816	1.0760	g solid
Target wt% Coal-carbon/carbon source in trimmed sludge, dry basis	9.44	9.44	6.10	2.87	0.00	0.00	6.10	total wt% dry basis

Table A-1. SRNL Acid, Trim Chemical, Dewater and Redox Calculations								
Run #	**SB10-1**	**SB10-2**	**SB10-3**	**SB10-5**	**SB10-7**	**SB10-8**	**SB10-9**	**Units**
Total Coal-carbon in fresh Sludge	46.740	46.720	31.977	15.995	0.000	0.000	25.561	g
Total Coal-carbon in trimmed Sludge	46.739	46.720	31.977	15.995	0.000	0.000	32.969	g
Mass of Coal to add (CF =.08)	0.00	0.00	0.00	0.00	0.00	0.00	0.00	g
Calculated wt% coal after trim additions	9.44	9.44	6.10	2.87	0.00	0.00	6.10	wt%
Target sodium oxalate in trimmed sludge per gm total solids	0.14	0.14	0.09	0.04	0.00	0.00	0.07	total wt% dry basis
Total Sodium Oxalate in fresh Sludge	0.672	0.672	0.460	0.230	0.000	0.000	0.368	g
Total Sodium Oxalate in trimmed Sludge	0.672	0.672	0.460	0.230	0.000	0.000	0.368	g
Sodium oxalate to add (CF=0.463)	-0.0000015	-0.0000015	0.0000000	-0.0000012	0.0000000	0.0000000	-0.0000038	g
Calculated oxalate conc. after trim chemical additions	0.14	0.14	0.09	0.04	0.00	0.00	0.07	total wt% dry basis
Na2O calcined solids from sodium oxalate	0.31088	0.31075	0.21269	0.10639	0.00000	0.00000	0.17001	
Total mass of trim chemicals added	0.0	9.6	11.2	13.1	15.1	15.0	10.2	g
Calcined oxides added in trim chemicals	0.00	1.20	1.40	1.64	1.89	1.89	1.28	g
Total solids after trim addition	487.13	494.88	523.94	556.47	589.13	588.91	539.07	g
Match of actual to predicted total solids mass	101.61%	100.00%	100.00%	100.00%	100.00%	100.00%	100.20%	
Total Calcined solids after trim	367.47	368.51	398.87	432.54	466.25	466.08	399.17	g

Table A-1. SRNL Acid, Trim Chemical, Dewater and Redox Calculations								
Run #	**SB10-1**	**SB10-2**	**SB10-3**	**SB10-5**	**SB10-7**	**SB10-8**	**SB10-9**	**Units**
Water added to dilute and/or rinse trim chemicals	100.0	100.0	100.0	100.0	100.0	100.0	100.0	g
Mass of trimmed sludge	3,253.50	3,261.78	3,285.18	3,315.86	3,346.65	3,345.44	5,338.23	g
Calculated wt% total solids in SRAT receipt sludge	15.4	15.4	16.2	17.0	17.8	17.8	16.2	wt%
Sample mass of trimmed sludge	0.00	0.00	0.00	0.00	0.00	0.00	0.00	g
Mass of trimmed feeds reacted	3,253.50	3,261.78	3,285.18	3,315.86	3,346.65	3,345.44	5,338.23	g
Mass of equivalent sludge w/o ARP	3,153.50	3,203.65	3,231.20	3,266.36	3,301.54	3,300.32	3,324.54	g, used to calculate scaling factors, etc.
Sample removal ratio at start of ARP boil	1.000	1.000	1.000	1.000	1.000	1.000	1.000	
Sample removal ratio at start of SRAT	1.000	1.000	1.000	1.000	1.000	1.000	1.000	
Calcined solids at start of SRAT	367.5	368.5	398.9	432.5	466.3	466.1	399.2	g
STOICHIOMETRIC ACID CALCULATIONS								
Fresh feed NO_2^-	0.46	0.46	0.52	0.59	0.66	0.66	0.45	gmol
Fresh feed Manganese	0.38962	0.38946	0.40892	0.43075	0.45259	0.45242	0.35123	gmol
Fresh feed slurry Carbonate	0.5827	0.5824	0.5126	0.4376	0.3624	0.3623	0.4550	gmol
Fresh feed OH^-	1.8610	1.8603	2.0748	2.3114	2.5482	2.5473	1.9465	gmol
Fresh feed H+	0.0000	0.0000	0.0000	0.0000	0.0000	0.0000	-0.0984	gmol
Total Sludge Mercury	0.030289	0.030277	0.035330	0.041247	0.047543	0.047525	0.036422	gmol
Acid requirement per mole of Oxalate	0.01	0.01	0.00	0.00	0.00	0.00	0.12	gmol

Table A-1. SRNL Acid, Trim Chemical, Dewater and Redox Calculations								
Run #	**SB10-1**	**SB10-2**	**SB10-3**	**SB10-5**	**SB10-7**	**SB10-8**	**SB10-9**	**Units**
Fresh Feed Supernate Carbonate	0.38	0.38	0.35	0.30	0.26	0.26	0.31	gmol
Fresh Feed Calcium	0.27	0.27	0.27	0.28	0.29	0.29	0.24	gmol
Fresh Feed Magnesium	0.06	0.06	0.06	0.06	0.06	0.06	0.07	gmol
Fresh Feed Sodium	2.17	2.17	2.42	2.70	2.98	2.98	2.90	gmol
Fresh Feed Potassium	0.02	0.02	0.02	0.02	0.02	0.02	0.02	gmol
Fresh Feed Cesium	0.00	0.00	0.00	0.00	0.00	0.00	0.00	gmol
Fresh Feed Strontium	0.00	0.00	0.00	0.00	0.00	0.00	0.00	gmol
Fresh Feed Nickel	0.05	0.05	0.05	0.06	0.06	0.06	0.05	gmol
Fresh Feed Nitrate	0.25	0.25	0.26	0.28	0.30	0.30	0.49	gmol
Fresh Feed Sulfate	0.01	0.01	0.01	0.01	0.01	0.01	0.03	gmol
Fresh Feed Chloride	0.03	0.03	0.02	0.01	0.00	0.00	0.02	gmol
Fresh Feed Formate	0.00	0.00	0.00	0.00	0.00	0.00	0.00	gmol
Fresh Feed Phosphate	0.00	0.00	0.00	0.00	0.00	0.00	0.00	gmol
Hsu Total Stoichiometric Acid required	3.8676	3.8660	4.0174	4.1889	4.3608	4.3592	3.6532	gmol
Koopman Nominal Stoichiometric Acid required	4.5135	4.5117	4.8365	5.1977	5.5594	5.5573	4.3798	gmol
Koopman Minimum Stoichiometric Acid required	3.8026	3.8011	4.0880	4.4068	4.7261	4.7243	3.7310	gmol
Cation Nominal Stoichiometric Acid required	3.7406	3.7391	4.0671	4.4307	4.7950	4.7932	4.0595	gmol
Cation Minimum Stoichiometric Acid required	3.1562	3.1549	3.4537	3.7846	4.1161	4.1146	3.5327	gmol
Percent Acid in Excess Stoichiometric Ratio	96.780	150.000	100.000	100.000	100.000	150.000	150.000	%

Table A-1. SRNL Acid, Trim Chemical, Dewater and Redox Calculations								
Run #	**SB10-1**	**SB10-2**	**SB10-3**	**SB10-5**	**SB10-7**	**SB10-8**	**SB10-9**	**Units**
Actual acid to add to SRAT	3.6802	5.7016	4.0880	4.4068	4.7261	7.0865	5.5964	gmol
Acid required in moles per liter of starting sludge (untrimmed, less receipt samples)	1.3129	2.0349	1.4604	1.5735	1.6867	2.5300	2.5013	gmol/L

Appendix B: Analytical Results from Experiments

Table B-1. Analytical Results for SRAT Product and SME Product Filtered Slurries

Process Science Analytical Laboratory									
Date: 7/12/10									
ICP-AES elemental supernate (mg/L)									
Sample ID	**Lab ID**	**Ag**	**Al**	**Ba**	**Ca**	**Cd**	**Cr**	**Cu**	**Fe**
10-SB10-1-3566 (A)	10-0793	<0.100	3.39	128	3270	<0.010	0.354	1.68	<0.010
10-SB10-1-3566 (B)	10-0793	<0.100	2.67	128	3270	<0.010	0.391	1.63	<0.010
10-SB10-1-3570 (A)	10-0794	<0.100	2.09	132	5460	<0.010	0.261	2.18	<0.010
10-SB10-1-3570 (B)	10-0794	<0.100	2.07	131	5380	<0.010	0.381	2.20	<0.010
10-SB10-2-3588 (A)	10-0797	<0.100	543	197	3180	<0.010	5.52	42.7	510
10-SB10-2-3588 (B)	10-0797	<0.100	536	203	3200	<0.010	5.40	41.9	532
10-SB10-2-3592 (A)	10-0798	<0.100	30.3	178	4860	0.958	0.501	9.60	4850
10-SB10-2-3592 (B)	10-0798	<0.100	30.5	176	4830	1.01	0.654	9.51	4780
10-SB10-3-3837 (A)	10-0912	<0.100	4.88	126	3383	<0.010	0.383	NM	<0.010
10-SB10-3-3837 (B)	10-0912	<0.100	4.92	130	3426	<0.010	0.470	NM	<0.010
10-SB10-3-3841 (A)	10-0913	<0.100	2.00	111	5174	<0.010	0.295	NM	<0.010
10-SB10-3-3841 (B)	10-0913	<0.100	1.97	111	5189	<0.010	0.192	NM	<0.010
10-SB10-5-3859 (A)	10-0914	<0.100	4.10	70.4	3663	<0.010	0.160	NM	<0.010
10-SB10-5-3859 (B)	10-0914	<0.100	4.22	71.1	3648	<0.010	0.270	NM	<0.010
10-SB10-5-3863 (A)	10-0915	<0.100	2.03	41.5	4808	<0.010	<0.010	NM	<0.010
10-SB10-5-3863 (B)	10-0915	<0.100	1.93	41.1	4784	<0.010	<0.010	NM	<0.010
10-SB10-7-3611 (A)	10-0795	<0.100	1.81	<0.010	3880	<0.010	<0.010	0.940	<0.010
10-SB10-7-3611 (B)	10-0795	<0.100	1.81	<0.010	3890	<0.010	<0.010	0.936	<0.010
10-SB10-7-3615 (A)	10-0796	<0.100	1.96	30.4	4710	<0.010	<0.010	1.05	<0.010
10-SB10-7-3615 (B)	10-0796	<0.100	1.84	30.4	4590	<0.010	<0.010	1.06	<0.010
10-SB10-8-3632 (A)	10-0799	<0.100	192	78.5	3830	<0.010	5.85	43.6	17.4
10-SB10-8-3632 (B)	10-0799	<0.100	186	77.9	3910	<0.010	5.75	43.5	17.4
10-SB10-8-3637 (A)	10-0800	<0.100	2.61	82.0	5060	<0.010	0.461	1.26	235
10-SB10-8-3637 (B)	10-0800	<0.100	2.39	81.6	5270	<0.010	0.430	1.22	236
10-SB10-9-3815 (A)	10-0916	<0.100	169	7.62	2322	<0.010	4.66	NM	34.4
10-SB10-9-3815 (B)	10-0916	<0.100	164	7.63	2345	<0.010	4.56	NM	35.0
10-SB10-9-3819 (A)	10-0917	<0.100	125	7.75	2388	<0.010	4.08	NM	751
10-SB10-9-3819 (B)	10-0917	<0.100	126	7.59	2339	<0.010	4.00	NM	762

Sample ID	Lab ID	K	Mg	Mn	Ni	P	Pb	Pd
10-SB10-1-3566 (A)	10-0793	424	287	4620	90.0	<1.00	<0.010	<1.00
10-SB10-1-3566 (B)	10-0793	423	290	4620	92.1	<1.00	<0.010	<1.00
10-SB10-1-3570 (A)	10-0794	896	525	4610	3.29	<1.00	0.185	<1.00
10-SB10-1-3570 (B)	10-0794	867	526	4560	3.42	<1.00	<0.010	<1.00
10-SB10-2-3588 (A)	10-0797	448	331	7240	494	<1.00	11.1	<1.00
10-SB10-2-3588 (B)	10-0797	438	342	7280	496	<1.00	11.3	<1.00
10-SB10-2-3592 (A)	10-0798	780	586	10800	670	<1.00	5.03	<1.00
10-SB10-2-3592 (B)	10-0793	782	576	10700	672	<1.00	4.88	<1.00
10-SB10-3-3837 (A)	10-0912	451	299	4846	158	<1.00	<0.010	0.225
10-SB10-3-3837 (B)	10-0912	464	307	5018	162	<1.00	<0.010	0.208
10-SB10-3-3841 (A)	10-0913	994	520	4905	2.51	<1.00	<0.010	0.128
10-SB10-3-3841 (B)	10-0913	1020	518	4811	2.47	<1.00	<0.010	0.138
10-SB10-5-3859 (A)	10-0914	457	329	3612	119	<1.00	<0.010	0.159
10-SB10-5-3859 (B)	10-0914	458	336	3662	123	<1.00	<0.010	0.136
10-SB10-5-3863 (A)	10-0915	860	480	1577	1.22	<1.00	<0.010	0.149
10-SB10-5-3863 (B)	10-0915	856	484	1589	1.21	<1.00	<0.010	0.189
10-SB10-7-3611 (A)	10-0795	501	380	3730	<0.010	<1.00	<0.010	<1.00
10-SB10-7-3611 (B)	10-0795	505	387	3700	<0.010	<1.00	<0.010	<1.00
10-SB10-7-3615 (A)	10-0796	819	495	1180	1.04	<1.00	<0.010	<1.00
10-SB10-7-3615 (B)	10-0796	808	494	1180	1.13	<1.00	<0.010	<1.00
10-SB10-8-3632 (A)	10-0799	496	423	8640	487	<1.00	3.56	<1.00
10-SB10-8-3632 (B)	10-0799	477	421	8730	476	<1.00	3.28	<1.00
10-SB10-8-3637 (A)	10-0800	762	583	8380	54.5	<1.00	0.803	<1.00
10-SB10-8-3637 (B)	10-0800	757	584	8440	54.6	<1.00	1.25	<1.00
10-SB10-9-3815 (A)	10-0916	445	399	6546	283	<1.00	<0.010	0.144
10-SB10-9-3815 (B)	10-0916	429	398	6497	282	<1.00	<0.010	0.140
10-SB10-9-3819 (A)	10-0917	445	406	6715	319	<1.00	0.988	0.125
10-SB10-9-3819 (B)	10-0917	448	406	6548	320	<1.00	0.771	0.096

Sample ID	Lab ID	Pr	Rh	Ru	S	Si	Ti	Zn	Zr
10-SB10-1-3566 (A)	10-0793	1.02	9.23	<1.00	8.26	155	<0.010	<0.010	0.030
10-SB10-1-3566 (B)	10-0793	0.967	9.01	<1.00	13.8	159	<0.010	<0.010	0.017
10-SB10-1-3570 (A)	10-0794	3.23	0.521	<1.00	23.3	42.9	<0.010	<0.010	0.030
10-SB10-1-3570 (B)	10-0794	3.29	0.512	<1.00	24.6	42.1	<0.010	<0.010	0.020
10-SB10-2-3588 (A)	10-0797	2.20	2.94	1.57	18.6	168	<0.010	14.9	0.560
10-SB10-2-3588 (B)	10-0797	2.22	2.94	1.59	21.8	166	<0.010	14.4	0.581
10-SB10-2-3592 (A)	10-0798	4.41	0.665	<1.00	23.3	83.0	<0.010	20.1	0.355
10-SB10-2-3592 (B)	10-0798	4.47	0.625	<1.00	32.0	83.8	<0.010	20.1	0.379
10-SB10-3-3837 (A)	10-0912	1.17	14.2	0.210	20.8	73.1	<0.010	0.308	0.036
10-SB10-3-3837 (B)	10-0912	1.23	14.2	0.332	25.3	74.0	<0.010	0.203	0.027
10-SB10-3-3841 (A)	10-0913	2.98	0.494	<0.010	31.8	32.4	<0.010	<0.010	0.025
10-SB10-3-3841 (B)	10-0913	2.94	0.484	<0.010	25.9	32.3	<0.010	<0.010	0.018
10-SB10-5-3859 (A)	10-0914	1.41	17.7	1.29	33.2	31.7	<0.010	<0.010	0.029
10-SB10-5-3859 (B)	10-0914	1.37	18.1	0.976	33.8	32.0	<0.010	<0.010	0.023
10-SB10-5-3863 (A)	10-0915	2.59	0.667	<0.010	41.8	19.6	<0.010	<0.010	0.023
10-SB10-5-3863 (B)	10-0915	2.63	0.660	<0.010	33.7	19.4	<0.010	<0.010	0.023
10-SB10-7-3611 (A)	10-0795	<0.010	0.447	<1.00	0.912	0.603	<0.010	<0.010	0.008
10-SB10-7-3611 (B)	10-0795	<0.010	0.447	<1.00	0.967	0.436	<0.010	<0.010	0.012
10-SB10-7-3615 (A)	10-0796	2.45	0.966	<1.00	48.6	36.2	<0.010	<0.010	0.022
10-SB10-7-3615 (B)	10-0796	2.54	0.954	<1.00	50.4	36.4	<0.010	<0.010	0.017
10-SB10-8-3632 (A)	10-0799	2.05	32.5	21.7	32.6	25.4	<0.010	13.9	0.170
10-SB10-8-3632 (B)	10-0799	2.04	32.5	21.4	38.4	25.7	<0.010	13.8	0.203
10-SB10-8-3637 (A)	10-0800	3.28	0.600	<1.00	32.9	105	<0.010	2.56	0.059
10-SB10-8-3637 (B)	10-0800	3.28	0.604	<1.00	32.8	107	<0.010	2.58	0.060
10-SB10-9-3815 (A)	10-0916	0.478	2.16	0.270	169	141	0.087	5.69	0.050
10-SB10-9-3815 (B)	10-0916	0.457	2.13	<0.010	160	140	0.086	5.61	0.046
10-SB10-9-3819 (A)	10-0917	0.572	1.88	<0.010	165	161	0.041	9.30	0.080
10-SB10-9-3819 (B)	10-0917	0.571	1.85	<0.010	166	155	0.040	8.99	0.073

Anions, mg/L								
Sample ID	Lab ID	F	Cl	NO2	NO3	SO4	C2O4	HCO2
10-SB10-1-3566 (A)	10-0793	<100	144	1610	56600	<100	<100	84500
10-SB10-1-3566 (B)	10-0793	<100	144	1640	58100	<100	<100	84800
10-SB10-1-3570 (A)	10-0794	<100	401	<100	100000	<100	<100	11400
10-SB10-1-3570 (B)	10-0794	<100	401	<100	102000	<100	<100	11300
10-SB10-2-3588 (A)	10-0797	<100	200	<100	75300	<100	<100	40000
10-SB10-2-3588 (B)	10-0797	<100	200	<100	74200	<100	<100	39600
10-SB10-2-3592 (A)	10-0798	<100	366	<100	109000	377	<100	41400
10-SB10-2-3592 (B)	10-0798	<100	366	<100	109000	377	<100	40000
10-SB10-3-3837 (A)	10-0912	<100	214	2060	57700	<1000	<100	17900
10-SB10-3-3837 (B)	10-0912	<100	214	2090	56200	<1000	<100	18200
10-SB10-3-3841 (A)	10-0913	<100	443	<100	93600	<1000	<100	25100
10-SB10-3-3841 (B)	10-0913	<100	443	<100	92100	<1000	<100	24900
10-SB10-5-3859 (A)	10-0914	<100	238	5230	38000	<1000	<100	33600
10-SB10-5-3859 (B)	10-0914	<100	238	5180	37500	<1000	<100	34200
10-SB10-5-3863 (A)	10-0915	<100	364	1030	57900	<1000	<100	49200
10-SB10-5-3863 (B)	10-0915	<100	364	1030	56100	<1000	<100	49100
10-SB10-7-3611 (A)	10-0795	<100	261	6440	20000	<100	<100	48500
10-SB10-7-3611 (B)	10-0795	<100	261	6420	21500	<100	<100	49400
10-SB10-7-3615 (A)	10-0796	<100	366	2920	28100	<100	<100	66400
10-SB10-7-3615 (B)	10-0796	<100	366	2960	27000	<100	<100	66400
10-SB10-8-3632 (A)	10-0799	<100	247	404	26000	319	<100	83300
10-SB10-8-3632 (B)	10-0799	<100	247	404	25800	319	<100	83400
10-SB10-8-3637 (A)	10-0800	<100	346	<100	33400	226	<100	86400
10-SB10-8-3637 (B)	10-0800	<100	346	<100	32000	226	<100	84900
10-SB10-9-3815 (A)	10-0916	<100	219	<100	59300	<1000	724	56000
10-SB10-9-3815 (B)	10-0916	<100	219	<100	56000	<1000	724	56100
10-SB10-9-3819 (A)	10-0917	<100	212	<100	56800	<1000	703	49900
10-SB10-9-3819 (B)	10-0917	<100	212	<100	57000	<1000	703	49400

Sample	Lab ID	Density	pH
10-SB10-1-3566 (A)	10-0793	1.0635	4.83
10-SB10-1-3566 (B)	10-0793	1.0633	
10-SB10-1-3570 (A)	10-0794	1.1044	5.46
10-SB10-1-3570 (B)	10-0794	1.1043	
10-SB10-2-3588 (A)	10-0797	1.0784	2.84
10-SB10-2-3588 (B)	10-0797	1.0784	
10-SB10-2-3592 (A)	10-0798	1.1202	3.46
10-SB10-2-3592 (B)	10-0798	1.1202	
10-SB10-3-3837 (A)	10-0912	1.0677	4.31
10-SB10-3-3837 (B)	10-0912	1.0677	
10-SB10-3-3841 (A)	10-0913	1.1027	5.88
10-SB10-3-3841 (B)	10-0913	1.1027	
10-SB10-5-3859 (A)	10-0914	1.0673	4.74
10-SB10-5-3859 (B)	10-0914	1.0673	
10-SB10-5-3863 (A)	10-0915	1.0929	6.22
10-SB10-5-3863 (B)	10-0915	1.0929	
10-SB10-7-3611 (A)	10-0795	1.0690	5.22
10-SB10-7-3611 (B)	10-0795	1.0689	
10-SB10-7-3615 (A)	10-0796	1.0896	6.49
10-SB10-7-3615 (B)	10-0796	1.0896	
10-SB10-8-3632 (A)	10-0799	1.0831	4.01
10-SB10-8-3632 (B)	10-0799	1.0831	
10-SB10-8-3637 (A)	10-0800	1.0998	4.63
10-SB10-8-3637 (B)	10-0800	1.0998	
10-SB10-9-3815 (A)	10-0916	1.0752	3.47
10-SB10-9-3815 (B)	10-0916	1.0753	
10-SB10-9-3819 (A)	10-0917	1.0766	3.59
10-SB10-9-3819 (B)	10-0917	1.0766	

Table B-2. Analytical Results for Composite Dewater Samples

Process Science Analytical Laboratory											
Date: 6/10/10, 7/13/10											
Lab ID: 10-0906-0908, 10-0769-0772											
Units: mg/L											
Sample ID	**Lab ID**	**F**	**Cl**	**NO2**	**NO3**	**SO4**	**C2O4**	**HCO2**		**Density**	**pH**
10-SB10-1-3569 (A)	10-0769	<100	<100	<100	2170	<100	<100	198		1.0089	1.8
10-SB10-1-3569 (B)	10-0769	<100	<100	<100	2100	<100	<100	201			
10-SB10-2-3591 (A)	10-0771	<100	<100	<100	335	<100	<100	4560		1.0106	2.3
10-SB10-2-3591 (B)	10-0771	<100	<100	<100	345	<100	<100	4680			
10-SB10-3-3839 (A)	10-0909	<100	<100	<100	1870	<100	<100	273		0.99928	1.8
10-SB10-3-3839 (B)	10-0909	<100	<100	<100	1790	<100	<100	274		0.99929	
10-SB10-5-3861 (A)	10-0910	<100	<100	121	3410	<100	<100	340		1.00012	1.6
10-SB10-5-3861 (B)	10-0910	<100	<100	121	3350	<100	<100	339		1.00012	
10-SB10-7-3614 (A)	10-0770	<100	<100	<100	3360	<100	<100	418		1.0112	1.7
10-SB10-7-3614 (B)	10-0770	<100	<100	<100	3300	<100	<100	415			
10-SB10-8-3636 (A)	10-0772	<100	<100	<100	2350	<100	<100	4180		1.0111	1.9
10-SB10-8-3636 (B)	10-0772	<100	<100	<100	2230	<100	<100	4030			
10-SB10-9-3817 (A)	10-0911	<100	<100	<100	912	<100	<100	3490		0.96311	2.1
10-SB10-9-3817 (B)	10-0911	<100	<100	<100	917	<100	<100	3550		0.96312	

Table B-3. Analytical Results for REDOX Samples

SRNL Process Science Analytical Laboratory						
Date: 7/15/10						
Lab ID: 10-1013 through 10-1029						
Units: absorbance					**Fe(2+)**	**Fe(2+)**
Sample	**Lab ID**	**Fe(2+)**	**Fe(3+)**	**Fe(total)**	**Fe(3+)**	**Fe(total)**
EA		0.026	0.093	0.119	0.280	0.218
10-SB10-3890 (A)	10-1013	0.050	0.207	0.257	0.242	0.195
10-SB10-3890 (B)	10-1013	0.051	0.207	0.258	0.246	0.198
10-SB10-3891 (A)	10-1014	0.096	0.192	0.288	0.500	0.333
10-SB10-3891 (B)	10-1014	0.096	0.192	0.288	0.500	0.333
10-SB10-3892 (A)	10-1015	0.112	0.193	0.305	0.580	0.367
10-SB10-3892 (B)	10-1015	0.113	0.190	0.303	0.595	0.373
10-SB10-3893 (A)	10-1016	0.053	0.286	0.339	0.185	0.156
10-SB10-3893 (B)	10-1016	0.054	0.286	0.340	0.189	0.159
10-SB10-3894 (A)	10-1017	0.053	0.213	0.266	0.249	0.199
10-SB10-3894 (B)	10-1017	0.053	0.212	0.265	0.250	0.200
10-SB10-3895 (A)	10-1018	0.079	0.220	0.299	0.359	0.264
10-SB10-3895 (B)	10-1018	0.080	0.219	0.299	0.365	0.268
10-SB10-3896 (A)	10-1019	0.033	0.239	0.272	0.138	0.121
10-SB10-3896 (B)	10-1019	0.034	0.236	0.270	0.144	0.126
10-SB10-3897 (A)	10-1020	0.080	0.167	0.247	0.479	0.324
10-SB10-3897 (B)	10-1020	0.081	0.166	0.247	0.488	0.328
10-SB10-3898 (A)	10-1021	<0.010	0.230	0.230	All Fe3+	All Fe3+
10-SB10-3898 (B)	10-1021	<0.010	0.231	0.231	All Fe3+	All Fe3+
10-SB10-3899 (A)	10-1022	0.083	0.182	0.265	0.456	0.313
10-SB10-3899 (B)	10-1022	0.080	0.185	0.265	0.432	0.302
10-SB10-3900 (A)	10-1023	0.012	0.231	0.243	0.052	0.049
10-SB10-3900 (B)	10-1023	0.011	0.233	0.244	0.047	0.045
10-SB10-3901 (A)	10-1024	0.102	0.191	0.293	0.534	0.348

SRNL Process Science Analytical Laboratory						
Date: 7/15/10						
Lab ID: 10-1013 through 10-1029						
Units: absorbance					**Fe(2+)**	**Fe(2+)**
Sample	**Lab ID**	**Fe(2+)**	**Fe(3+)**	**Fe(total)**	**Fe(3+)**	**Fe(total)**
10-SB10-3901 (B)	10-1024	0.103	0.190	0.293	0.542	0.352
10-SB10-3902 (A)	10-1025	0.077	0.194	0.271	0.397	0.284
10-SB10-3902 (B)	10-1025	0.078	0.193	0.271	0.404	0.288
10-SB10-3903 (A)	10-1026	0.058	0.224	0.282	0.259	0.206
10-SB10-3903 (B)	10-1026	0.057	0.224	0.281	0.254	0.203
10-SB10-3904 (A)	10-1027	0.074	0.264	0.338	0.280	0.219
10-SB10-3904 (B)	10-1027	0.074	0.262	0.336	0.282	0.220
10-SB10-3905 (A)	10-1028	0.058	0.210	0.268	0.276	0.216
10-SB10-3905 (B)	10-1028	0.059	0.210	0.269	0.281	0.219
10-SB10-3908 (A)	10-1029	0.087	0.174	0.261	0.500	0.333
10-SB10-3908 (B)	10-1029	0.087	0.176	0.263	0.494	0.331

Table B-4. Analytical Results for NaOH Quenched Samples

Process Science Analytical Laboratory								
Date: 6/11/10								
Lab ID: 10-0777-0788, 10-0930-0941								
Units: mg/L								
Sample ID	**Lab ID**	**F**	**Cl**	**NO2**	**NO3**	**SO4**	**C2O4**	**HCO2**
10-SB10-1-3567 (A)	10-0777	<100	<100	1750	41400	<100	<100	10200
10-SB10-1-3567 (B)	10-0777	<100	<100	1780	40900	<100	<100	9950
10-SB10-1-3572 (A)	10-0778	<100	<100	<100	68900	<100	<100	13100
10-SB10-1-3572 (B)	10-0778	<100	<100	<100	66900	<100	<100	13100
10-SB10-1-3575 (A)	10-0779	<100	<100	<100	67600	<100	<100	11900
10-SB10-1-3575 (B)	10-0779	<100	<100	<100	68600	<100	<100	11700
10-SB10-2-3589 (A)	10-0783	<100	<100	<100	47800	<100	<100	27400
10-SB10-2-3589 (B)	10-0783	<100	<100	<100	49100	<100	<100	26900
10-SB10-2-3594 (A)	10-0784	<100	<100	<100	66900	<100	<100	27300
10-SB10-2-3594 (B)	10-0784	<100	<100	<100	68000	<100	<100	28100
10-SB10-2-3597 (A)	10-0785	<100	<100	<100	64400	<100	<100	24500
10-SB10-2-3597 (B)	10-0785	<100	<100	<100	66500	<100	<100	25100
10-SB10-3-3838 (A)	10-0930	<100	184	2190	43000	<100	<100	14900
10-SB10-3-3838 (B)	10-0930	<100	185	2190	41400	<100	<100	14700
10-SB10-3-3843 (A)	10-0931	<100	345	<100	67100	<100	<100	19700
10-SB10-3-3843 (B)	10-0931	<100	346	<100	67300	<100	<100	19600
10-SB10-3-3844 (A)	10-0932	<100	360	<100	64300	<100	<100	18400
10-SB10-3-3844 (B)	10-0932	<100	361	<100	63900	<100	<100	18300
10-SB10-3-3852 (A)	10-0933	<100	368	<100	63000	<100	<100	20100
10-SB10-3-3852 (B)	10-0933	<100	367	<100	63700	<100	<100	20400
10-SB10-5-3860 (A)	10-0934	<100	185	4600	28100	<100	<100	26800
10-SB10-5-3860 (B)	10-0934	<100	185	4560	28100	<100	<100	27100
10-SB10-5-3865 (A)	10-0935	<100	286	635	41400	<100	<100	39500
10-SB10-5-3865 (B)	10-0935	<100	285	635	41600	<100	<100	40600

Process Science Analytical Laboratory								
Date: 6/11/10								
Lab ID: 10-0777-0788, 10-0930-0941								
Units: mg/L								
Sample ID	**Lab ID**	**F**	**Cl**	**NO2**	**NO3**	**SO4**	**C2O4**	**HCO2**
10-SB10-5-3866 (A)	10-0936	<100	290	<100	41300	<100	<100	37100
10-SB10-5-3866 (B)	10-0936	<100	292	<100	41600	<100	<100	37100
10-SB10-5-3874 (A)	10-0937	<100	283	<100	39700	<100	<100	36900
10-SB10-5-3874 (B)	10-0937	<100	283	<100	40300	<100	<100	39200
10-SB10-7-3612 (A)	10-0780	<100	<100	5800	13400	<100	<100	41600
10-SB10-7-3612 (B)	10-0780	<100	<100	5930	13600	<100	<100	41100
10-SB10-7-3617 (A)	10-0781	<100	<100	2300	18700	<100	<100	55500
10-SB10-7-3617 (B)	10-0781	<100	<100	2220	18800	<100	<100	56300
10-SB10-7-3620 (A)	10-0782	<100	<100	1250	18000	<100	<100	52700
10-SB10-7-3620 (B)	10-0782	<100	<100	1380	18300	<100	<100	53800
10-SB10-8-3633 (A)	10-0786	<100	<100	830	17200	<100	<100	61300
10-SB10-8-3633 (B)	10-0786	<100	<100	843	16900	<100	<100	61500
10-SB10-8-3639 (A)	10-0787	<100	<100	<100	19900	<100	<100	67500
10-SB10-8-3639 (B)	10-0787	<100	<100	<100	20000	<100	<100	68000
10-SB10-8-3642 (A)	10-0788	<100	<100	<100	17200	<100	<100	58800
10-SB10-8-3642 (B)	10-0788	<100	<100	<100	17100	<100	<100	59800
10-SB10-9-3816 (A)	10-0938	<100	182	<100	42700	<100	<100	33500
10-SB10-9-3816 (B)	10-0938	<100	182	<100	42500	<100	<100	33100
10-SB10-9-3821 (A)	10-0939	<100	198	<100	42200	<100	<100	29700
10-SB10-9-3821 (B)	10-0939	<100	198	<100	42400	<100	<100	30200
10-SB10-9-3822 (A)	10-0940	<100	295	<100	56600	<100	<100	34700
10-SB10-9-3822 (B)	10-0940	<100	294	<100	57000	<100	<100	37700
10-SB10-9-3830 (A)	10-0941	<100	313	<100	57900	<100	<100	37400
10-SB10-9-3830 (B)	10-0941	<100	310	<100	58600	<100	<100	37800

Appendix C: Offgas Composition Results from Experiments

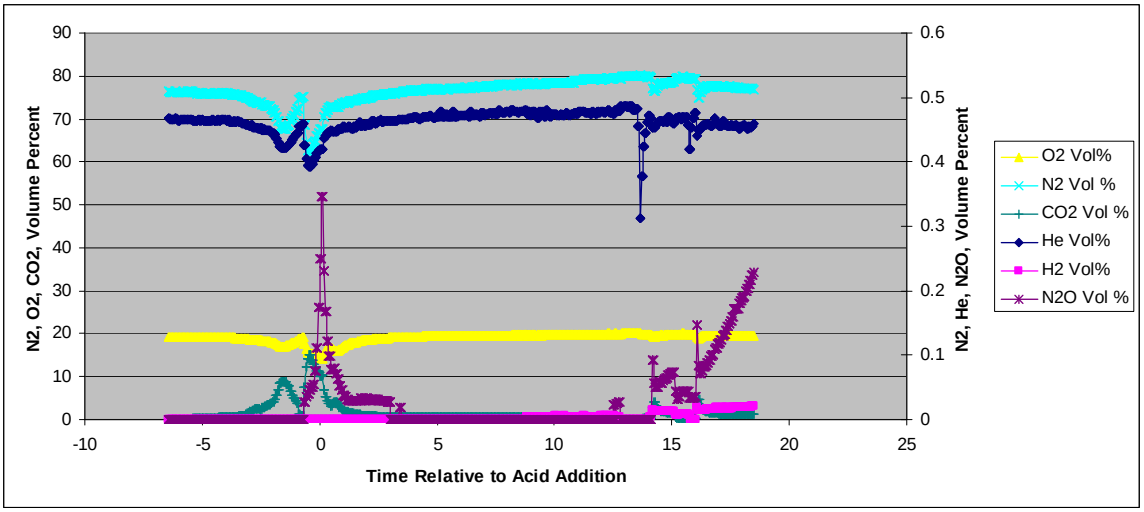

Figure C-1. SB10-1 Offgas Graph

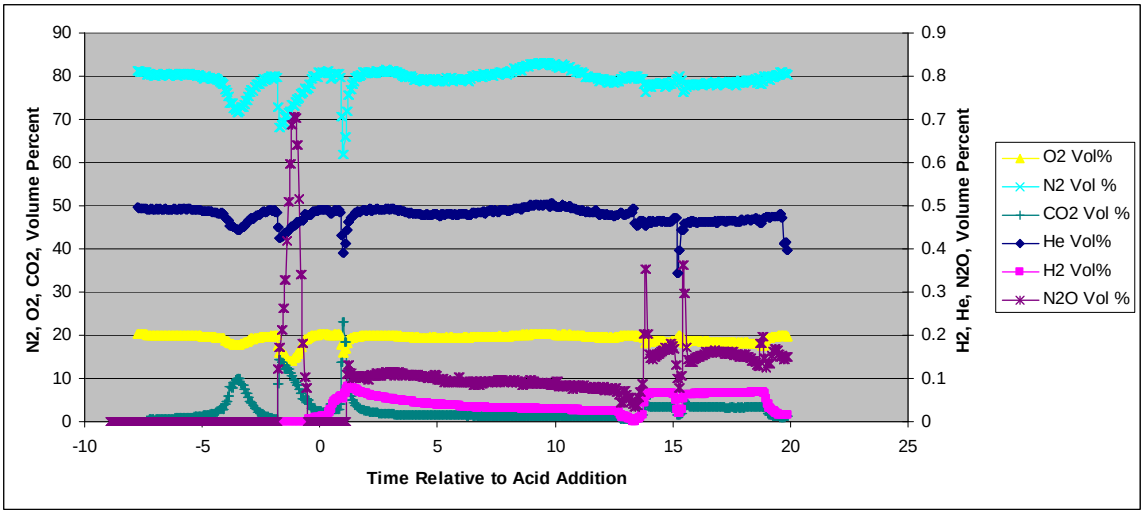

Figure C-2. SB10-2 Offgas Graph

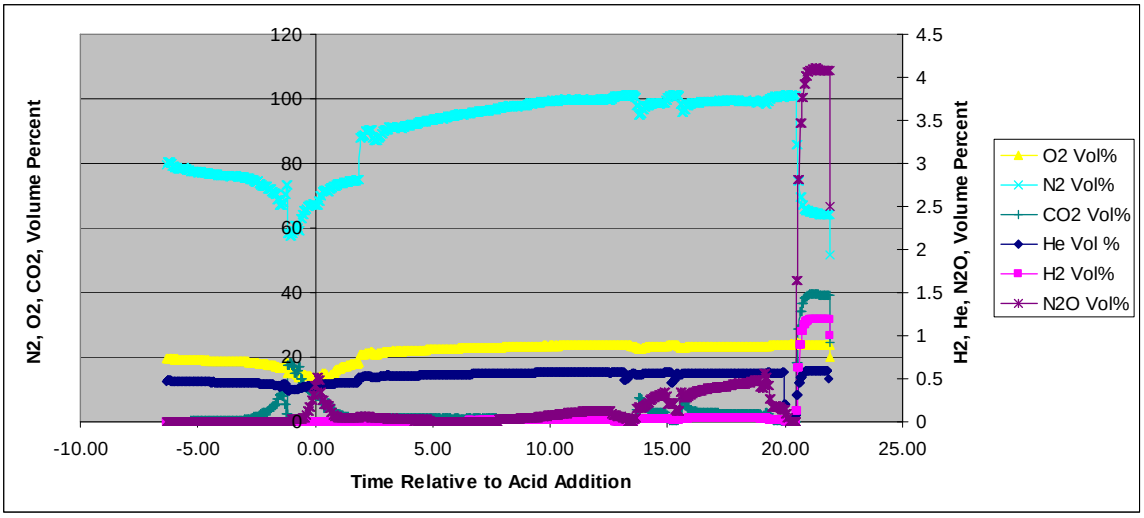

Figure C-3. SB10-3 Offgas Graph

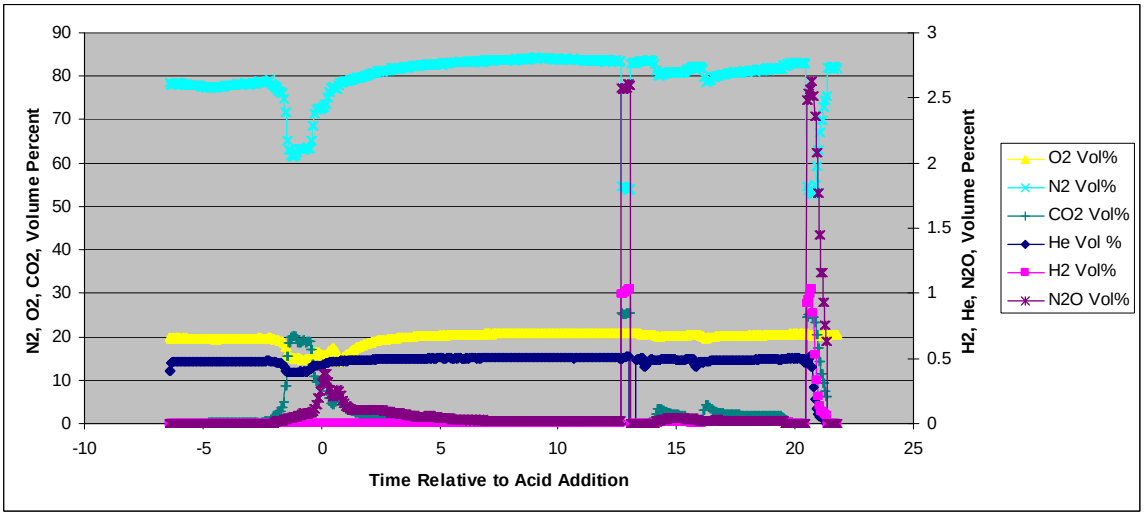

Figure C-4. SB10-5 Offgas Graph

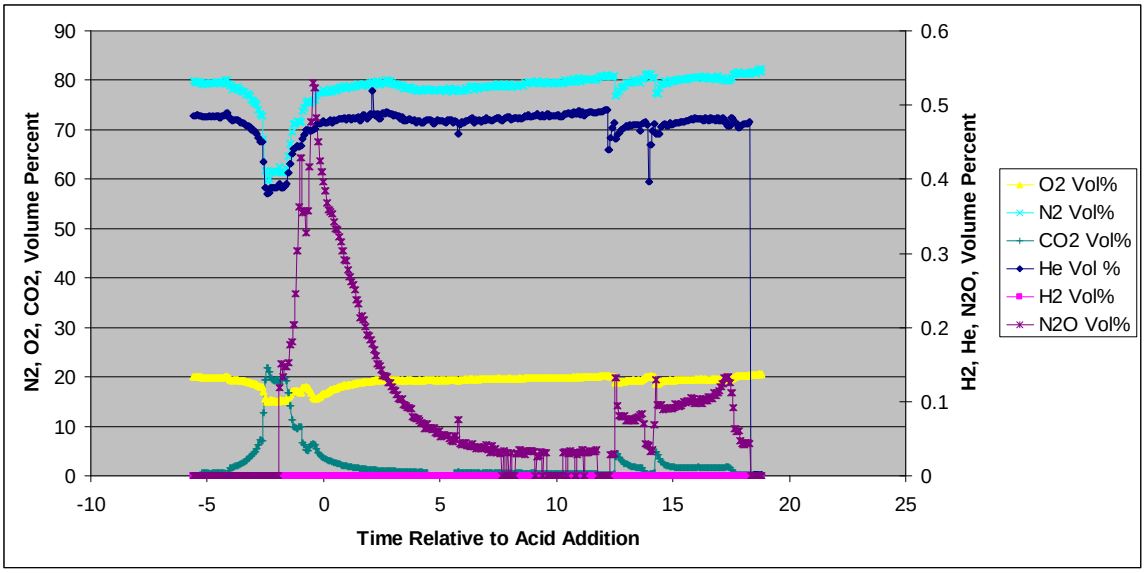

Figure C-5. SB10-7 Offgas Graph

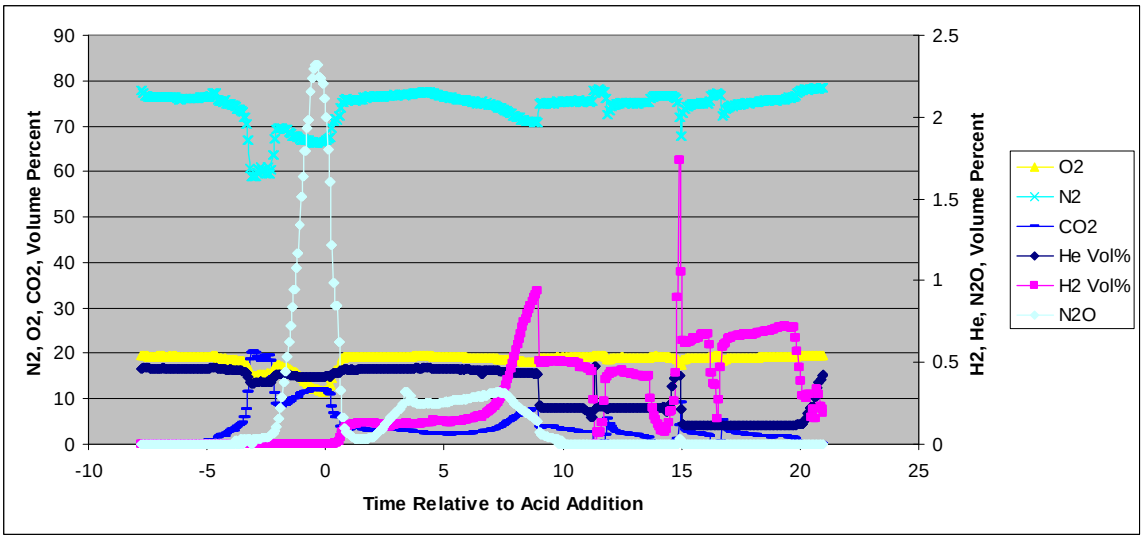

Figure C-6. SB10-8 Offgas Graph

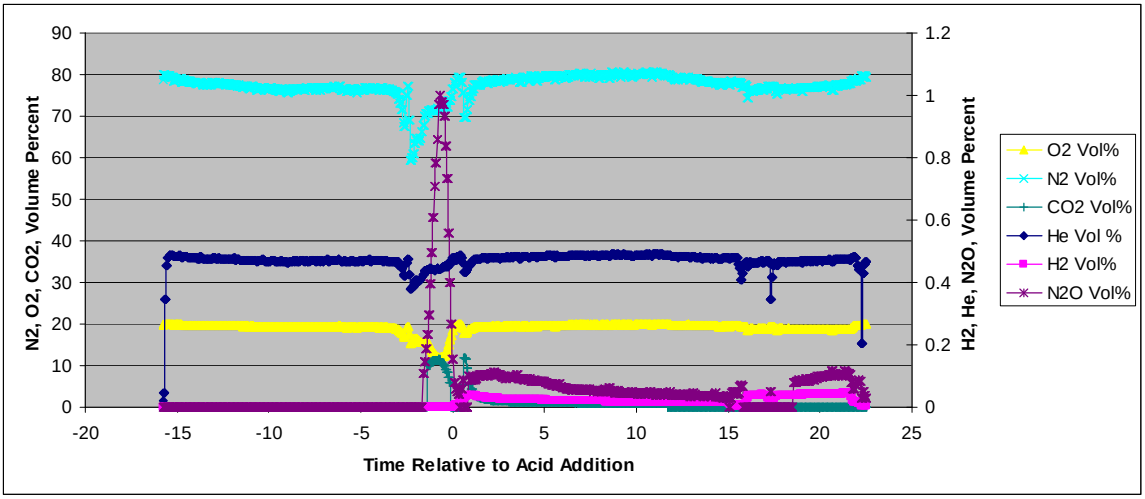

Figure C-7. SB10-9 Offgas Graph

Appendix D: Predicted Compositions of SB10 Baseline Melter Feeds

Table D-1. Composition of SB10-1 Baseline Melter Feed at 1.5 GPM

Insoluble Solids	lb/hr		Soluble Solids	lb/hr
Fe(OH)3	113.4707		Ca(COOH)2	
Al(OH)3	28.2329		Ca(NO3)2	19.0638
MnO2	11.6667		Cu(COOH)2	
Ca(OH)2	1.5115		Cu(NO3)2	
Mg(OH)2	0.6035		KCOOH	
HgO	0.0137		KNO3	1.2778
Ni(OH)2	2.4969		Mg(COOH)2	0.0000
Cr(OH)3	0.6266		Mg(NO3)2	2.9267
Cu(OH)2	0.1821		Mn(COOH)2	9.4924
TiO2	0.4514		Mn(NO3)2	
SiO2	223.7553		NaCl	
Na2O	22.1956		NaF	
Zn(OH)2	0.2404		NaCOOH	9.1568
K2O			NaNO3	70.4007
RuO2			NaNO2	
RhO2	0.0518		Na3PO4	
PdO			Ni(COOH)2	
B2O3	22.1956		Ni(NO3)2	
Li2O	22.1956		La(COOH)3	
BaSO4	0.8063		La(NO3)3	
PbSO4			Zn(COOH)2	
La(OH)3			Zn(NO3)2	
ZrO2	1.1749		Na2CO3	
CaCO3			Na2C2O4	
CaSO4	0.1381		Na2SO4	0.0659
MgO	0.0000		Fe(NO3)3	
Coal-carbon	19.8558		Si(OH)4	
NaTi2O5H			HCOOH	
Total_1	471.8653		Total_2	112.3841
			H2O	527.3363
			Total	1111.5857

Table D-2. Composition of SB10-2 Baseline Melter Feed at 1.5 GPM

Insoluble Solids	lb/hr		Soluble Solids	lb/hr
Fe(OH)3	101.2382		Ca(COOH)2	
Al(OH)3	26.7981		Ca(NO3)2	18.0661
MnO2	1.7851		Cu(COOH)2	
Ca(OH)2	1.8592		Cu(NO3)2	
Mg(OH)2	0.5217		KCOOH	
HgO	0.0097		KNO3	1.1436
Ni(OH)2	1.6126		Mg(COOH)2	
Cr(OH)3	0.6477		Mg(NO3)2	3.2482
Cu(OH)2	0.1386		Mn(COOH)2	24.7226
TiO2	0.4027		Mn(NO3)2	
SiO2	213.0266		NaCl	
Na2O	21.1309		NaF	
Zn(OH)2	0.2140		NaCOOH	10.8766
K2O			NaNO3	36.3974
RuO2			NaNO2	
RhO2	0.0504		Na3PO4	
PdO			Ni(COOH)2	
B2O3	21.1309		Ni(NO3)2	1.7887
Li2O	21.1309		La(COOH)3	
BaSO4	0.7516		La(NO3)3	
PbSO4			Zn(COOH)2	
La(OH)3	0		Zn(NO3)2	0.0379
ZrO2	1.1429		Na2CO3	
CaCO3			Na2C2O4	
CaSO4	0.1444		Na2SO4	0.0735
MgO			Fe(NO3)3	19.0370
Coal-carbon	15.1481		Si(OH)4	0.2245
NaTi2O5H	0.0981		HCOOH	
Total_1	428.9824		Total_2	115.6236
			H2O	533.1815
			Total	1077.7875

Table D-3. Composition of SB10-3 Baseline Melter Feed at 1.5 GPM.

Insoluble Solids	lb/hr		Soluble Solids	lb/hr
FeOOH	135.9715		Ca(COOH)2	
Al(OH)3	37.7853		Ca(NO3)2	20.8762
MnO2	8.2320		Cu(COOH)2	
Ca(OH)2			Cu(NO3)2	
Mg(OH)2	0.7428		KCOOH	
HgO	0.0186		KNO3	1.6559
Ni(OH)2	2.6964		Mg(COOH)2	
Cr(OH)3	0.6579		Mg(NO3)2	2.7410
Cu(OH)2			Mn(COOH)2	9.5532
TiO2	0.3678		Mn(NO3)2	
SiO2	228.4196		NaCl	0.5853
Na2O	24.0115		NaF	
Zn(OH)2	0.2524		NaCOOH	18.3139
K2O			NaNO3	60.2865
RuO2			NaNO2	
RhO2	0.2798		Na3PO4	
PdO			Ni(COOH)2	
B2O3	24.0115		Ni(NO3)2	
Li2O	24.0115		La(COOH)3	
BaSO4	0.9271		La(NO3)3	
PbSO4	0.2430		Zn(COOH)2	
La(OH)3			Zn(NO3)2	
ZrO2	1.4097		Na2CO3	
CaCO3			Na2C2O4	
CaSO4			Na2SO4	0.0813
MgO			Fe(NO3)3	
Coal-carbon	12.6492		Si(OH)4	0.0723
NaTi2O5H			HCOOH	
Total_1	502.6879		Total_2	114.1588
			H2O	517.2712
			Total	1134.1179

Table D- 4. Composition of SB10-5 Baseline Melter Feed at 1.5 GPM.

Insoluble Solids	lb/hr		Soluble Solids	lb/hr
Fe(OH)3	127.5660		Ca(COOH)2	
Al(OH)3	41.3559		Ca(NO3)2	19.3947
MnO2	12.1037		Cu(COOH)2	
Ca(OH)2			Cu(NO3)2	
Mg(OH)2	0.6730		KCOOH	
HgO	0.0186		KNO3	1.2368
Ni(OH)2	2.5534		Mg(COOH)2	
Cr(OH)3	0.6318		Mg(NO3)2	2.5957
Cu(OH)2			Mn(COOH)2	2.5951
TiO2	0.1710		Mn(NO3)2	
SiO2	222.0141		NaCl	0.5162
Na2O	23.3420		NaF	
Zn(OH)2	0.2424		NaCOOH	57.8967
K2O			NaNO3	37.0447
RuO2			NaNO2	
RhO2	0.2687		Na3PO4	
PdO			Ni(COOH)2	
B2O3	23.3420		Ni(NO3)2	
Li2O	23.3420		La(COOH)3	
BaSO4	0.8516		La(NO3)3	
PbSO4	0.3000		Zn(COOH)2	
La(OH)3	0.0000		Zn(NO3)2	
ZrO2	1.4153		Na2CO3	
CaCO3			Na2C2O4	
CaSO4			Na2SO4	0.1263
MgO			Fe(NO3)3	
Coal-carbon	6.7266		Si(OH)4	0.0437
NaTi2O5H			HCOOH	
Total_1	486.9181		Total_2	121.3776
			H2O	521.3157
			Total	1129.6114

Table D- 5. Composition of SB10-7 Baseline Melter Feed at 1.5 GPM.

Insoluble Solids	lb/hr		Soluble Solids	lb/hr
Fe(OH)3	111.5852		Ca(COOH)2	
Al(OH)3	41.0774		Ca(NO3)2	16.0985
MnO2	16.6026		Cu(COOH)2	
Ca(OH)2	2.6461		Cu(NO3)2	
Mg(OH)2	0.6256		KCOOH	
HgO	0.0301		KNO3	0.8421
Ni(OH)2	2.4425		Mg(COOH)2	
Cr(OH)3	0.6453		Mg(NO3)2	2.7549
Cu(OH)2	0.1875		Mn(COOH)2	1.5869
TiO2			Mn(NO3)2	
SiO2	229.7239		NaCl	
Na2O	23.2556		NaF	
Zn(OH)2	0.2166		NaCOOH	89.8018
K2O			NaNO3	7.6854
RuO2			NaNO2	2.2379
RhO2	0.0534		Na3PO4	
PdO			Ni(COOH)2	
B2O3	23.2556		Ni(NO3)2	
Li2O	23.2556		La(COOH)3	
BaSO4	0.7264		La(NO3)3	
PbSO4			Zn(COOH)2	
La(OH)3			Zn(NO3)2	
ZrO2	1.2923		Na2CO3	
CaCO3			Na2C2O4	
CaSO4	0.0336		Na2SO4	0.1541
MgO			Fe(NO3)3	
Coal-carbon			Si(OH)4	
NaTi2O5H			HCOOH	
Total_1	477.6553		Total_2	121.1616
			H2O	524.0349
			Total	1122.8518

Table D- 6. Composition of SB10-8 Baseline Melter Feed at 1.5 GPM.

Insoluble Solids	lb/hr		Soluble Solids	lb/hr
Fe(OH)3	112.3814		Ca(COOH)2	
Al(OH)3	41.6885		Ca(NO3)2	16.6232
MnO2	13.8747		Cu(COOH)2	
Ca(OH)2	2.5273		Cu(NO3)2	
Mg(OH)2	0.7532		KCOOH	
HgO	0.0003		KNO3	0.8571
Ni(OH)2	2.7477		Mg(COOH)2	
Cr(OH)3	0.6978		Mg(NO3)2	3.1397
Cu(OH)2			Mn(COOH)2	6.2181
TiO2			Mn(NO3)2	
SiO2	240.2285		NaCl	
Na2O	24.3356		NaF	
Zn(OH)2	0.2519		NaCOOH	93.4471
K2O			NaNO3	4.5075
RuO2			NaNO2	
RhO2	0.0543		Na3PO4	
PdO			Ni(COOH)2	
B2O3	24.3356		Ni(NO3)2	
Li2O	24.3356		La(COOH)3	
BaSO4	0.7746		La(NO3)3	
PbSO4			Zn(COOH)2	
La(OH)3			Zn(NO3)2	
ZrO2	1.4272		Na2CO3	
CaCO3			Na2C2O4	
CaSO4	0.1412		Na2SO4	0.1156
MgO			Fe(NO3)3	
Coal-carbon			Si(OH)4	
NaTi2O5H			HCOOH	
Total_1	490.5552		Total_2	124.9082
			H2O	517.1523
			Total	1132.6157

Table D- 7. Composition of SB10-9 Baseline Melter Feed at 1.5 GPM.

Insoluble Solids	lb/hr		Soluble Solids	lb/hr
Fe(OH)3	103.6527		Ca(COOH)2	
Al(OH)3	36.5090		Ca(NO3)2	15.8231
MnO2			Cu(COOH)2	
Ca(OH)2			Cu(NO3)2	
Mg(OH)2	0.3780		KCOOH	
HgO	0.0083		KNO3	1.1239
Ni(OH)2	1.8241		Mg(COOH)2	
Cr(OH)3	0.5167		Mg(NO3)2	3.9443
Cu(OH)2			Mn(COOH)2	18.1184
TiO2	0.2804		Mn(NO3)2	
SiO2	212.2828		NaCl	0.5163
Na2O	22.2792		NaF	
Zn(OH)2	0.2198		NaCOOH	41.0757
K2O			NaNO3	57.0053
RuO2			NaNO2	
RhO2	0.1994		Na3PO4	
PdO			Ni(COOH)2	
B2O3	22.2792		Ni(NO3)2	0.5307
Li2O	22.2792		Pb(NO3)2	0.3127
BaSO4	0.7387		La(COOH)3	
PbSO4			La(NO3)3	
Ce(OH)3			Zn(COOH)2	
La(OH)3			Zn(NO3)2	0.0218
ZrO2	1.1743		Na2CO3	0.0221
CaCO3			Na2C2O4	
CaSO4	1.8575		Na2SO4	0.9643
MgO			Fe(NO3)3	2.9719
Coal-carbon	9.6223		Si(OH)4	0.3299
NaTi2O5H	10.2108		HCOOH	
Total_1	446.3124		Total_2	142.7604
			H2O	511.9979
			Total	1101.0707

Distribution:

A. B. Barnes, 999-W
D. A. Crowley, 773-43A
S. D. Fink, 773-A
B. J. Giddings, 786-5A
C. C. Herman, 999-W
S. L. Marra, 773-A
F. M. Pennebaker, 773-42A
C. J. Bannochie, 773-42A
J. M. Gillam, 766-H
B. A. Hamm, 766-H
J. F. Iaukea, 704-30S
A. V. Staub, 704-27S
J. E. Occhipinti, 704-S
D. K. Peeler, 999-W
J. W. Ray, 704-S
H. B. Shah, 766-H
D. C. Sherburne, 704-S
M. E. Stone, 999-W
J. M. Bricker, 704-27S
T. L. Fellinger, 704-26S
E. W. Holtzscheiter, 704-15S
M. T. Keefer, 766-H
C. L. Atseff, 766-H
C. J. Johnson, 766-H
R. T. McNew, 766-H
S. C Shah, 766-H
A. Samadi-Dezfouli, 766-H
C. I. Aponte, 766-H
E. W. Daniel, 999-W
J. D. Newell, 999-W
A I. Fernandez, 999-W
D. C. Koopman, 999-W
J. M. Pareizs, 773-A
C. J. Bannochie, 773-42A
D. P. Lambert, 999-W
A. S. Choi, 773-42A
R. E. Eibling, 999-W